

AD-A096 113

AIRESEARCH MFG CO OF ARIZONA PHOENIX
REGENERATIVE ENGINE ANALYSIS PROGRAM (REAP).(U)
JAN 81 R W HELDENBRAND, W S MILLER

F/G 21/5

DAAK51-79-C-0057

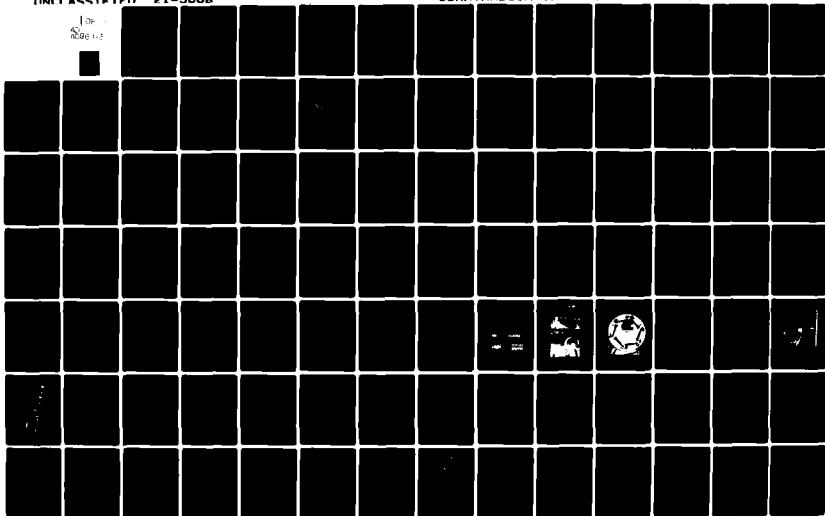
UNCLASSIFIED

21-3668

USAAVRADCOM-TR-81-D-2

NL

100
200



USAAVRADCOM-TR-81-D-2

AD A 096113

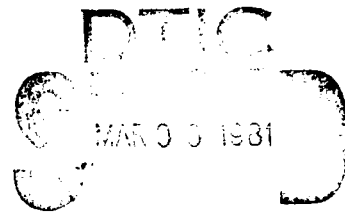
LEVEL II



12

REGENERATIVE ENGINE ANALYSIS PROGRAM (REAP)

R. W. Heldenbrand, W. S. Miller
AIRESEARCH MANUFACTURING CO. OF ARIZONA
111 S. 34th St., P. O. Box 5217
Phoenix, Ariz. 85010



January 1981

Final Report for Period October 1979 - May 1980

Approved for public release;
distribution unlimited.

Prepared for
APPLIED TECHNOLOGY LABORATORY
U. S. ARMY RESEARCH AND TECHNOLOGY LABORATORIES (AVRADCOM)
Fort Eustis, Va. 23604

DDC FILE COPY

81 3 09 038

APPLIED TECHNOLOGY LABORATORY POSITION STATEMENT

The results of previous regenerative engine technology programs have become somewhat obsolete by intervening technology development. In 1980, the Army supported several engine design investigations to update the regenerative cycle engine data for helicopter application. Results of this effort will be utilized in conjunction with parallel efforts at other engine companies and in-house to formalize future efforts directly related to small fuel efficient gas turbine engines.

Mr. Albert E. Easterling of the Propulsion Technical Area, Aeronautical Technology Division, served as project engineer for this effort.

DISCLAIMERS

The findings in this report are not to be construed as an official Department of the Army position unless so designated by other authorized documents.

When Government drawings, specifications, or other data are used for any purpose other than in connection with a definitely related Government procurement operation, the United States Government thereby incurs no responsibility nor any obligation whatsoever; and the fact that the Government may have formulated, furnished, or in any way supplied the said drawings, specifications, or other data is not to be regarded by implication or otherwise as in any manner licensing the holder or any other person or corporation, or conveying any rights or permission, to manufacture, use, or sell any patented invention that may in any way be related thereto.

Trade names cited in this report do not constitute an official endorsement or approval of the use of such commercial hardware or software.

DISPOSITION INSTRUCTIONS

Destroy this report when no longer needed. Do not return it to the originator.

Unclassified

SECURITY CLASSIFICATION OF THIS PAGE (When Data Entered)

REPORT DOCUMENTATION PAGE		READ INSTRUCTIONS BEFORE COMPLETING FORM
1. REPORT NUMBER 18 USAAVRADCOM 19 TR-81-D-2 ✓	2. GOVT ACCESSION NO. AD-A096 113	3. RECIPIENT'S CATALOG NUMBER
4. TITLE (and Subtitle) 6 REGENERATIVE ENGINE ANALYSIS PROGRAM (REAP)	5. TYPE OF REPORT & PERIOD COVERED 9 Final Report October 1979 - May 1980	6. PERFORMING ORG. REPORT NUMBER 14 21-3668 ✓
7. AUTHOR(s) 10 R. W. Heldenbrand W. S. Miller	8. CONTRACT OR GRANT NUMBER(s) 15 DAAK51-79-C-0057	
9. PERFORMING ORGANIZATION NAME AND ADDRESS AiResearch Manufacturing Co. of Arizona 111 S. 34th St., P. O. Box 5217 Phoenix, Arizona 85010	10. PROGRAM ELEMENT PROJECT, TASK AREA & WORK UNIT NUMBERS 16 612209 11162209AH76 00 306 EK	
11. CONTROLLING OFFICE NAME AND ADDRESS Applied Technology Laboratory, US Army Research and Technology Laboratories (AVRADCOM) Fort Eustis, Virginia 23604	12. REPORT DATE 11 January 1981 1700	13. NUMBER OF PAGES 142
14. MONITORING AGENCY NAME & ADDRESS (if different from Controlling Office) 12 143	15. SECURITY CLASS. (of this report) Unclassified	15a. DECLASSIFICATION/DOWNGRADING SCHEDULE
16. DISTRIBUTION STATEMENT (of this Report) Approved for public release; distribution unlimited.		
17. DISTRIBUTION STATEMENT (of the abstract entered in Block 20, if different from Report)		
18. SUPPLEMENTARY NOTES		
19. KEY WORDS (Continue on reverse side if necessary and identify by block number) Regenerative Recuperator Heat Exchanger Turboshaft Engine		
20. ABSTRACT (Continue on reverse side if necessary and identify by block number) This report presents the results of a 7-month program to conduct a preliminary design analysis of a 500-SHP fuel-efficient regenerative turboshaft engine and to identify promising heat-exchanger concepts for such engines. A technology level consistent with that available in a 1980 demonstrator engine is assumed. Ninety engine/heat exchanger configuration and cycle combinations were examined. These included variations of compressor-stage configuration, compressor pressure ratio, turbine design-point inlet temperature, heat-exchanger effectiveness, and		

1
F

DD FORM 1473 1 JAN 73 EDITION OF 1 NOV 65 IS OBSOLETE

Unclassified
SECURITY CLASSIFICATION OF THIS PAGE (When Data Entered)

404776

13

Unclassified

SECURITY CLASSIFICATION OF THIS PAGE(When Data Entered)

Block 20. Abstract - continued.

Heat-exchanger pressure loss. These engine combinations were evaluated and screened on the basis of fuel economy, weight and cost, and several promising configurations were chosen for more detailed analysis. The most promising of these was selected for preliminary design. The study results indicate that an engine configuration with a cycle pressure ratio of 10:1, a turbine temperature of 2300°F; and a heat exchanger with an effectiveness of 0.70 is most suitable for the 1980 environment. However, with fuel costs projected to increase, the analyses indicate that a tubular heat exchanger with an effectiveness approaching 0.80 would be more attractive.

Accession For	
NTIS GRA&I	<input checked="" type="checkbox"/>
DTIC TAB	<input type="checkbox"/>
Unannounced	<input type="checkbox"/>
Justification	
Evaluation	
Distribution	
Availability Codes	
Dist	Avail and/or Special
A	

I
B

Unclassified

SECURITY CLASSIFICATION OF THIS PAGE(When Data Entered)

SUMMARY

In September 1979, the U.S. Army Research and Technology Laboratory awarded the AiResearch Manufacturing Company of Arizona a contract, DAAK51-79-C-0057, to conduct an analysis of regenerative turboshaft engines suitable for helicopter application. The objectives of the program were to identify promising heat-exchanger concepts and to conduct a preliminary design and analysis of a fuel-efficient, regenerative turboshaft engine.

During the program study, 90 engine/heat-exchanger cycle and configuration combinations were screened. These included variations of compressor-staging arrangement, compressor pressure ratio, turbine design-point rotor inlet temperature, heat-exchanger effectiveness, and heat-exchanger pressure loss. Component efficiencies and turbine-cooling flows were also varied as appropriate to the configuration and cycle conditions. Screening was performed on the basis of a figure of merit that considered fuel consumption, weight, and cost.

The basic engine configuration consists of a high-pressure spool that includes a centrifugal compressor, a reverse-flow annular combustor, and a cooled radial turbine; a low-pressure spool that includes a two-stage, variable-geometry axial turbine that drives the output shaft through a spur reduction-gear set; and a tubular heat exchanger mounted aft of the engine to receive the turbine exhaust gas directly. An inlet-particle separator is incorporated as an integral part of the engine inlet and output shaft reduction gearbox, and the accessory gearbox is mounted aft of the inlet-particle separator on top of the engine. The engine is of modular construction and incorporates an integral lubrication system.

Both plate-fin and tubular heat-exchanger types were considered in the study; however, from the standpoint of configuration arrangement, installation, and weight, it was concluded early in the study that even though costs may be higher, the tubular configuration offered more advantages than the plate-fin. Therefore, a tubular unit was used as the baseline throughout the 90-engine parametric analysis. Subsequently, comparisons with plate-fin units were made for specific engine configurations and conditions.

As part of the initial heat-exchanger-design analysis, a wide variety of configuration arrangements and features were considered in an effort to identify promising concepts for helicopter applications. The aero/thermodynamic characteristics of heat exchangers is well understood, and thus, improvements in pressure loss and heat-transfer characteristics were not considered immediately possible. However, two areas were identified in which future improvements are considered to be feasible. They are advanced materials and improved fabrication methods. The

development of advanced materials with improved physical properties will allow reductions in both weight and volume with improved heat-transfer characteristics. The development of improved fabrication methods, with a reduction in hand-labor requirements, is required in order to reduce costs.

A most promising cycle was selected from the screening process for more detailed evaluation and preliminary design. This engine has the following characteristics at standard sea-level static conditions:

<u>Characteristic</u>	<u>500 SHP</u>	<u>250 SHP</u>
Compressor stages	1	1
Compressor pressure ratio	10.0:1	5.48:1
Air flow rate, lb/s	3.26	1.77
Turbine inlet temperature, °F	2300	2300
Specific fuel consumption, lb/hr-hp	0.425	0.437
Specific power, hp/lb/s	153.4	--
Heat exchanger effectiveness, %	70	73
Heat exchanger pressure loss, %	10	5.7
Length, in.	52.2	--
Maximum diameter, in.	21.9	--
Weight, lb	299.0	--
Acquisition cost, K\$	151.3	--

Since a principal reason for performing this study involved the escalation in cost of fuel and its uncertain future availability, a brief examination of the sensitivity of the heat-exchanger configuration to fuel cost was conducted. This examination showed that as fuel costs increase, a higher heat-exchanger effectiveness is desirable. The examination also verified that a tubular heat exchanger is preferable to a plate-fin configuration.

During the course of the study, engine-configuration and performance characteristics were reviewed with airframe manufacturers to determine what advantages or disadvantages might be introduced by the addition of the heat exchanger. The consensus was that any fuel saving was an advantage, weight and balance were manageable problems, and drag resulting from heat-exchanger bulk would not be a limiting factor.

As a result of this study, it was concluded that SFC was the prime mover in the selection of future helicopter propulsion systems, and the added bulk, weight, and cost associated with the heat exchanger were of significantly less concern than in previous studies and could be accommodated by the airframe manufacturer.

PREFACE

A parametric study and preliminary design analysis of fuel-efficient regenerative turboshaft engines suitable for helicopter application was conducted by the AiResearch Manufacturing Companies of Arizona and California for the U.S. Army Research and Technology Laboratory under Contract DAAK51-79-C-0057. The study was initiated in October 1979 and completed in May 1980.

The study was performed under the cognizance of Mr. A. E. Easterling of USARTL. The AiResearch Program Manager was Mr. R. W. Heldenbrand. Engine analysis efforts were performed by Mr. F. W. Lewis, who acted as technical director for those tasks, and Messrs. R. C. Davis and B. J. Gray. Heat-exchanger analyses were performed by Mr. W. S. Miller, and Mr. S. J. Lee.

The assistance of Bell Helicopter Textron, Ft. Worth, Texas, and Hughes Helicopter, Culver City, California, in providing helpful suggestions and constructive advice during this study is gratefully acknowledged.

TABLE OF CONTENTS

	<u>Page</u>
SUMMARY	3
PREFACE	5
LIST OF ILLUSTRATIONS	9
LIST OF TABLES.....	12
INTRODUCTION	14
ENGINE PARAMETRIC STUDY	16
HEAT-EXCHANGER PARAMETRICS	24
PERFORMANCE	24
WEIGHT	27
COST.....	30
FIGURE OF MERIT (FOM).....	32
PROMISING CYCLES	39
CONFIGURATION VARIANTS	52
Fixed-Geometry Power Turbine	52
Low-Speed Power Turbine	56
Bypass Heat Exchanger	56
HEAT-EXCHANGER ANALYSIS	60
CANDIDATE RECUPERATOR TYPES	60
FLOW-PATH CONFIGURATIONS.....	60
PLATE-FIN VERSUS TUBULAR.....	65
TUBULAR DESIGN PARAMETERS	70
PARAMETRIC STUDY	77
WEIGHT MODEL	83
COST MODEL	86
REFINED RECUPERATOR DESIGNS	86
PLATE-FIN CHARACTERISTICS FOR ENGINE NO. 36	88
MOST PROMISING CYCLE PRELIMINARY DESIGN.....	92
ENGINE DEFINITION	92
HEAT EXCHANGER DEFINITION.....	101
DESIGN PHYSICAL CHARACTERISTICS	102

TABLE OF CONTENTS (CONTD)

	<u>Page</u>
TEN YEAR TECHNOLOGY ADVANCEMENTS	110
ENGINE TECHNOLOGY	110
HEAT-EXCHANGER TECHNOLOGY	111
WEIGHT REDUCTION	111
VOLUME REDUCTION	112
COST REDUCTION	112
ADVANCED MATERIALS	113
LOW-COST FABRICATION METHODS	117
FUEL SENSITIVITY	119
INSTALLATION CHARACTERISTICS	125
SPECIAL DEVELOPMENT ASPECTS	128
CONCLUSIONS	139
RECOMMENDATIONS	142

LIST OF ILLUSTRATIONS

<u>Figure</u>	<u>Title</u>	<u>Page</u>
1	Baseline Engine.....	17
2	90-Engine Parametric Study.....	18
3	Power Turbine Efficiency Characteristics.....	22
4	Regenerative Engine Turbine Cooling Airflow	23
5	Regenerative Engine Specific Fuel Consumption	26
6	WATE - Weight Analysis of Turbine Engines	28
7	Regenerative Engine Parametric Analysis (Engine Weights).....	31
8	Regenerative Engine Parametric Analysis (Bare Engine Cost)	33
9	Regenerative Engine Parametric Analysis (Heat Exchange Costs).....	34
10	Regenerative Engine Parametric Analysis (Total Engine Cost)	37
11	Regenerative Engine Parametric Analysis (Figures of Merit)	38
12	Specific Power for 90 Engines	40
13	Engine 34 Performance.....	43
14	Engine 70 Performance	44
15	Engine 88A Performance	45
16	Selected Cycle	46
17	Engine 34 and 34A Cross-Section Drawing	48
18	Engine 70 Cross-Section Drawing.....	49
19	Engine 88A Cross-Section Drawing.....	50
20	Fixed- and Variable-Geometry Power Turbine Engine Performance	54

LIST OF ILLUSTRATIONS (CONTD)

<u>Figure</u>	<u>Title</u>	<u>Page</u>
21	Engine 34C, Low-Speed (20,000 RPM) Power Turbine Engine	57
22	Possible Recuperator Flow Configuration	62
23	T-53 Gas Turbine Engine Recuperator	63
24	T-78 Recuperator	64
25	Heat Transfer Surfaces	66
26	T-63 Regenerator Core Assembly	67
27	Fin-Tubeplate Subassemblies GT-601 Recuperator	68
28	Recuperated Engine Cycle	69
29	Weight Comparison of Typical Tubular and Plate-Fin Units (Stainless Steel Unit)	71
30	Tubular Heat Exchanger Surface Geometries	72
31	Tubular Recuperator, Study Effect of Tube Ring Dimple on Recuperator Characteristics	74
32	Tubular Recuperator, Study Effect of Pressure Drop and Tube Diameter on Recuperator Characteristics	75
33	Tubular Recuperator, Study Effect of Tube Bundle Spacing on Recuperator Characteristics	76
34	Estimated Off-Design Pressure Drop, 500 HP Engine Recuperator ($\Delta P/P_T = 5\%$)	82
35	Tubular Unit Off-Design Performance	84
36	Estimated Off-Design Performance Plate-Fin Recuperator for 500 HP Engine No. 36	85
37	Plate-Fin Module Configuration for Engine 36	89
38	Estimated Off-Design Performance (Engine No. 36: $E = 0.8$, $\Delta P/P_T = 10\%$)	90
39	Estimated Off-Design Pressure Drop (Engine No. 36: $\Delta P/P_T = 10\%$, $E = 0.8$)	91

LIST OF ILLUSTRATIONS (CONTD)

<u>Figure</u>	<u>Title</u>	<u>Page</u>
40	Turboshaft Engine TSE Model 1071	93
41	TSE Model 1071 Performance	96
42	TSE Model 1071 Performance	97
43	TSE Model 1071 Performance	98
44	Recuperator Outline, Turbine Exhaust	103
45	Estimated Recuperator Off-Design Performance.....	108
46	Estimated Recuperator Off-Design Pressure Loss.....	109
47	Application of High-Temperature Nitriding Process to Modified Type 321 Stainless Steel Sheet.....	115
48	Master Rupture Plot Showing Temperatures for 1-Percent Creep in 10,000 Hours	116
49	Fuel Sensitivity.....	121
50	Fuel Sensitivity Trends	122
51	Heat-Exchanger Trades.....	124
52	Engine 34 Compressor Map	130
53	Sensitivity of Tubing Blockage to Recuperator Performance	132
54	Sensitivity of Tubing Blockage to Recuperator Pressure Drop.....	133
55	Recuperator Weight as a Function of Tube Wall Thickness	135
56	Sensitivity of Fouling on Tube Outside Surface to Recuperator Performance	136
57	Comparison Between Tubular and Plate-Fin Heat Exchanger	138
58	Fuel Conserved by a Recuperated Engine at 50 Percent IRP	140

LIST OF TABLES

<u>Table</u>	<u>Title</u>	<u>Page</u>
1	Regenerative Engine Analysis Study 90-Engine Cycle Screening Average Part-Load Shaft Power.....	20
2	Component Efficiency.....	20
3	REAP Parametric Analysis Part Load Cycle Losses Assumed.....	25
4	Full Load Performance	25
5	Heat Exchanger Weight Model	29
6	Figure of Merit Analysis.....	36
7	Promising Cycles Design-Point Program Conditions.....	41
8	Promising Cycles Off-Design Program Conditions.....	42
9	Regenerative Engine Analysis Parametric Study Summary	51
10	Fixed-Geometry Power Turbine Engines	53
11	Figures of Merit, Fixed-Geometry Power Turbine Engines	55
12	Low-Speed Power Turbine Comparison.....	58
13	Bypass Heat Exchanger Comparison	58
14	Tubular Recuperator Design Parameter Ranges	73
15	Selected Parameter Values	78
16	500 HP Engine Tubular Recuperator Design Study.....	78
17	Screening Study Results.....	78
18	Preliminary Recuperator Characteristics	79
19	Tubular Heat Exchanger Cost Model Elements	87
20	Refined Recuperator Design Characteristics	88

LIST OF TABLES (CONTD)

<u>Table</u>	<u>Title</u>	<u>Page</u>
21	Plate-Fin Characteristics For Engine Nos. 34 and 36.....	89
22	TSE Model 1071 Cycle Parameters SEA Level Static, 59°F.....	94
23	TSE Model 1071 Materials.....	95
24	TSE Model 1071 Trends and Limits.....	99
25	TSE Model 1071 Estimated Weight.....	100
26	TSE Model 1071 Estimated Acquisition Cost.....	101
27	Recuperator Design Requirement for Phase III 500-HP Helicopter Engine.....	102
28	Recuperator Design Summary.....	104
29	Recuperator Weight Summary.....	106
30	Preliminary Design Recuperator Performance Summary at Design Point.....	106
31	Estimated 10-Year Technology Improvements.....	110
32	Figure of Merit (FOM) Equation.....	120

INTRODUCTION

During the past 15 years, studies have been made in an effort to establish the benefits of regenerative gas turbines for helicopters. In these studies, the trade-offs of weight and cost associated with the heat exchanger were examined in relation to mission duration and heat-exchanger effectiveness. In general, it was concluded that for the missions considered, the additional weight (and attendant bulk and cost) was not worth the fuel saved. For these studies, fuel cost was a relatively insignificant factor, and the cost associated with the heat exchangers were excessive by comparison. Furthermore, the installation of an additional component, for which maintenance requirements were not defined, and survivability was uncertain on an already weight-sensitive vehicle, was not considered worth the risk.

However, in the last five years, several factors have resulted in a renewed interest in the helicopter regenerative engine cycle. Principal among these are the rapidly increasing cost of fuel and the combined uncertainty of its future availability. In addition, advances in helicopter aerodynamic and propulsion technology have tended to reduce the vehicles sensitivity to the installed weight of the heat exchanger. Brief experience with development units in a ground vehicle installation and one flight unit¹ indicate that heat-exchanger maintenance should not be a serious problem. Finally, as a result of the fuel situation and its anticipated intensification, the civilian sector has shown interest in the regenerative cycle.

Survivability/vulnerability continue to be an issue, but some data exists that shows a recuperator reduces the IR signature. It was beyond the scope of this study to address survivability/vulnerability.

In view of the above, the Applied Technology Laboratory funded three regenerative engine analysis programs to identify promising heat-exchanger concepts and to conduct a preliminary design and analysis of a fuel-efficient, regenerative, turboshaft engine suitable for helicopter application. This document presents the results of the study performed by the AiResearch Manufacturing Company of Arizona.

¹Privoznik, Edward J., "T63 Regenerative Engine Program", Allison Division, General Motors Corporation; USAAVLABS Technical Report 68-9, U.S. Army Aviation Materiel Laboratories, Fort Eustis, Virginia, May 1963, AD675444.

The requirements for the turboshaft engine itself were as follows:

- 500-SHP class
- Front drive
- Free output-shaft speed of 20,000 rpm
- Integral inlet-particle separator
- Modular construction
- Minimum SFC (specific fuel consumption) at cruise power (50-percent intermediate)
- Technology level consistent with current demonstration.

In addition, for the parametric studies, cycle parameters were also specified. However, other than the ranges of effectiveness and overall pressure loss, no constraints were placed on the heat exchanger with respect to configuration, type, or materials. Thus, the designers were allowed to optimize the heat exchangers with respect to location and flow paths, choice of tubular or plate-fin types, and selection of best materials for the operating temperatures.

Since a major part of the program was to provide a definition of engine performance, installation characteristics, and cost, with a primary objective of minimizing engine weight, a formula was derived for a figure of merit (FOM) that included SFC, weight, and cost considerations as follows:

$$FOM = K_1 \frac{SFC}{SFC_{BL}} + K_2 \frac{WT}{WT_{BL}} + K_3 \frac{\$}{\$_{BL}}$$

where the relationship among the K coefficients is based on life-cycle cost analyses and depends on details such as fuel cost, mission type, and mission duration. Once the values for the K coefficients were defined and confirmed after consultation with airframe manufacturers, the equation was used to screen a variety of configuration and cycle combinations. As the study progressed, the FOM equation was modified to reflect fuel cost and mission variations in order to examine trends; however, these modified FOM equations were not used to alter or otherwise adjust the results obtained with the initial parametric screening.

ENGINE PARAMETRIC STUDY

The initial task of the regenerative engine analysis study was to perform a multi-cycle parametric analysis of regenerative turboshaft engine configurations in order to select a most promising cycle for further detailed analysis and preliminary design. The baseline engine configuration used for this parametric analysis is shown in Figure 1. This engine incorporates an integral particle separator; a main reduction gearbox; a top-mounted accessory gearbox; a single-stage centrifugal compressor; a reverse-flow annular combustor; a single-stage laminated-construction, cooled radial turbine; a two-stage axial power turbine; and a two-pass cross-counterflow tubular heat exchanger.

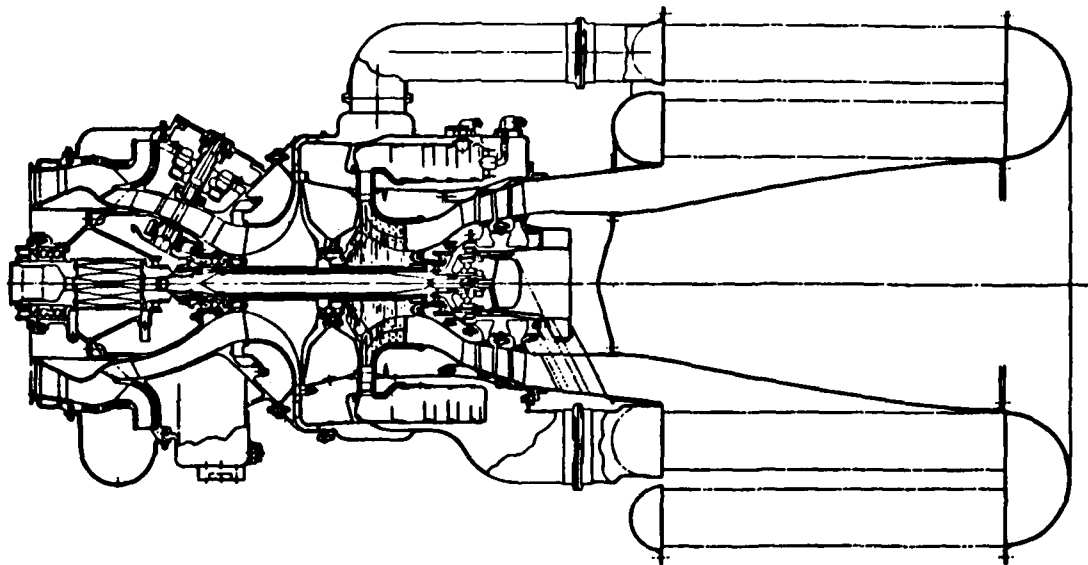
CYCLE VARIABLES

The cycle and configuration variables used for the parametric analysis were as follows:

- Single-stage compressors with pressure ratios of 7:1 and 10:1
- Two-stage compressors with pressure ratios of 7:1, 10:1 and 13:1
- Turbine rotor inlet temperatures of 2100°F, 2200°F, and 2300°F
- Heat-exchanger effectivenesses of 60, 70, and 80 percent
- Heat exchanger pressure losses of 5 and 10 percent.

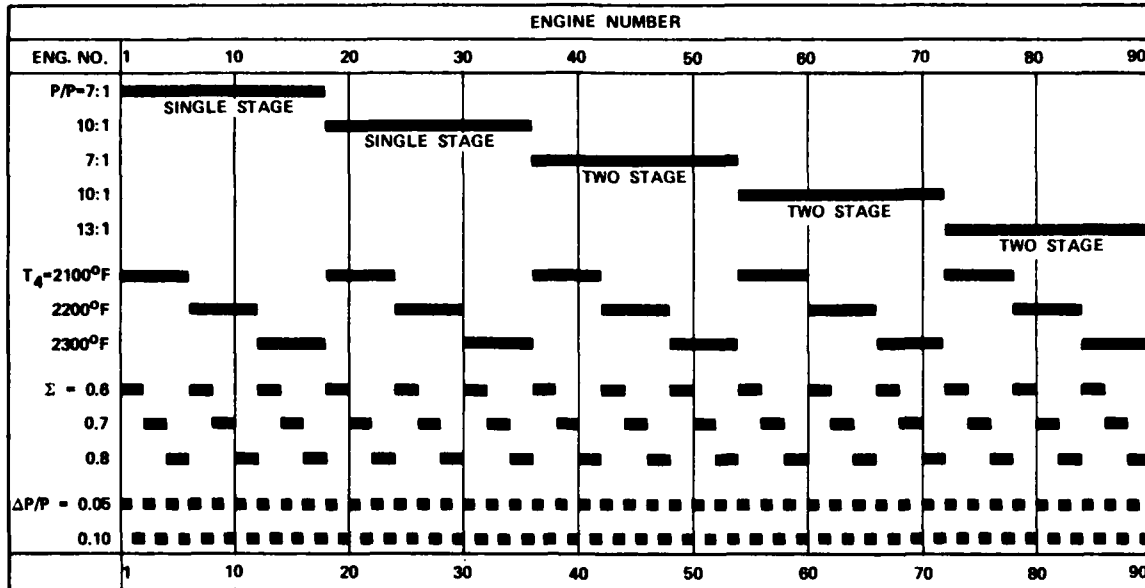
The combination of these variables result in five families of engines with a total of 90 different cycles. Throughout the study, a given cycle combination was identified and referred to by an engine number, as indicated in Figure 2. In addition to the above variables, other cycle parameters, including component efficiencies and turbine cooling flows, were varied appropriately, as discussed in subsequent paragraphs.

In order to provide a low specific fuel consumption over a broad power range, it was assumed that all 90 cycles incorporated a variable-geometry power turbine. To verify the advantage of this feature, six of the engine cycles were selected for study with fixed-geometry power turbines. These and other variants of the baseline configuration, including a lower speed power turbine designed to eliminate the need for a reduction gearbox, a bypass heat exchanger, and compressor inlet-guide vanes, are discussed in a subsequent section.



2
F

Figure 1. Baseline Engine.



2
B

Figure 2. 90-Engine Parametric Study.

The compressor components selected for the five engine families were based on current AiResearch technology. The single-stage, 7:1 compressors were derived from the Model TSE36-10 turboshaft engine. The single-stage, 10:1 compressor was based on the predicted performance for a research unit being tested at AiResearch under USARTL sponsorship. The two-stage, 7:1 compressor was derived from the Model GT601 truck engine currently under development. The two-stage, 10:1 compressor was taken from the Model TPE331 turboprop engine. The two-stage, 13:1 compressor was based on an advanced compressor design for the Model TPE331 turboprop engine. As the study progressed, an additional 13:1 compressor was added. This compressor was taken from a Model GT1801 tank engine currently under study, and incorporated inlet guide vanes.

In order to facilitate the screening of the 90 engines, performance-cycle calculations were performed on a design-point basis at the 500-SHP design point and at 50 ±5 percent of that power. The selection of compressor and turbine match points at the part-power condition was based on previous experience with the constraint that the calculated available shaft power must be between 225 and 275 SHP. The actual values were spread over that full range with the average for each of the five engine families as shown in Table 1. Variations among the families was due primarily to compressor-match estimation, as explained later.

Design considerations in setting up the engine models were as follows: Since the variable-geometry power turbine allows for power modulation at a constant gas-generator turbine-inlet temperature, then, for any chosen operating point, all other points along the operating line are readily predictable from the relationships:

$$\left(\frac{W\sqrt{T}}{P}\right)_{GG} = \text{CONSTANT}$$

All engines were matched with a minimum of five-percent compressor surge margin, where surge margin is defined as:

$$SM = \left[\frac{\frac{W\sqrt{\theta}}{\delta} \frac{P}{P} \text{ OPERATING POINT}}{\frac{W\sqrt{\theta}}{\delta} \frac{P}{P} \text{ SURGE LINE}} - 1 \right] \times 100$$

and the operating line was adjusted, if necessary, to obtain the minimum-range margin. This required that the full-power match points be modified from peak efficiency as shown in Table 2. This table also shows the efficiencies for the gas generator and power turbines. It should be noted that the turbine efficiencies were the same at full load and part load during the screening process. However, the gas generator turbine efficiency was reduced as cycle pressure ratio increased, consistent with the higher turbine-work requirements.

TABLE 1. REGENERATIVE ENGINE ANALYSIS STUDY 90-ENGINE
CYCLE SCREENING AVERAGE PART-LOAD SHAFT POWER

Compressor Family	Average Part Load SHP
Single-stage 7:1	262.3
Single-stage 10:1	267.9
Two-stage 7:1	265.5
Two-stage 10:1	235.2
Two-stage 13:1	282.3

TABLE 2. COMPONENT EFFICIENCY

	Single-Stage		Two-Stage		
	7:1	10:1	7:1	10:1	13:1
Peak η	78.5	77.0	81.0	79.2	77.7
Actual η Full/Part	77/75.2	76.8/77.4	80/80.7	78.2/75.1	75.2/70.8
Actual Corrected Speed, $\%N/\sqrt{\theta}$	100	101	100	98	99
Gas Generator Turbine η (Radial)	91.0	89.5	91.0	89.5	88.0
Power turbine η (Axial)	88.5	88.5	88.5	88.5	88.5

Table 2 also shows that the actual compressor match points were not at the peak efficiency. Further, because of the surge-margin constraint and the resulting nature of the turbine operating lines, some of the compressors experienced a large change in efficiency from the full-load condition to the part-load condition, whereas other compressors showed a modest gain from full load to part load. The efficiency of the two-stage 13:1 compressor at part load was so low that during the more detailed analysis of the three more promising cycles later in the study, the original compressor was abandoned in favor of a configuration with inlet guide vanes. The part-load compressor efficiency of fixed-geometry power turbine engines was approximately one-percent higher than that of the variable-geometry power turbine engines. This was principally the result of a difference in safe operating line and the higher corrected speed at part power of the fixed-geometry engines.

In establishing the models for the 90 engine cycles, the variable power turbine efficiency was held constant for the full- and part-load points. This assumption was justified on the basis of the characteristics shown in Figure 3. The left side of this figure shows the design-point power turbine efficiency characteristic versus pressure ratio as a function of corrected speed. The right side shows the ratio of the power turbine cycle efficiency to design-point efficiency versus the area ratio of the variable-inlet nozzle. Under the conditions assumed for this program, the power turbine pressure ratio changes only a small amount from full load to part load. Thus, with the slight reduction in corrected speed, efficiency tends to remain constant. Further, the power turbine inlet nozzle vane area was intentionally opened at full load to obtain slightly lower than peak efficiency so that the part-load efficiency at the smaller nozzle area would be increased or equal to that at full load.

Cooling flows for the gas generator turbine stator and rotor were varied as a function of cycle pressure ratio and gas generator turbine rotor inlet temperature, as shown in Figure 4. The cooling-flow rate is higher for the variable-geometry power-turbine configuration since, with the variable-geometry power turbine, the gas-generator turbine inlet temperature is constant over the load range from 100 percent to less than 50 percent. Thus, the higher cooling-air-flow rate provides a gas generator turbine life equal to that for the fixed-geometry power-turbine configuration. A rotor life of 5000 hours was assumed for this application. As noted in Figure 4, the rotor cooling flows are the combined disk and blade flows. The gas generator stator-cooling flows, which were not charged to the cycle, are identical for both power-turbine configurations. In addition to the cooling flows shown in Figure 4, a constant 1.5 percent of the core flow was used for the first-stage power turbine disk cooling.

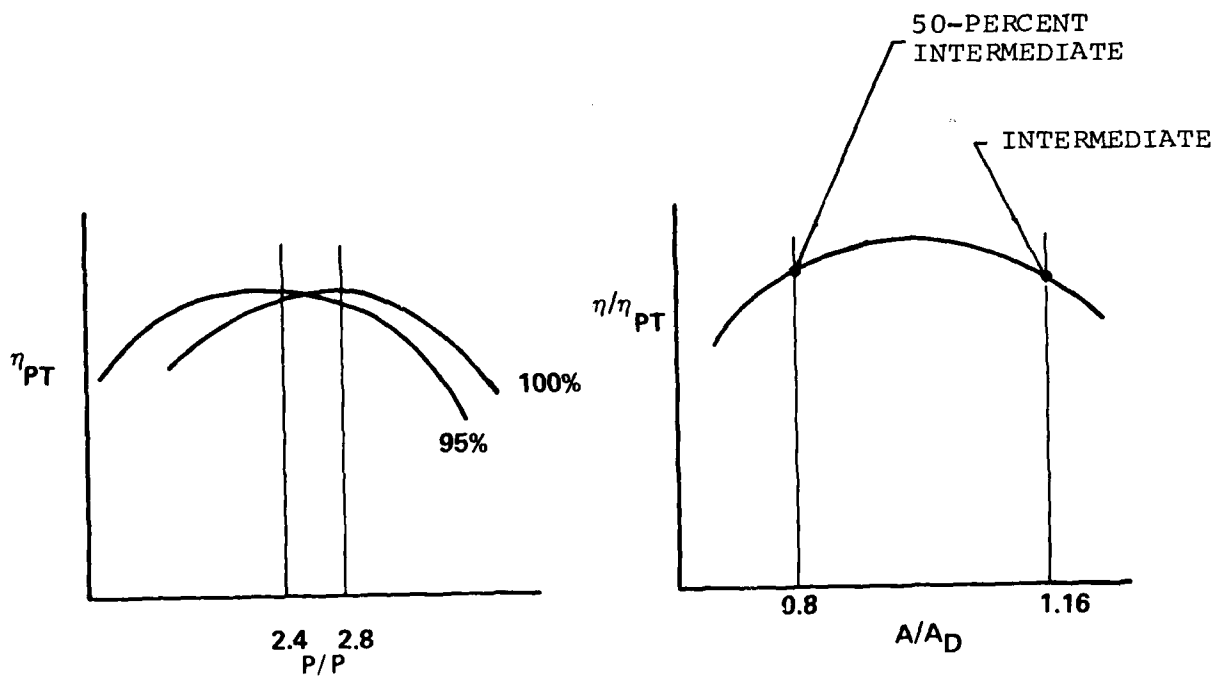


Figure 3. Power Turbine Efficiency Characteristics.

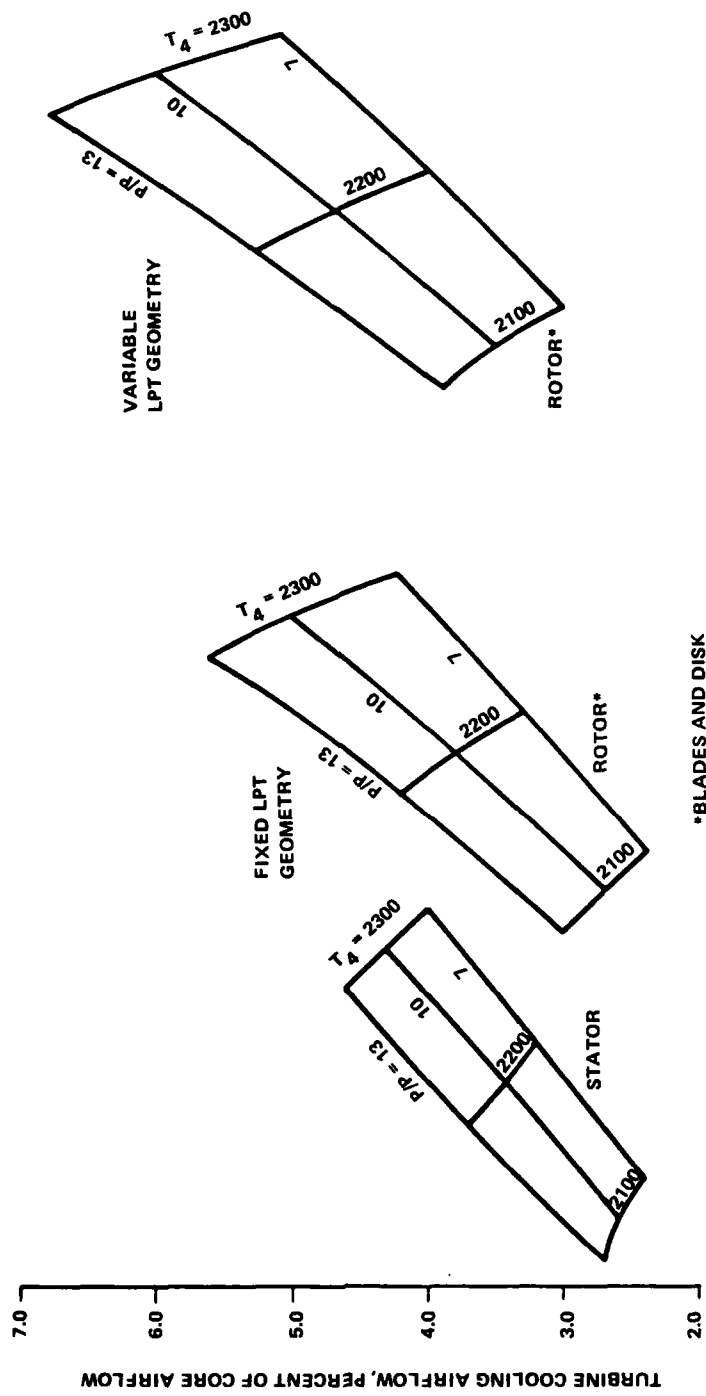


Figure 4. Regenerative Engine Turbine Cooling Airflow.

HEAT-EXCHANGER PARAMETRICS

The two general classes of heat exchangers considered for gas-turbine applications are the periodic or rotary regenerator in which heat is alternately absorbed and rejected by a mass of material that rotates through fixed fluid streams, and the fixed-boundary recuperator in which compressor discharge air and turbine exhaust gas exchange thermal energy directly through the separating heat-transfer surface. Because the rotary regenerators suffer from wear and leakage at cycle pressure ratios above 6:1, this study was limited to fixed-boundary recuperators.

Among the fixed-boundary heat exchangers, two design concepts were considered--the plate-fin and the tubular construction. For the 90-engine cycle parametric analysis, a tubular heat exchanger of an annular cross counterflow basic configuration was selected based principally on consideration of weight and packaging. This basic configuration was expanded into 18 groups based on heat-exchanger effectiveness, overall pressure loss, and cycle pressure ratio. Within each of the five engine families, a nominal heat exchanger was designed for flow rates in the middle of the family range. Characteristics such as weight, geometry, and number of tubes for other heat exchangers in each family were obtained by scaling from the nominal configuration.

A detailed discussion of the heat-exchanger design analysis for the 90-engine parametric study is given in a subsequent section. A comparison of tubular and plate-fin configurations is also given.

PERFORMANCE

Cycle calculations for the 90-engine cycles at the full- and part-load conditions were performed using an AiResearch engine-design-point computer program identified as 770. Program 770 accepts various cycle parameters as inputs and can either calculate airflow required for a specified shaft horsepower or thrust, or calculate output thrust or shaft horsepower for a specified airflow. The program will also accommodate various spool arrangements, as well as recuperators and intercoolers. The losses assumed for the cycle calculations are given in Table 3.

The evaluation of the 90 engines and cycles was performed on the basis of performance at the 50-percent load condition. Therefore, carpet plots of SFC were prepared for each of the five engine families as functions of gas generator turbine inlet temperature, heat-exchanger effectiveness, and heat-exchanger pressure loss. The SFC values for the 90-engine cycles at the sea-level, standard-day, static, 50-percent load condition are shown in Figure 5. Full load performance for selected engines is given in Table 4. The cycles with the highest compressor efficiencies at part load--the single-stage 10:1 and the two-stage 7:1--have

TABLE 3. REAP PARAMETRIC ANALYSIS PART LOAD
CYCLE LOSSES ASSUMED

Efficiencies

Combustor	0.998
Combined Shafts and Gearbox	0.980

Pressure Losses ($\Delta P/P$)

Inlet Particle Separator	0.025
Combustor	0.035
Inter-Turbine Duct	0.015
Turbine Diffuser	0.015
Heat Exchanger, Hot Side	0.035
Heat Exchanger, Cold Side	0.015
Heat Exchanger, Ducts	0.040

Leakages (Percent Compressor Flow)

Compressor P/P = 7:1	0.40
Compressor P/P = 10:1	0.65
Compressor P/P = 13:1	0.85

Cooling Flow (Percent Core Flow)

VG Power Turbine Disk	1.5
-----------------------	-----

TABLE 4. FULL LOAD PERFORMANCE

Engine No.	1	30	38	64	89
Compressor Stages	1	1	2	2	2
Compressor Pressure Ratio	7:1	10:1	7:1	10:1	13:1
Turbine Rotor Inlet Temp.	2100	2200	2100	2200	2300
Heat Exchanger Effectiveness	0.6	0.8	0.6	0.7	0.8
Heat Exchanger Pressure Loss	0.05	0.10	0.10	0.10	0.05
Output Shaft Horsepower	500	500	500	500	500
Specific Fuel Consumption	0.445	0.415	0.448	0.423	0.426
Specific Power	141.3	146.9	139.9	151.0	154.9

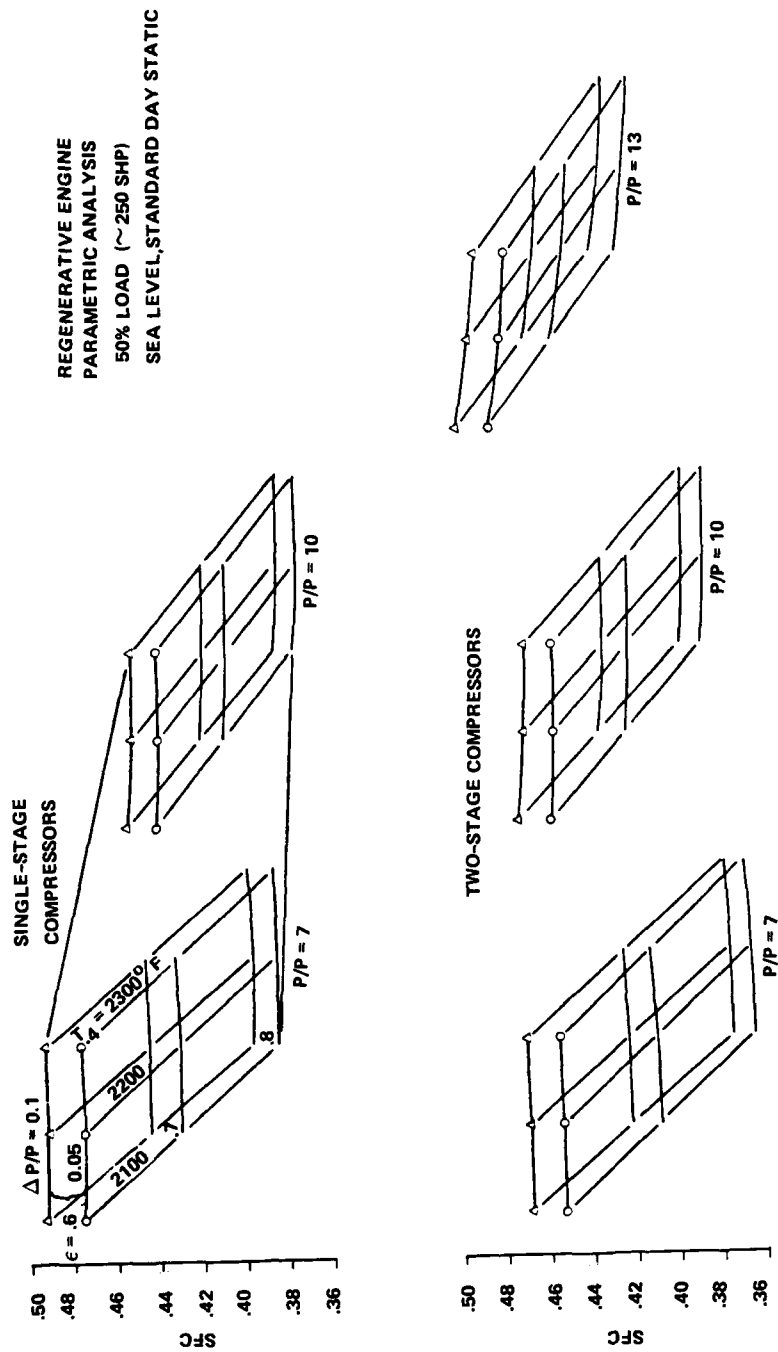


Figure 5. Regenerative Engine Specific Fuel Consumption.

the lowest overall SFCs. However, because of other cycle conditions, principally slight differences in flow rates and recuperator temperatures, the single-stage 10:1 cycle engines have slightly lower SFCs at the lower recuperator effectiveness. The SFCs shown in Figure 5 were used as a part of the FOM evaluation.

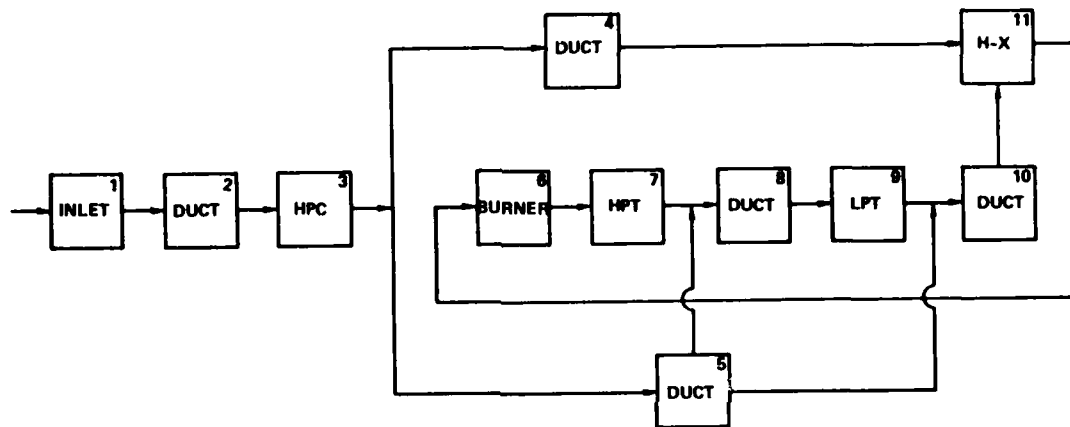
WEIGHT

The weights of the bare engine were calculated with a computer program developed by the Boeing Airplane Company² primarily for large engines and subsequently modified by AiResearch for small engines. The program, entitled WATE (Weight Analysis of Turbine Engines) accepts as inputs the geometric, thermodynamic, mechanical, and aerodynamic design data of the engine components. It provides individual component weights based on data given as inputs as well as data generated internally. The program has been calibrated with the known weight of the AiResearch production Model TFE731 turbofan engine and, prior to use in this study, was also calibrated against the component weights estimated for a similar turboshaft engine. The use of the WATE program allowed the rapid evaluation of a large number of similar components with the ability to account for relatively small changes in turbine temperatures and air-flow rates.

The flow path for the WATE program as structured for the regenerative engine analysis study is given in Figure 6. The program output provides weights for each of the numbered components and sums them for a total engine weight. While the program did calculate a heat-exchanger weight (H-X, Item 11), that weight was not used. Instead, the heat-exchanger weights were calculated separately, as discussed below.

The weights of the heat exchanger were calculated as a part of the heat-exchanger design analysis and, for the 90-engine parametric analysis, were based on the tube weight times an empirical "wrap-up" factor that accounts for manifolds, headers, and support structure. The wrap-up factor for the tubular configuration used in this study is based on a current production heat exchanger and provides reasonably accurate results. A summary of the weight model for the heat exchangers is given in Table 5.

²ONAT, E., and G.W. Klees, "A Method to Estimate Weight and Dimensions of Large and Small Gas Turbine Engines", Boeing Military Airplane Development; NASA-Lewis Research Center CR159431, January 1979.



INPUT: - CONFIGURATION DATA
 - THERMODYNAMIC DATA
 - MECHANICAL AND AERODYNAMIC DESIGN DATA

Figure 6. WATE - Weight Analysis of Turbine Engines.

TABLE 5. HEAT EXCHANGER WEIGHT MODEL

-
- Tube weight based on computer calculations for 0.007-inch wall thickness tubing
 - Total weight based on "wrap-up" factor for DC-10 precooler

Wrap-up Includes

Does Not Include

Egg-crate headers (2)

Hot gas ducting tubing for U-bends

Manifolds (2)

Sound suppression baffles

Tube support plates

Antifretting ferrules

Side plates

Bracing

Mounts

- Total weight = 1.85 x tube weight

The weights of the engine and the combined engine and heat-exchanger weights of the 90 engines are given in Figure 7. As shown, the engine weights are relatively constant within each family, with the lower turbine inlet temperature engines slightly heavier. However, the total weight with the heat exchanger is strongly influenced by the heat-exchanger effectiveness and somewhat less influenced by heat-exchanger pressure drop. As would be expected, a higher effectiveness requires a larger and heavier tube bundle, and similarly, a lower-pressure drop requires larger tubes, greater tube spacing, or some combination of these, which results in greater weight. These, and other factors that affect the heat-exchanger design are discussed in subsequent sections.

COST

Costs are a sensitive part of any study; however, in order to provide a reasonably valid evaluation of the large number of engines considered in this study, it was considered necessary to address costs on an equal basis with weight. Accordingly, it was initially planned to use a form of the Materials Index Factor (MIF) method to estimate component costs for each of the 90 engines rather than any of the less sophisticated methods that employ basic performance and cycle parameters in relatively simple equations. The MIF method has been successfully applied to engines similar to those examined in this study; however, it soon became apparent that the detailed manufacturing, weight, and materials indices (required for each engine component) exceeded the scope and resources of this study. Accordingly, a less complex approach was taken in which the cost of each component was estimated based on the known cost of a counterpart component in a similar engine. The procedure used was as follows:

- (1) Determine the component weight from the WATE program
- (2) Determine the ratio of cost to weight of the known counterpart component in a similar engine. (The weight of the counterpart component was adjusted to account for any material or configuration differences. This could involve a simple change from titanium to steel, or a more complex change involving numbers of turbo-machinery blades and their aspect ratios.)
- (3) Determine an escalation cost index that accounts for materials and labor cost differences due to the time differential between the known component and the study engine component.

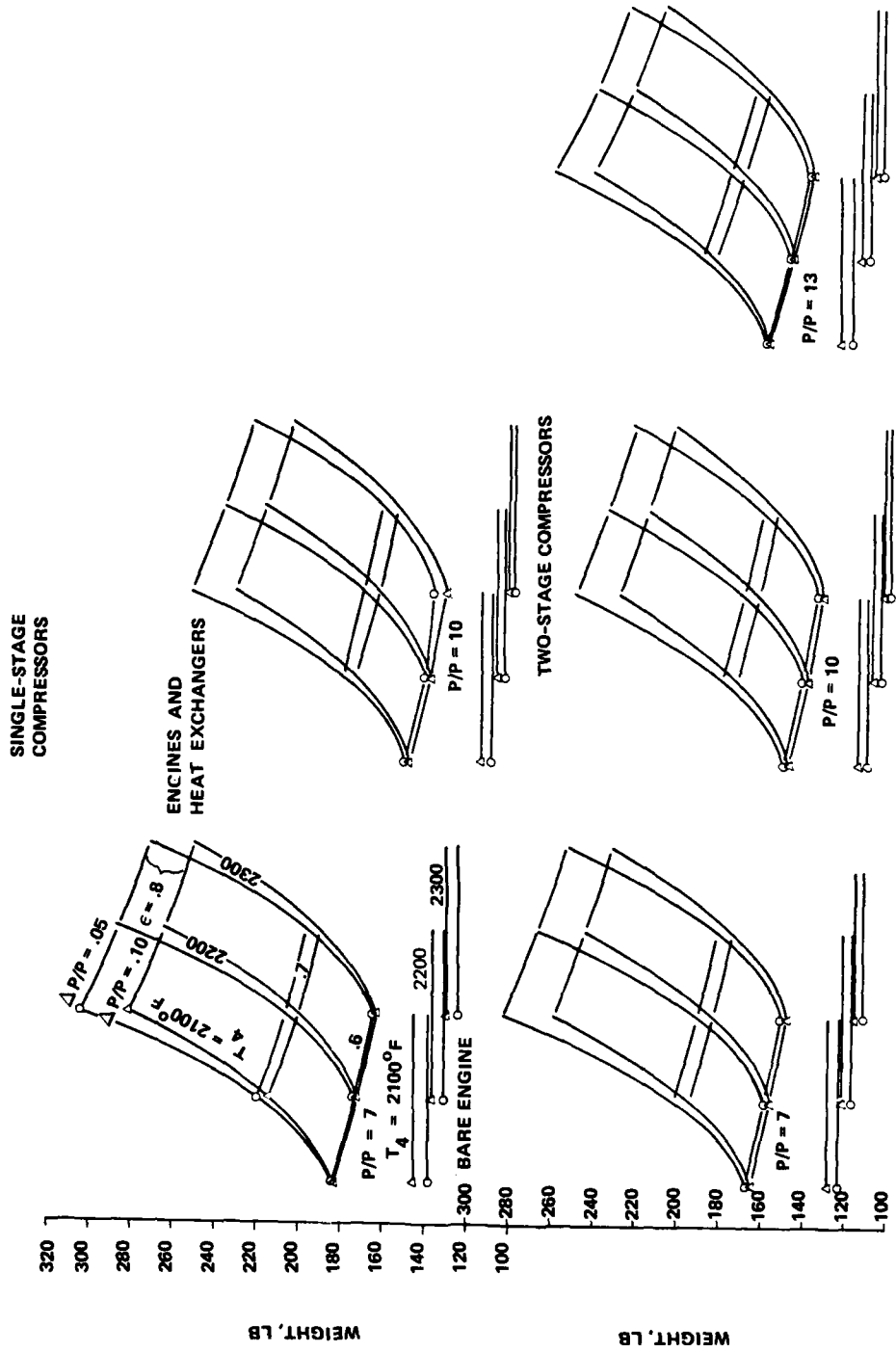


Figure 7. Regenerative Engine Parametric Analysis (Engine Weights).

The individual component weights were calculated by combining the three factors defined above as follows:

$$\begin{array}{rcccl}
 \text{WATE} & & \text{COUNTERPART} & & \\
 \text{COMPONENT} & & \text{COMPONENT} & & \\
 \text{WEIGHT} & \times & \text{COST} & & \\
 & & \text{-----} & & \\
 & & \text{ADJUSTED} & \times & \text{ESCALATION} & = & \text{1980} \\
 & & \text{COUNTERPART} & & \text{COST} & & \text{COMPONENT} \\
 & & \text{COMPONENT} & & \text{INDEX} & & \text{COST} \\
 & & \text{WEIGHT} & & & & \\
 \end{array}$$

The component costs were then summed to obtain a total engine (less heat exchanger) cost; the results are shown in Figure 8.

It should be noted that the costs shown in Figure 8 are a parametric summation of the acquisition costs estimated to manufacture the parts associated with each engine in constant 1980 dollars. These rough, order-of-magnitude costs are considered valid for relative parametric evaluations.

Heat-exchanger costs were estimated with an equation that related the number of tubes, tube length, tube weight, and appropriate material indices. The equation is described in the heat-exchanger analysis section. The heat-exchanger costs, shown in Figure 9, are also based on mature units with a production rate of 300 per year. As indicated in Figure 9, two materials were assumed for the heat-exchanger designs; Type 347 stainless steel was assumed for all units with hot-side inlet temperatures less than 1340°F; Inconel 625, a more expensive material, was assumed for all units with hot-side inlet temperatures equal to or greater than 1340°F. The discontinuities in the plots in Figure 9 are the points at which material changes occur.

The total costs for the engines with heat exchangers are given in Figure 10. Also shown are the points at which heat-exchanger material changes occur.

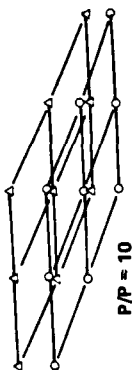
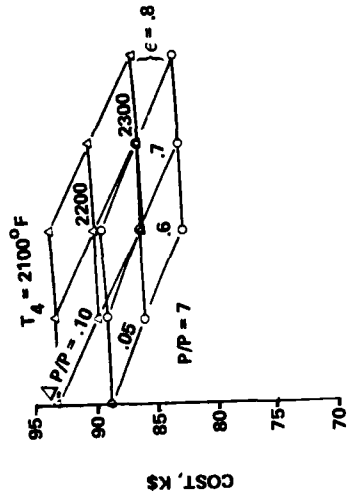
FIGURE OF MERIT (FOM)

The final evaluation of the 90-engine cycles was performed with an FOM equation that was developed with life-cycle-cost techniques. The form of the equation was:

$$\text{FOM} = K_1 \frac{\text{SFC}}{\text{SFC}_{\text{AV}}} + K_2 \frac{\text{WT}}{\text{WT}_{\text{AV}}} + K_3 \frac{\text{COST}}{\text{COST}_{\text{AV}}}$$

in which low values of FOM are superior to high values. The three K factors were derived from life-cycle-cost analyses. These analyses are based on a simplified life-cycle cost (LCC) model developed by AiResearch for a military helicopter mission and

SINGLE-STAGE COMPRESSORS



TWO-STAGE COMPRESSORS

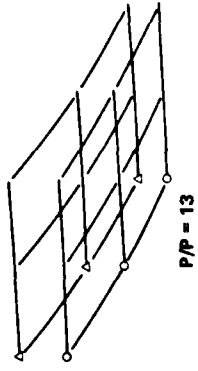
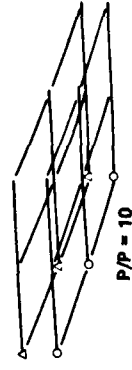
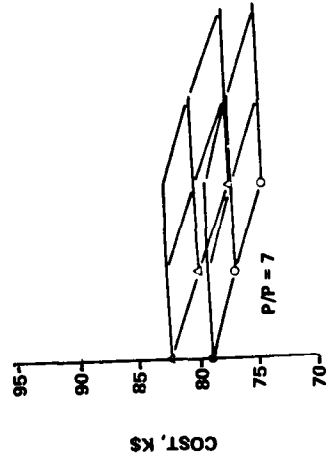


Figure 8. Regenerative Engine Parametric Analysis (Bare Engine Cost).

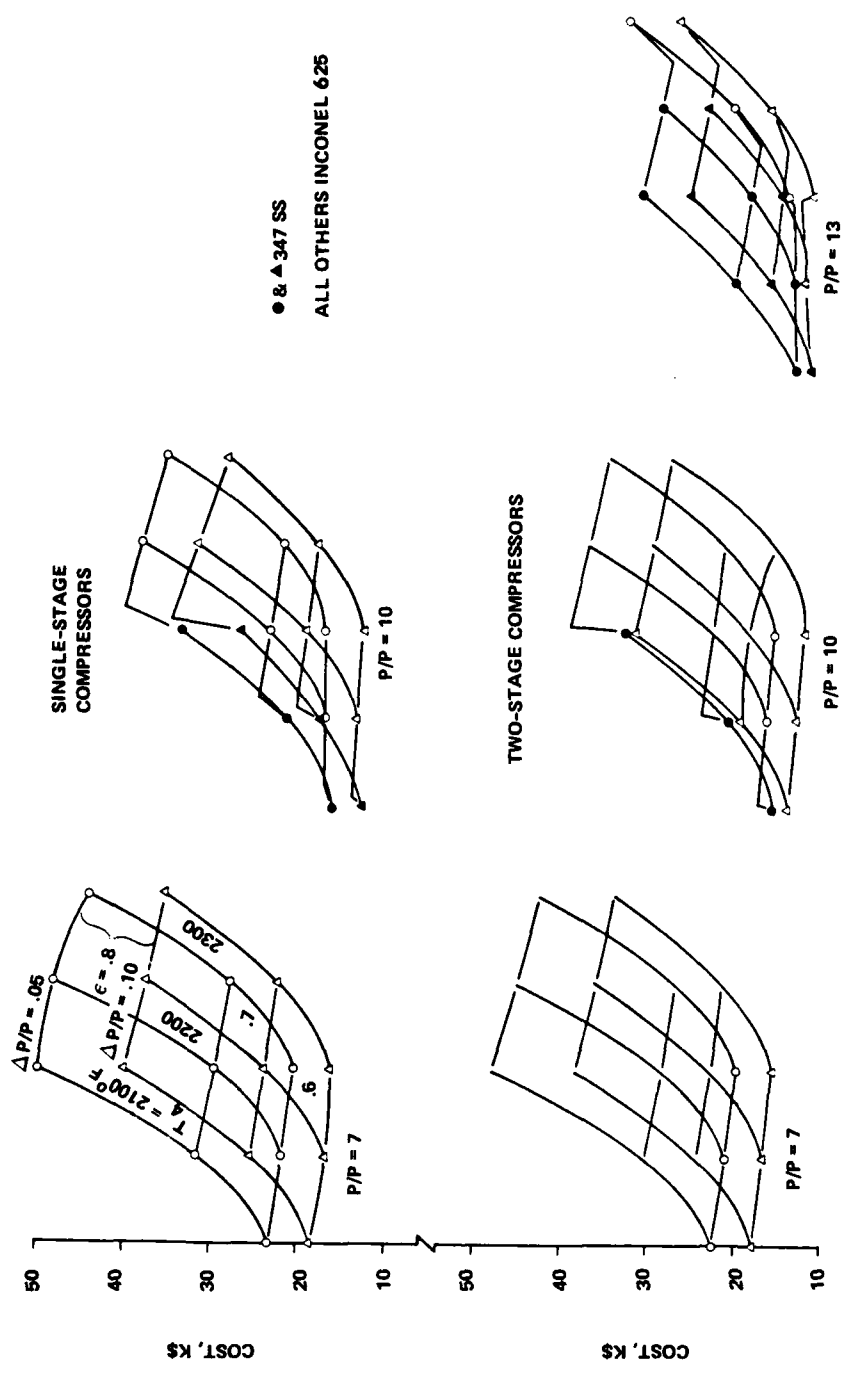


Figure 9. Regenerative Engine Parametric Analysis (Heat Exchange Costs).

scenario that incorporates interactive resizing of the airframe and engine for a constant mission and includes airframe effects in the LCC sensitivities. These analyses reflected the relative importance of the SFC, weight, and cost ratios in the overall analyses. The K factors are structured so that their sum is unity; thus the total of the three FOM terms did not vary greatly from unity. The values in the denominator of each term are the average of the 90 values calculated. For consistency, these average values were used in all subsequent FOM analyses, including those for the more promising cycles examined later in the study.

Two FOM equations were used for the parametric evaluation:

$$\text{FOM} = 0.55 \frac{\text{SFC}}{\text{SFC}_{\text{AV}}} + 0.14 \frac{\text{WT}}{\text{WT}_{\text{AV}}} + 0.31 \frac{\text{COST}}{\text{COST}_{\text{AV}}} \quad (1)$$

$$\text{FOM} = 0.56 \frac{\text{SFC}}{\text{SFC}_{\text{AV}}} + 0.19 \frac{\text{WT}}{\text{WT}_{\text{AV}}} + 0.25 \frac{\text{COST}}{\text{COST}_{\text{AV}}} \quad (2)$$

Equation (1) was based on a military attack mission with a duration of 2.5 hours and on a fuel cost of \$0.60 per gallon. Equation (2) was based on a cruise mission with a longer duration of 3.4 hours and the same fuel cost. Additional equations, based on somewhat different missions and higher fuel costs, were developed later in the study; however, they did not influence the basic results of the parametric evaluation.

Equation (1) was used for the initial FOM evaluation of the 90-engine cycles. A computer program was used to perform the calculation and to rank the 10 engines with the lowest FOMs. The printout from this program is shown in Table 6, and Figure 11 shows carpet plots of the 90 engines' FOMs for Equation (1). It is clear from Table 6 and Figure 11 that the single-stage 10:1 compressor engines are superior, with Engine 34 having the lowest FOM. This conclusion might have been inferred from the SFC, weight, and cost plots of Figures 5, 7 and 10. However, the influence coefficients in the FOM equation can have a normalizing effect that is not always predictable.

Equation (2) was used to evaluate the engines for the longer mission. The 10 engines with the lowest FOM were the same as for Equation (1), with the ranking identical except that Engines 26 and 28 had exchanged positions. Engine 34, again, had the lowest FOM, followed by Engines 32, 33, and 31, in that order.

In order to check the validity of these FOM equations, an inquiry was made of Bell Helicopter Textron. Bell responded that in their opinion, the equations were satisfactory and that the three influence coefficients were of the right magnitude.

TABLE 6. FIGURE OF MERIT ANALYSIS

ENG ***	SFC **	WEIGHT *****	REL COST *****	FDM **	ENG **	SFC **	WEIGHT *****	RFL COST *****	FDM **	ENG **	SFC **	WEIGHT *****	REL COST *****	FDM **	ENG **	SFC **	WEIGHT *****	FDM **	REL COST *****	FDM **
1	.47517	184.1	1.060	1.070	31	.43655	139.5	.823	.916	61	.45511	143.9	.832	.916	61	.45511	143.9	.916	.832	.945
2	.49246	183.2	1.027	1.082	32	.44877	133.6	.776	.912	62	.46907	141.3	.804	.912	62	.46907	141.3	.912	.804	.952
3	.42983	219.8	1.179	1.075	33	.40461	163.4	.891	.909	63	.42051	171.8	.923	.909	63	.42051	171.8	.909	.923	.949
4	.44442	213.4	1.126	1.073	34	.41521	155.9	.853	.909	64	.43234	164.6	.884	.909	64	.43234	164.6	.909	.884	.947
5	.38373	304.9	1.447	1.160	35	.37221	225.6	1.089	.978	65	.38519	236.8	1.129	.978	65	.38519	236.8	.978	1.129	1.015
6	.39558	281.9	1.338	1.125	36	.38116	206.4	1.004	.949	66	.39506	217.6	1.042	.949	66	.39506	217.6	.949	1.042	.987
7	.47446	173.8	1.014	1.048	37	.45311	167.2	.965	1.001	67	.45479	137.1	.799	1.001	67	.45479	137.1	1.001	.799	.930
8	.49130	172.5	.973	1.056	38	.46845	165.2	.927	1.007	68	.46820	134.4	.769	1.007	68	.46820	134.4	1.007	.769	.936
9	.42951	207.3	1.127	1.050	39	.40921	201.4	1.080	1.005	69	.42033	163.4	.882	1.005	69	.42033	163.4	1.005	.882	.930
10	.44377	200.7	1.075	1.047	40	.42207	194.2	1.023	.998	70	.43214	156.3	.816	.998	70	.43214	156.3	.998	.816	.970
11	.38380	286.8	1.393	1.131	41	.36458	282.8	1.336	1.086	71	.38536	224.3	1.076	1.086	71	.38536	224.3	1.086	1.076	.989
12	.39561	264.6	1.272	1.092	42	.37491	259.5	1.224	1.047	72	.39532	205.5	.991	1.047	72	.39532	205.5	1.047	.991	.962
13	.47510	165.5	.971	1.029	43	.45369	158.5	.930	.984	73	.48195	163.9	.884	.984	73	.48195	163.9	.984	.884	1.010
14	.49164	163.8	.937	1.039	44	.46874	156.3	.892	.990	74	.49749	162.9	.890	.990	74	.49749	162.9	.990	.890	.970
15	.43064	197.0	1.075	1.028	45	.41011	190.7	1.037	.985	75	.45263	194.2	.983	.985	75	.45263	194.2	.985	.983	1.025
16	.44468	190.4	1.024	1.025	46	.42277	183.4	.982	.979	76	.46646	188.2	.957	.979	76	.46646	188.2	.979	.957	1.030
17	.38540	271.7	1.310	1.096	47	.36579	267.0	1.277	1.058	77	.42297	264.6	1.141	1.058	77	.42297	264.6	1.058	1.141	.989
18	.39690	250.5	1.210	1.065	48	.37599	244.6	1.171	1.022	78	.43506	246.3	1.094	1.022	78	.43506	246.3	1.022	1.094	1.075
19	.43863	152.0	.855	.937	49	.45541	151.5	.894	.970	79	.47638	152.6	.847	.970	79	.47638	152.6	.970	.847	.983
20	.45153	149.5	.831	.944	50	.47027	149.1	.857	.976	80	.49119	150.8	.855	.976	80	.49119	150.8	.976	.855	1.003
21	.40651	181.8	.932	.941	51	.41253	181.8	.996	.969	81	.44720	180.4	.921	.969	81	.44720	180.4	.969	.921	.989
22	.41741	175.2	.901	.941	52	.42478	174.6	.941	.962	82	.46038	173.9	.892	.962	82	.46038	173.9	.962	.892	.992
23	.37374	254.4	1.109	1.007	53	.36869	253.8	1.222	1.035	83	.41766	245.2	1.067	1.035	83	.41766	245.2	1.035	1.067	1.043
24	.38282	233.6	1.034	.980	54	.37848	232.3	1.119	1.000	84	.42919	227.4	1.017	1.000	84	.42919	227.4	1.000	1.017	1.030
25	.43689	143.3	.843	.925	55	.45743	152.3	.844	.958	85	.47290	144.0	.829	.958	85	.47290	144.0	.958	.829	.977
26	.44915	140.6	.813	.929	56	.47186	150.0	.843	.974	86	.49719	141.8	.806	.974	86	.49719	141.8	.974	.806	.977
27	.40469	172.0	.935	.933	57	.42235	182.5	.919	.958	87	.44394	169.8	.916	.958	87	.44394	169.8	.958	.916	.976
28	.41550	164.4	.896	.929	58	.43485	175.2	.921	.970	88	.45667	163.3	.877	.970	88	.45667	163.3	.970	.877	.975
29	.37204	238.5	1.146	1.004	59	.38679	252.2	1.092	1.016	89	.41460	230.2	1.094	1.016	89	.41460	230.2	1.016	1.094	1.037
30	.38113	218.6	1.076	.980	60	.39670	231.8	1.098	1.016	90	.42575	212.8	1.029	1.016	90	.42575	212.8	1.016	1.029	1.019

AVG SFC = .42906
 AVG WEIGHT = 193.9
 AVG REL COST = 1.000

RANK ***	ENG **	FDM **
1	34	.909
2	32	.912
3	33	.913
4	31	.916
5	70	.920
6	25	.925
7	28	.929
8	26	.929
9	67	.930
10	69	.930

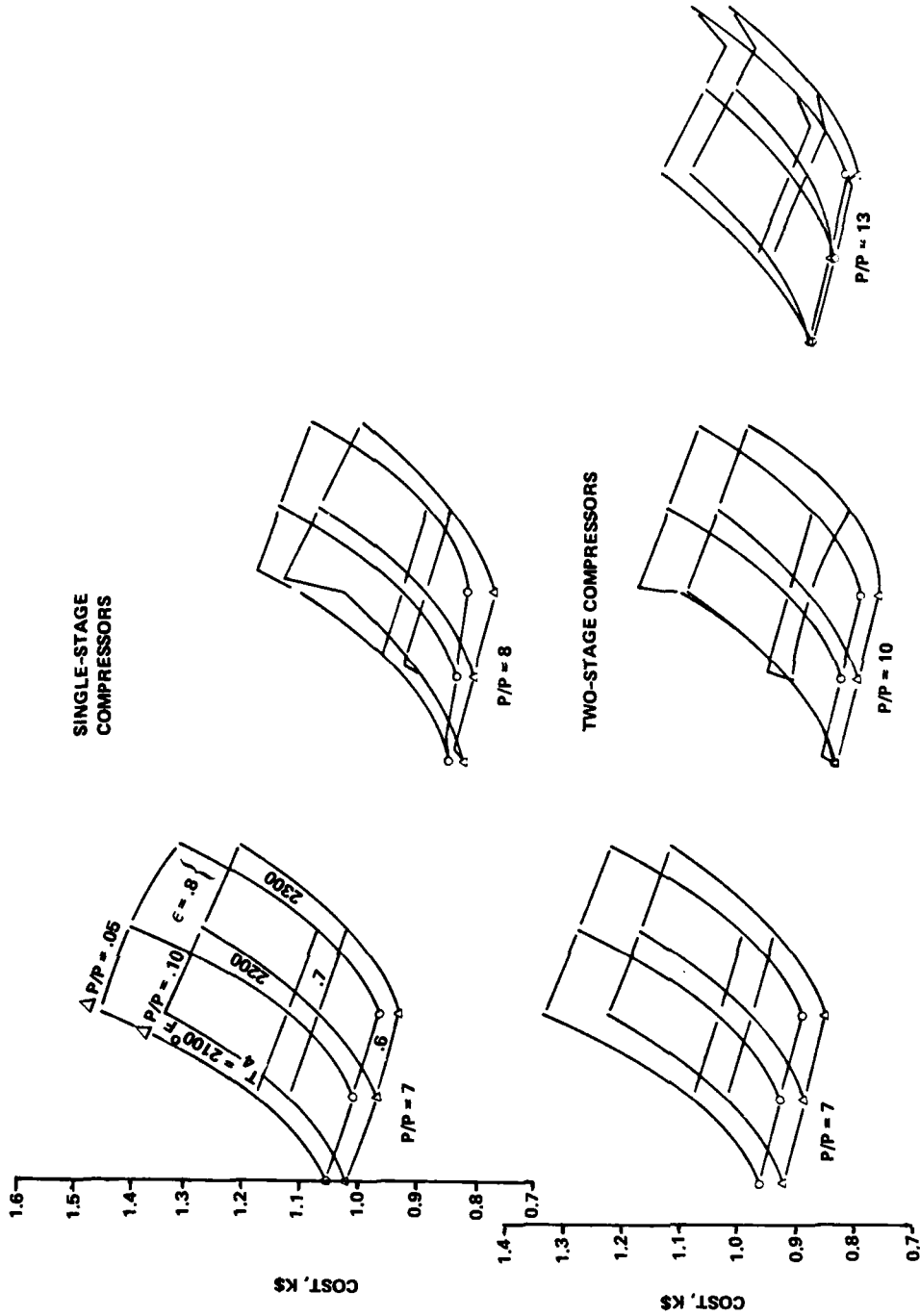
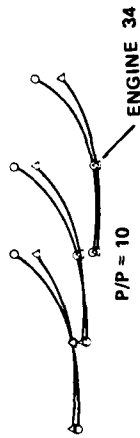
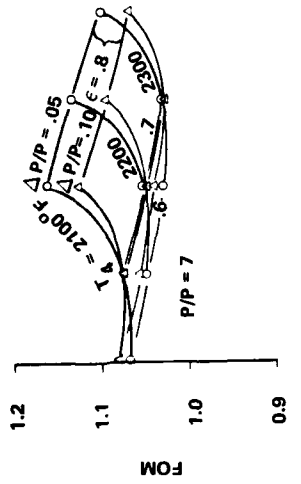


Figure 10. Regenerative Engine Parametric Analysis (Total Engine Cost).

SINGLE-STAGE COMPRESSORS



TWO-STAGE COMPRESSORS

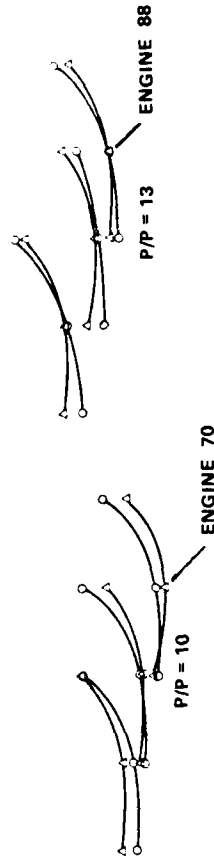
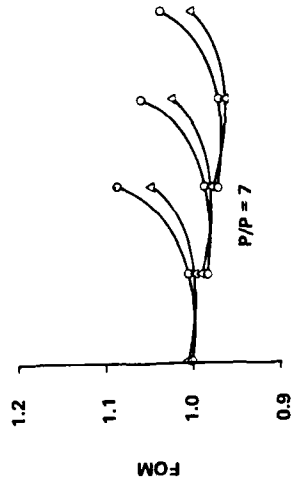


Figure 11. Regenerative Engine Parametric Analysis (Figures of Merit).

With the confirmation of the FOM equations from Bell, Engine 34, with a single-stage 10:1 compressor, was selected for more detailed analysis and as a leading candidate for the most promising cycle preliminary design. In addition, Engine 70 with a two-stage 10:1 compressor and Engine 88 with a two-stage 13:1 compressor were selected for more detailed analysis in order to evaluate configurations from different engine families. These choices were supported by the FOM values for these engines and also by their relatively high full-load specific powers, shown in Figure 12.

PROMISING CYCLES

The cycle conditions originally calculated by the design-point program for Engines 34, 70, and 88 are given in Table 7. Subsequently, off-design computer models were established for these engines, which included compressor and turbine performance maps, a schedule for variable power turbine efficiency as a function of power turbine-nozzle area, heat-exchanger effectiveness as a function of inlet-airflow rate, and heat-exchanger pressure loss ($\Delta P/P$) splits between the hot and cold sides as functions of inlet corrected-flow rates. The full- and part-load performance of these engines was defined with these models, and the results showed that the FOM for Engine 88 was considerably higher than anticipated due to poor part-load efficiency of the compressor. This compressor was therefore abandoned in favor of another design that incorporated inlet guide vanes to improve the part-load efficiency. Full- and part-load performance was then calculated for this engine, designated as Number 88A, with the off-design computer model, and the results are given in Table 8 with the results for Engines 34 and 70. A comparison of the detailed cycle values at the part-load conditions for the design-point program (Table 7) and the off-design program (Table 8) confirmed that the part-load compressor match points chosen for the initial parametric study with the 770 design-point program were satisfactory. The higher FOM values shown in Table 8 are due to the increased SFC, which is the result of the off-design program match at lower efficiencies for the high- and low-pressure turbines. The differences between the design-point and off-design-point program results are illustrated in Figures 13, 14, and 15, which show the SFC and individual component conditions for Engines 34, 70, and 88A. These figures show the off-design performance plotted versus shaft horsepower from full load to 50-percent load, as calculated by the off-design program and the 50-percent-load conditions as calculated by the design-point program.

The operating lines for each of these engines on their respective compressor maps are shown in Figure 16. As may readily be inferred from this figure and as discussed previously, the performance of these engines is extremely sensitive to the orientation of the operating line with respect to the compressor

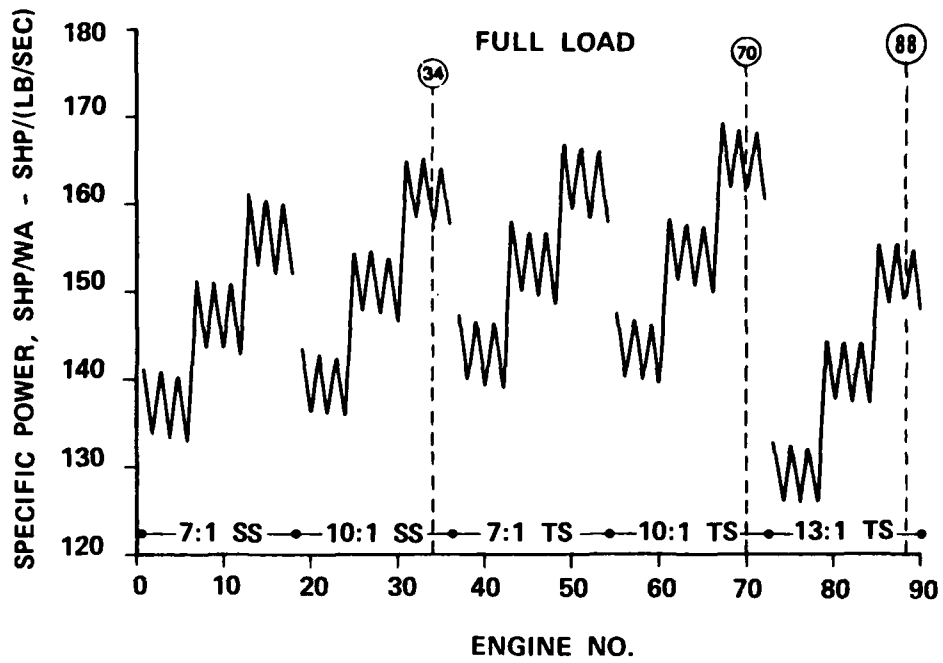


Figure 12. Specific Power for 90 Engines.

TABLE 7. PROMISING CYCLES DESIGN-POINT PROGRAM CONDITIONS

Engine Number	34	70	88
Compressor Stages	1	2	2
Turbine-Inlet Temperature, °F	2300	2300	2300
Output Shaft Power, shp	500	266	500
Compressor Pressure Ratio	10:1	5.7:1	10:1
Heat Exchanger Effectiveness	0.70	0.76	0.70
Heat Exchanger Total $\Delta P/P$	0.10	0.065	0.10
Specific Power, shp/lb/sec	157.7	--	161.4
Specific Fuel Consumption, lb/hr-hp	0.425	0.415	0.417
Figure of Merit	--	0.909	--
		0.920	--
		0.454	0.457
		0.70	0.76
		13:1	6.6:1
		500	230
		5.4:1	
		0.065	0.10
		148.3	--

TABLE 8. PROMISING CYCLES OFF-DESIGN PROGRAM CONDITIONS

Engine Number	34	70	88A
Compressor Stages	1	2	2
Turbine-Inlet Temperature, °F	2300	2300	2300
Output Shaft Power, shp	500	250	500
Compressor Pressure Ratio	10:1	5.5:1	10:1
Heat Exchanger Effectiveness	0.70	0.73	0.70
Heat Exchanger Total $\Delta P/P$	0.10	0.057	0.10
Specific Power, shp/lb/sec	157.5	--	161.3
Specific Fuel Consumption, lb/hr-hp	0.425	0.437	0.417
Figure of Merit	--	0.937	--

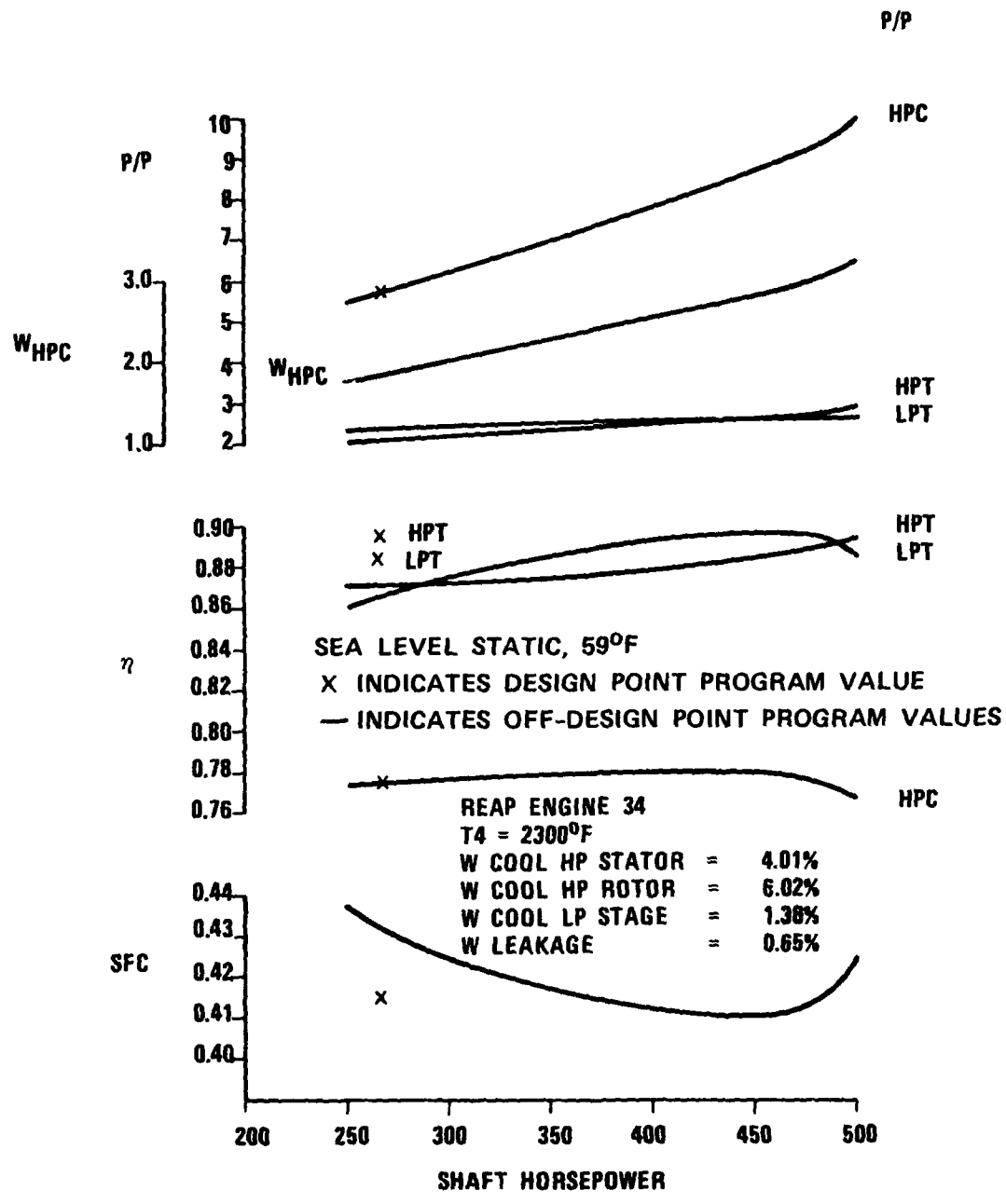


Figure 13. Engine 34 Performance.

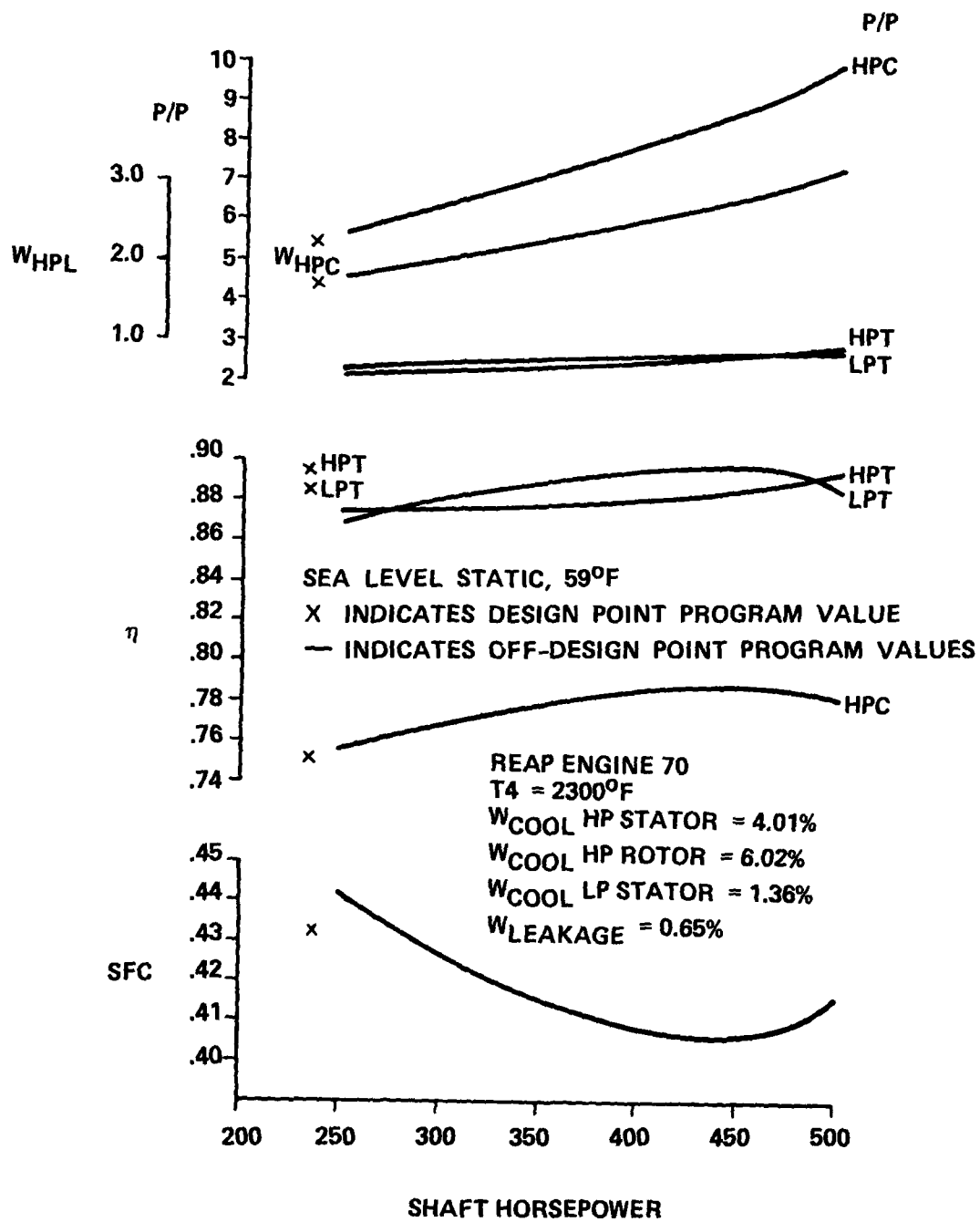


Figure 14. Engine 70 Performance.

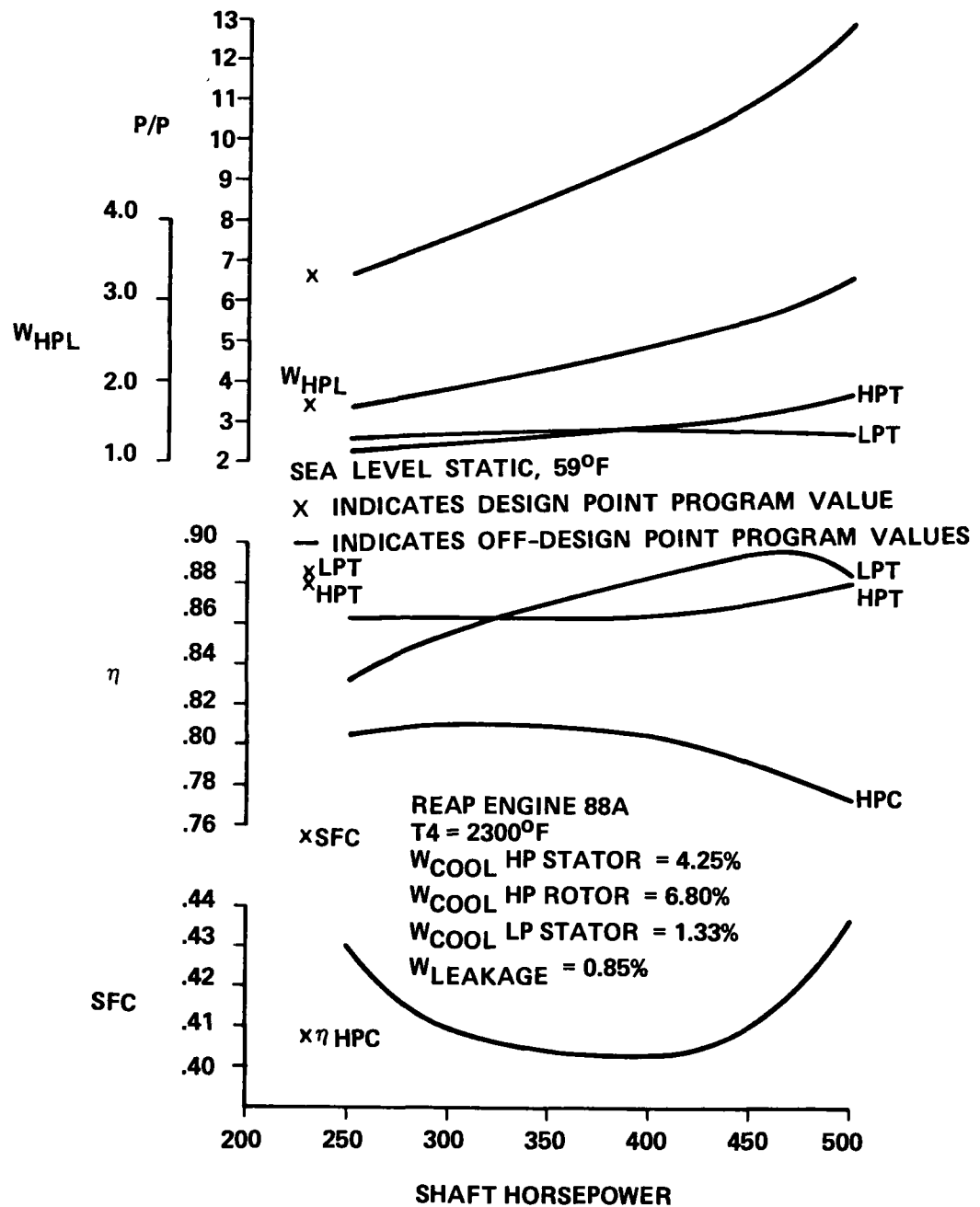
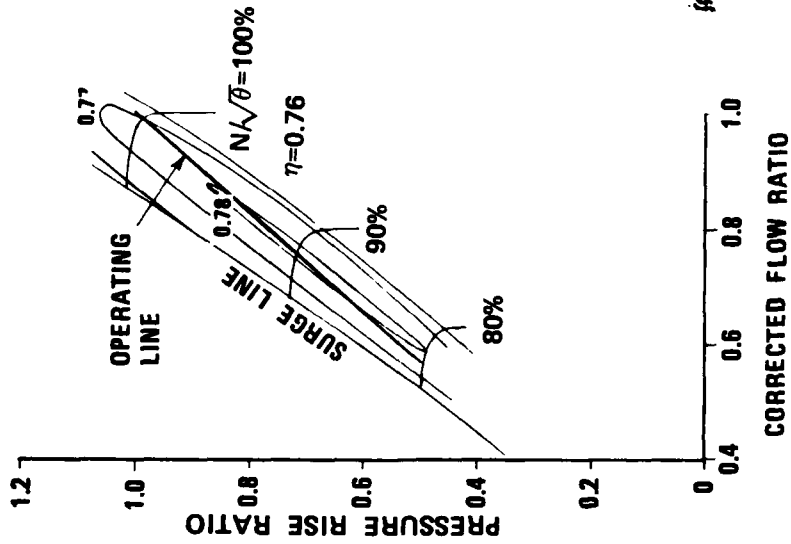
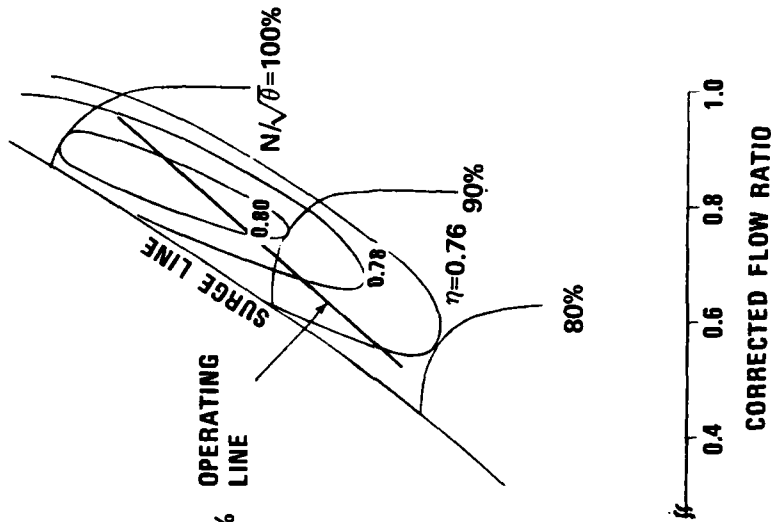


Figure 15. Engine 88A Performance.

ENGINE 34



ENGINE 70



ENGINE 88A

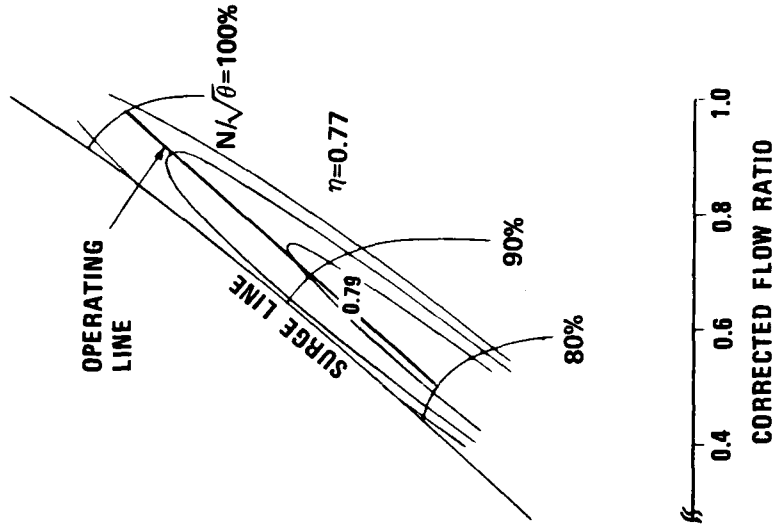


Figure 16. Selected Cycle.

surge line and the efficiency contours. For example, the operating line for Engines 34 and 88A are aligned so that they take maximum advantage of the peak efficiencies over a broad speed range, while the line for Engine 70 passes through the peak-efficiency island into an area of lower efficiency at the part-power, lower-speed regime. It may be noted that guide vanes (IGVs) were required for Engine 88A in order to control the locations of the engine operating line with respect to peak efficiencies and to the surge line. IGVs were not considered necessary for Engine 34 since the location of its operating line was satisfactory.

Cross-section drawings of Engines 34, 70, and 88A were prepared (along with drawings of the alternative configurations discussed in subsequent paragraphs) in order to facilitate estimates of weight and cost. The drawings, shown in Figures 17, 18, and 19, show the arrangement of the major components. Note that engine 34 is shown in the top half of Figure 17, while the bottom half shows Engine 34A, which incorporates the bypass recuperator discussed in the following section. Detailed weight and cost estimates were prepared from these drawings, and the results are summarized in Table 9 and compared with the results of the previous analyses.

The results show that the cost of Engine 34A is higher than 70 and 88A, which is surprising as 34A has less turbomachinery. Actually, the gas turbine portion of 34A is less expensive, but the recuperator cost is higher. The offsetting cost of the recuperator is most significant in the case of Engine 88A and is due to the higher cycle pressure ratio and its effect on heat exchanger core size.

The FOMs shown in Table 9 are based on Equation (1), defined earlier, and use the same average values of SFC, weight, and cost as were used for the 90-engine parametric study. The use of these average values was arbitrary; any similar values could have been used. The objective was simply to obtain FOM values near unity. Of more significance are the relative FOM values since they indicate the ranking within each group, and for the final group which includes the refinements of the off-design computer model and the detailed weight and cost analyses, it is seen that the relative FOM values are quite close. Although Engine 88A is the superior engine based on the FOM analysis, Engine 34 was chosen for preliminary design and evaluation of alternative configurations. Engine 88A was introduced late in the study (after engines 34, 70, and 88 were selected for further analyses) and was not developed to the degree that Engine 34 was.

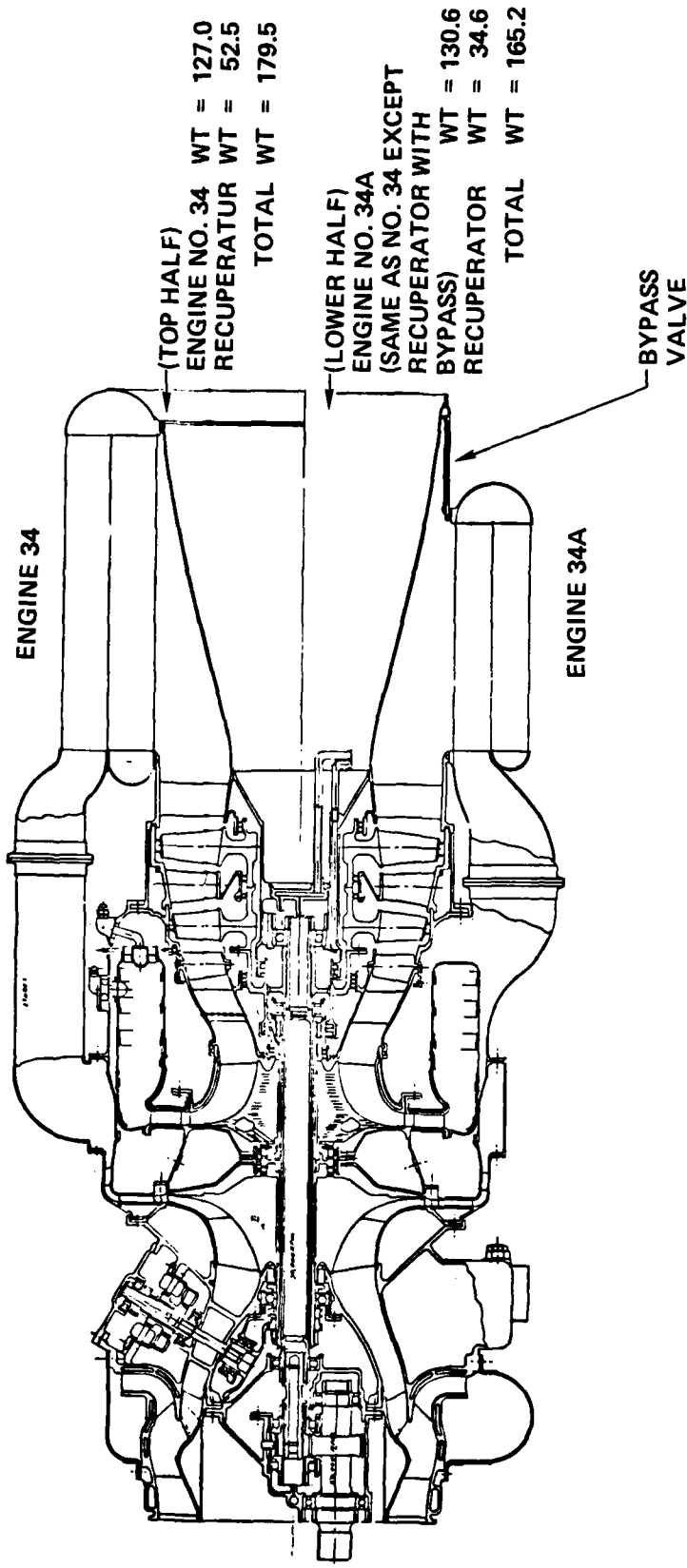
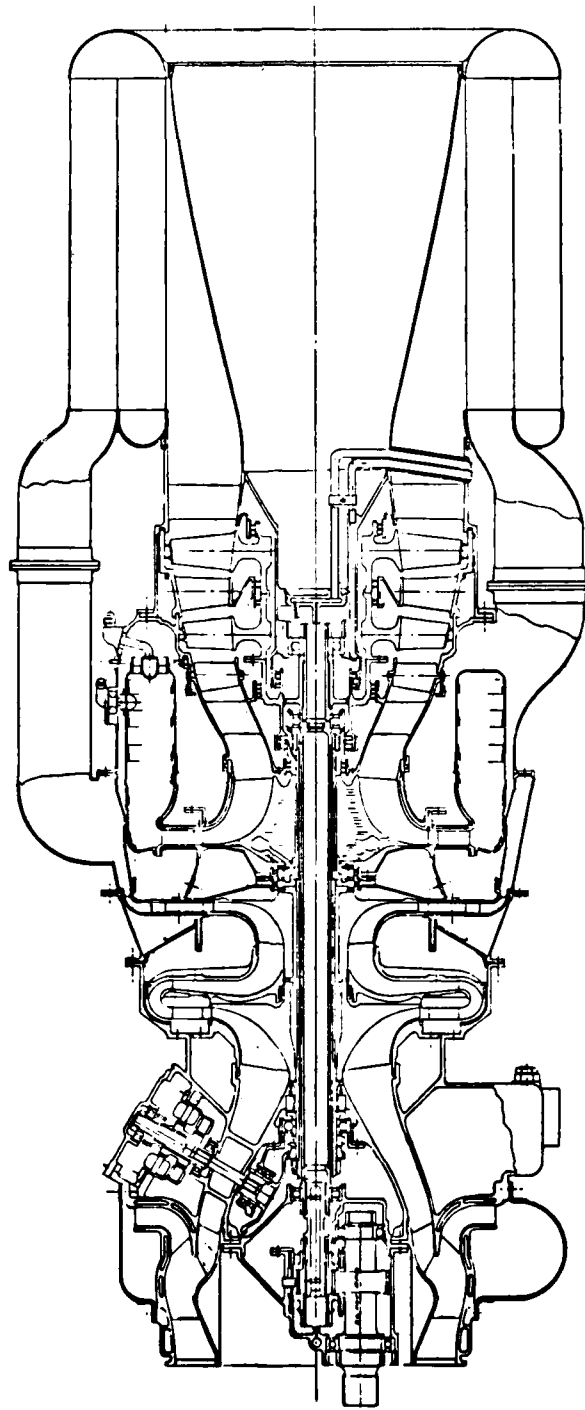


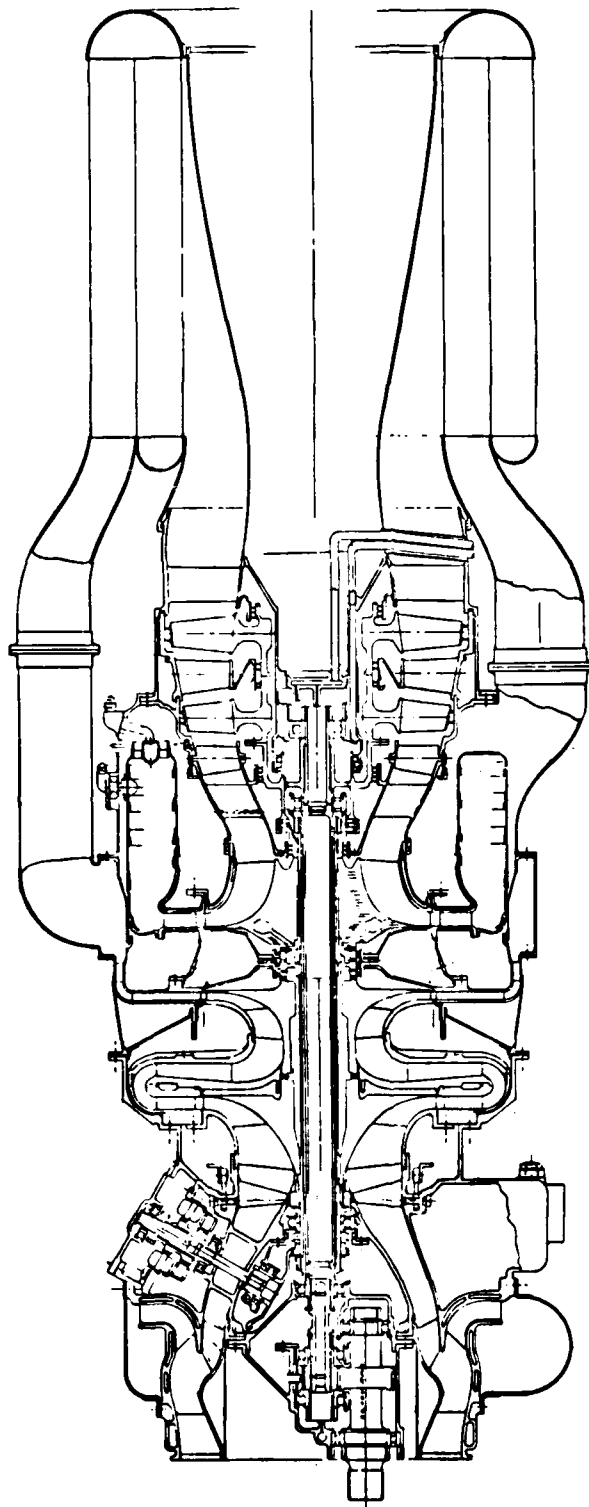
Figure 17. Engine 34 and 34A Cross-Section Drawing.

4
F



ENGINE NO. 70 WT = 136.0 LB
RECUPERATOR WT = 51.3 LB
TOTAL WT = 187.3 LB

Figure 18. Engine 70 Cross-Section Drawing.



ENGINE NO. 88A WT = 139.7 LB
RECUPERATOR WT = 49.6 LB
TOTAL WT = 189.3 LB

Figure 19. Engine 88A Cross-Section Drawing.

TABLE 9. REGENERATIVE ENGINE ANALYSIS
PARAMETRIC STUDY SUMMARY

STUDY PHASE	ENGINE		
	34	70	88
90-Engine Design-Point Parametric Analysis			
SFC (LB/HR-HP)	0.415	0.432	0.457
Weight (LB)	155.9	156.3	163.3
Cost (K\$)	90385	87728	94467
FOM	0.907	0.922	0.978
Relative FOM	1.000	1.016	1.078
Off-Design Program Study			(88A)
SFC (LB/HR-HP)	0.437	0.443	0.421
Weight (LB)	155.9	156.3	163.3
Cost (K\$)	90385	87728	94467
FOM	0.935	0.936	0.932
Relative FOM	1.000	1.001	0.996
Cross-Section Drawing Analysis			(88A)
SFC (LB/HR-HP)	0.437	0.443	0.421
Weight (LB)	179.5	187.3	189.3
Cost (K\$)	95004	96786	96511
FOM	0.966	0.984	0.957
Relative FOM	1.000	1.019	0.991

CONFIGURATION VARIANTS

Several variations on the basic-engine configuration were examined in order to determine their potential advantages or disadvantages. These included:

- Fixed-geometry power turbine
- Low-speed power turbine
- Bypass heat exchanger
- Plate-fin heat exchanger

The first three items are discussed in the following paragraphs. A discussion of the plate-fin heat exchanger is included in the detailed discussion of heat exchangers in a subsequent section.

Fixed Geometry Power Turbine

Since it has been generally established that variable-geometry power turbine engines will exhibit an advantageous specific fuel consumption at part-power conditions, the six engines defined in Table 10 were selected for examination with fixed-geometry power turbines to determine the magnitude of the variable power turbine advantage for the regenerative engine cycles under study. The match conditions for the fixed-geometry (FG) power turbine engines were essentially the same as those for the variable-geometry (VG) engines; however, because of leakage and other secondary effects, the FG power turbine efficiency was assumed to be slightly higher than that of the VG power turbines. The full-load power turbine efficiency for the FG engines was set at 90 percent. The part-load FG power turbine efficiencies were developed from another engine study. Principal engine parameters are given in Table 10 for the full load condition.

As expected, the part-load specific fuel consumption of the FG power turbine engines was significantly higher than that of the VG power turbine engines, as illustrated in Figure 20.

A further comparison of the FG power turbine engines was made with the FOM equation used for the 90-engine parametric analysis. Weights and costs were estimated in the same manner as for the 90 VG power turbine engines, and the same military attack mission FOM equation was applied. The results are given in Table 11 and compared with similar values for the VG power turbine versions of the same engines. These results show a clear advantage for the VG engines. Even though the VG engines weigh more than the FG engines, and the costs of the VG engines are higher, the SFC advantage dominates in the FOM equation.

TABLE 10. FIXED-GEOMETRY POWER TURBINE ENGINES

Engine Number	5	17	35	41	53	71
Compressor Stages	One	One	One	Two	Two	Two
Compressor Pressure Ratio	7:1	7:1	10:1	7:1	7:1	10:1
Turbine Inlet Temperature, °F	2100	2300	2300	2100	2300	2300
Heat Exchanger Effectiveness	0.8	0.8	0.8	0.8	0.8	0.8
Heat Exchanger Pressure Loss, $\Delta P/P$	0.05	0.05	0.05	0.05	0.05	0.05
HP Compressor Airflow, Lb/Sec	3.47	3.03	2.93	3.33	2.92	2.87
HP Turbine Pressure Ratio	2.38	2.25	2.92	2.30	2.18	2.86
LP Turbine Pressure Ratio	2.45	2.59	2.85	2.54	2.67	2.91
HP Compressor Efficiency	0.770	0.770	0.768	0.800	0.800	0.782
HP Turbine Efficiency	0.910	0.910	0.895	0.910	0.910	0.895
LP Turbine Efficiency	0.900	0.900	0.900	0.900	0.900	0.900
Output Shaft Horsepower	500	500	500	500	500	500
Specific Fuel Consumption, LB/HR-HP	0.388	0.378	0.384	0.374	0.366	0.377

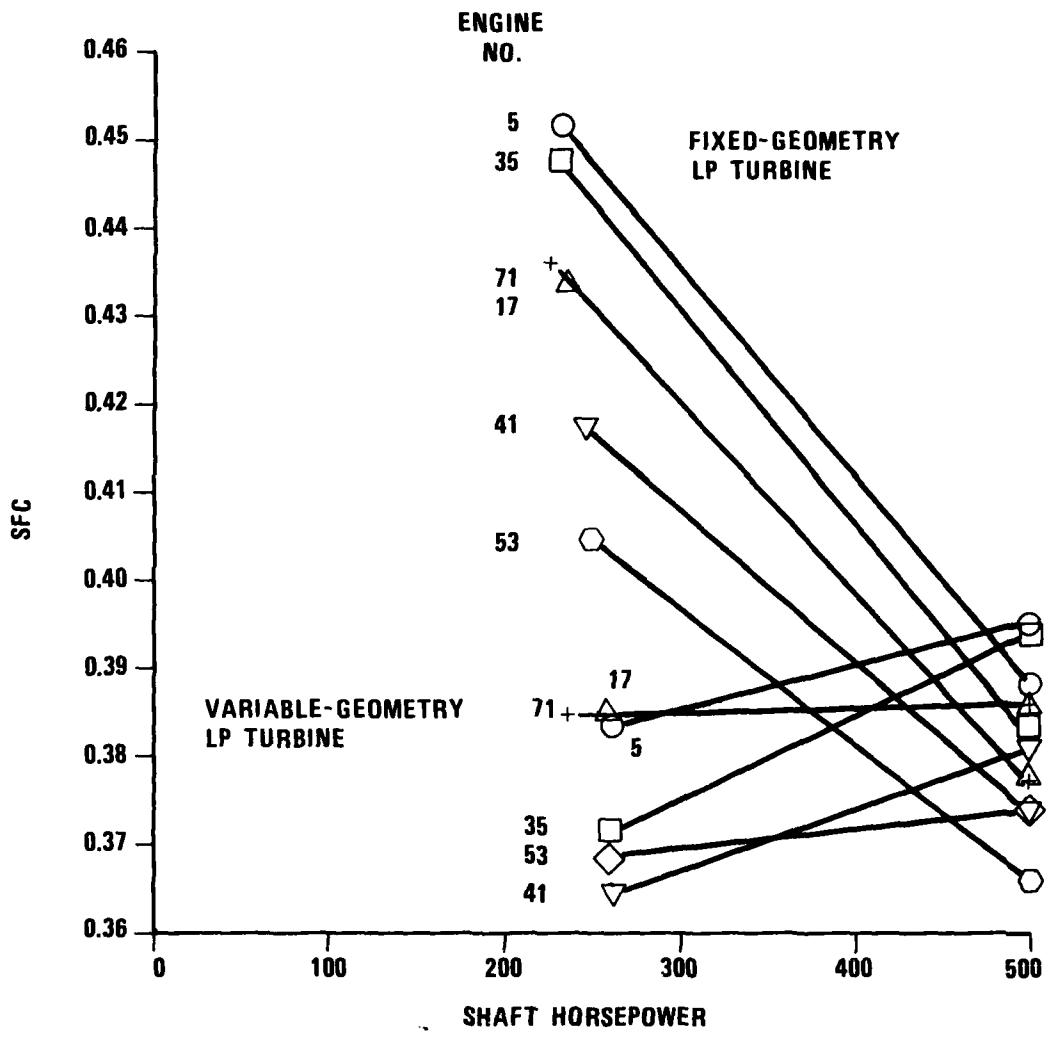


Figure 20. Fixed- and Variable-Geometry Power Turbine Engine Performance.

TABLE 11. FIGURES OF MERIT, FIXED-GEOMETRY POWER TURBINE ENGINES

ENGINE NO.	SHP*		SFC, LB/HR-HP		WEIGHT, LB		COST, K\$		FIGURE OF MERIT	
	FG	VG	FG	VG	FG	VG	FG	VG	FG	VG
5	236	263	0.452	0.384	302	305	118.8	138.8	1.143	1.116
17	240	257	0.434	0.385	269	272	116.9	126.7	1.090	1.058
35	235	261	0.448	0.372	224	226	85.7	106.0	0.985	0.948
41	248	266	0.418	0.365	280	283	107.9	121.5	1.052	1.025
53	251	260	0.405	0.369	252	254	107.5	117.3	1.014	0.997
71	238	230	0.435	0.385	222	224	85.0	105.0	0.965	0.960

$$FOM = 0.55 \frac{SFC}{SFC_{AV}} + 0.14 \frac{WEIGHT}{WEIGHT_{AV}} + 0.31 \frac{COST}{COST_{AV}}$$

*Sea-level static, 59°F

Low-Speed Power Turbine

A significant portion of the engine weight is represented by the main reduction gear train. To eliminate this weight, an alternative low-pressure turbine configuration was examined, with the single constraint that the ungeared output shaft speed remain at 20,000 rpm. The resulting engine configuration, designated Engine 34C, is shown in Figure 21. This engine configuration has no advantages over the basic Engine 34 as the comparison in Table 12 indicates. The power-turbine design requires five stages in order to meet the 20,000-rpm requirement while maintaining an efficiency level equal to that of the higher-speed two-stage design. As a result, the weight and cost are considerably higher than those of Engine 34, and the resulting FOM is also higher. The alternatives of using three or four stages were not examined since efficiency would suffer and SFC would increase, with the results that FOM would be higher. Accordingly, on the basis of FOM, it was decided that the configuration of Engine 34 would be retained.

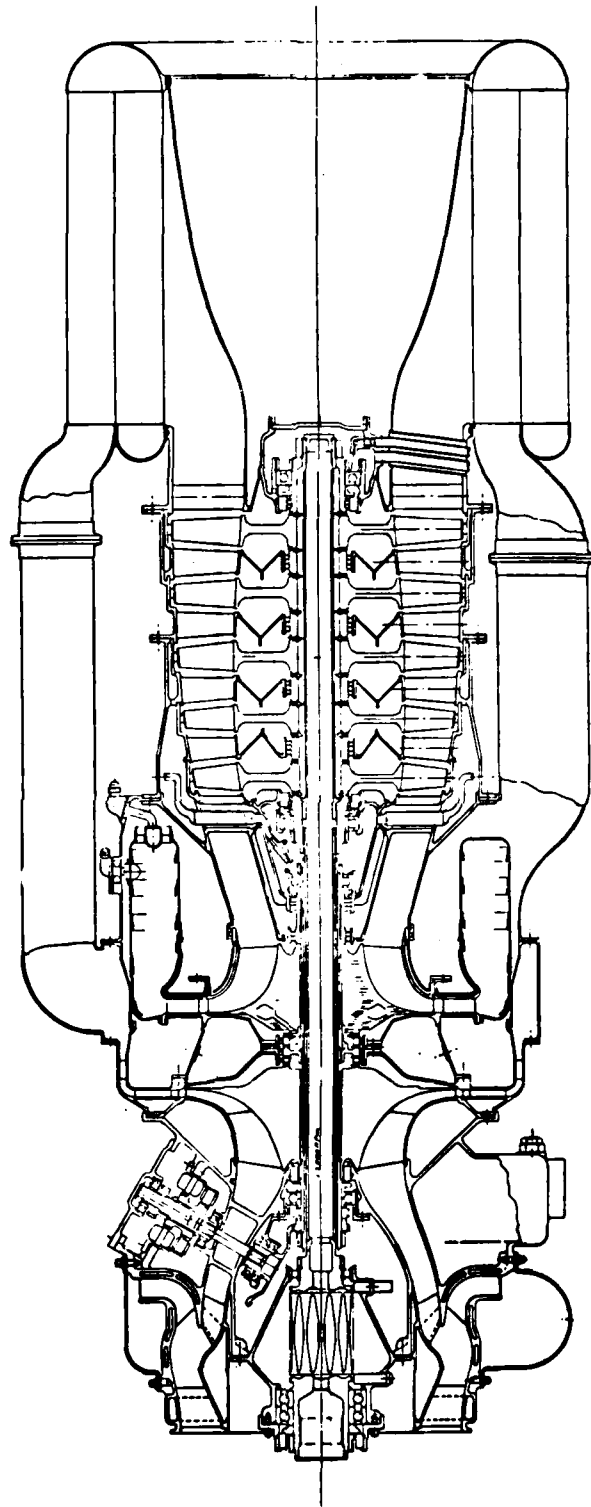
Bypass Heat Exchanger

Since most of the helicopter engine operation occurs at approximately 50 percent of intermediate rated power (IRP) with the resulting relatively lower compressor flow rate, an alternative configuration heat exchanger sized for the lower-flow rate offers a potential weight saving, while still providing the advantage of low SFC. However, at the higher-flow-rate, full-load condition, this heat exchanger must also have provision for bypassing some or all of the turbine exhaust gas around the smaller tube bundle in order to prevent excessive back pressure on the engine. Further, some compromise must be made in its design to preclude excessive pressure losses on the cold side during full-load operation, since the tubes must still carry all of the full-load compressor discharge airflow.

The configuration examined for this cycle variation is shown in the bottom half of Figure 17, designated Engine 34A. A comparison of the performance and cycle conditions for Engines 34 and 34A is given in Table 13. This table also shows the weights, costs and FOM for the two engines.

Several items in Table 13 warrant discussion. A comparison of the full-load, airflow rates shows in excess of a 6-percent reduction from the full heat exchanger to the bypass heat-exchanger configuration. This reduction is accounted for by the lower pressure loss in the heat exchanger hot side.

As would be expected, the bypass heat exchanger is considerably lighter weight than the full version; however, this is somewhat offset by the slightly increased engine weight due to the valves required for the bypass feature. The overall result is an



ENGINE NO. 34C WT = 137.1 LB
RECUPERATOR WT = 52.5 LB
TOTAL WT = 189.6 LB

Figure 21. Engine 34C, Low-Speed (20,000 RPM) Power Turbine Engine.

TABLE 12. LOW-SPEED POWER TURBINE COMPARISON

	Engine	
	34	34C
SFC, lb/hr-hp	0.437	0.437
Weight, lb	179.5	189.6
Cost, K\$	63.5	68.5
Relative FOM	1.000	1.031

TABLE 13. BYPASS HEAT EXCHANGER COMPARISON

Engine Power, shp	500		250	
	Full	Bypass	Full	Bypass
Heat Exchanger Type	Full	Bypass	Full	Bypass
SFC, lb/hr-hp	0.425	0.523	0.437	0.454
Airflow Rate, lb/sec	3.26	3.05	1.77	1.80
Heat Exchanger Effectiveness	0.700	--	0.728	0.700
Heat Exchanger Pressure Loss, $\Delta P/P$				
Cold Side	0.04	0.04	0.032	0.033
Hot Side	0.06	0.01	0.025	0.060
Weight, lb				
Engine	127.0	130.6		
Heat Exchanger	52.5	34.6		
Total	179.5	165.2		
Cost, K\$				
Engine	44.4	44.9		
Heat Exchanger	18.6	14.9		
Total	63.0	59.8		
Relative Figure of Merit			1.000	0.998

8-percent lower-weight system. It should be noted that the weight estimate for Engine 34A does not include the additional weight of the control system required for the bypass feature since that control system has not been defined.

Cost of the bypass heat exchanger is also lower than the cost of the full unit. However, the cost of the engine is slightly higher since the cost of the bypass valves is charged to the engine. As was noted in the discussion of weight in the previous paragraph, the cost estimate for Engine 34A does not include the additional cost of the bypass control system since that system was not defined.

The relative FOM for Engines 34 and 34A based on the factors available for this analysis indicate that these systems are essentially equal. However, with the additional complexity, weight, and cost of the bypass control system for which the definition was not within the scope of this study, Engine 34A would undoubtedly have a higher relative FOM and would be judged undesirable.

HEAT-EXCHANGER ANALYSIS

In recent years, recuperators have been applied to several vehicular applications where the environment is harsh due to the many start/stop cycles and vibrations. A similar environment can be expected for the present aircraft application of concern to this study. As a result of the recent work on vehicular recuperators, sophisticated structural-design techniques and thermal-analytical procedures have been developed.

Aircraft applications of heat exchangers result in the use of compact heat-transfer surfaces to minimize weight and volume. Not only are the weight and volume important, but the shape of the heat exchanger must lend itself to packaging. Packaging is always an important design constraint for aircraft applications and is one of the major reasons recuperators are not in use on existing aircraft. Advanced-design procedures in manifolding, ducting, and core fluid interface arrangements have been used in this study to aid in the packaging investigation. An essential feature of such an investigation is close coordination between the engine and recuperator designs to ensure efficient packaging.

CANDIDATE RECUPERATOR TYPES

There are two main types of heat exchangers currently being used as recuperators for gas turbine engine applications. One is the fixed-boundary recuperator, which is often referred to as a conventional direct-transfer heat exchanger, in which the compressor-discharge air and turbine exhaust gas exchange thermal energy directly through, and are separated by, the heat transfer surface itself. The other type is a periodic-flow recuperator, like the common Ljungstrom air preheater, in which the heat is alternately absorbed and rejected by a mass of material that rotates through fixed fluid streams, and is exposed periodically to the high-temperature gas and low-temperature air.

The periodic or rotary regenerator is well suited to low pressure ratio turbine engines. For operation at pressure ratios above approximately 6:1, however, these devices suffer from excessive wear and leakage of the seals between the high and low pressure gas streams. For this reason the rotary regenerator was not considered as a candidate for the present study where the high-performance engines of interest operate at pressure ratios above 6:1. The study was therefore limited to fixed-boundary recuperators.

FLOW-PATH CONFIGURATIONS

Among the fixed-boundary heat exchangers, two design concepts are most promising for the present application. These are the plate-fin and the tubular construction. For each of these concepts, a wide range of flow-arrangement options is available.

The choice of a particular combination of hot and cold flow paths depends largely on the desired thermal performance, on the turbo-machinery interface, and on the packaging envelope. These will be summarized here in light of present performance levels and packaging requirements.

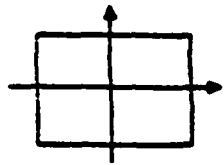
The two, basic-flow configurations considered in the study are crossflow and counterflow. As shown in Figure 22, these configurations can be combined into a number of passes to form more complex yet efficient flow arrangements. A number of these can be initially eliminated because of packaging restrictions. The recuperator has to occupy an annular space, having the turbine exhaust diffuser boundary at its inner diameter.

The most practical tubular flow configuration satisfying this requirement is the annular cross-counterflow design, with the tubes oriented in the direction of the turbine exhaust diffuser axis. Figure 23 gives an example of this configuration. An alternate approach consists of a circumferentially-arranged, cross-counterflow tubular unit. In the latter, the tube axes are oriented in a circumferential direction. The recuperator is split into a number of modules, which are arranged around the periphery of the annular space downstream of the turbine exhaust diffuser. Figure 24 is an example of this flow arrangement.

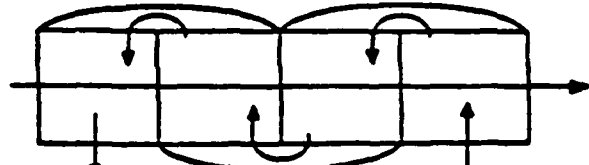
Selection of one arrangement in place of the other depends on the pressure-drop-split requirements between the exhaust gas and the high-pressure air circuits. As this split is varied, the tubular heat-exchanger configuration and size also vary. Thus, the design of the heat exchanger involves an iterative interaction with the engine thermodynamic cycle as well as with the engine-flow geometry. For the range of parameters for the present application, the annular configuration was selected. This configuration, shown in Figure 23, simplifies the manifolding and ducting, and costs less than the circumferential tube arrangement.

The above statements are also true for plate-fin recuperators, although these are characteristically less sensitive to pressure-drop split. Past studies of plate-fin recuperators applied to gas turbine engines with cycles within the range of the present application have shown that crossflow and counterflow units have the same weight for effectiveness levels, around 0.70. For effectiveness levels above this value, the counterflow configuration has a lower weight for the same packaging envelope. For this reason, crossflow plate-fin units were not considered in this study. Because of the flow arrangement inherent in the counterflow concept, a counterflow unit is difficult to package into an annular space. It must be divided into a number of modules, which increases the complexity of the installation. As shown subsequently, plate-fin designs are not competitive weight-wise with tubular designs for the present application, and their study was therefore not emphasized.

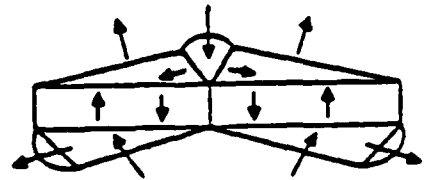
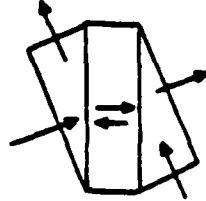
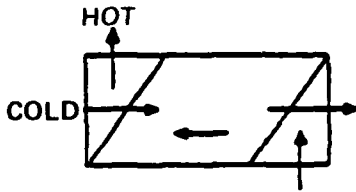
(1) PLATE-FIN DESIGNS



a. CROSSFLOW



b. MULTIPASS CROSS COUNTERFLOW



c. COUNTERFLOW CONFIGURATIONS

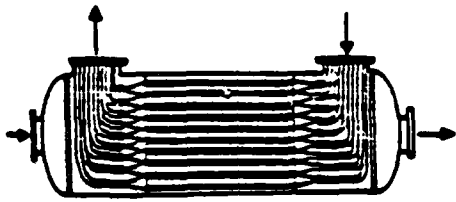
(2) TUBULAR DESIGNS



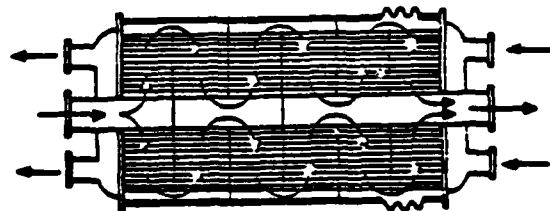
a. CROSS FLOW



b. MULTIPASS CROSS COUNTERFLOW



c. PURE COUNTERFLOW



d. ANNULAR CROSS COUNTERFLOW

Figure 22. Possible Recuperator Flow Configurations.

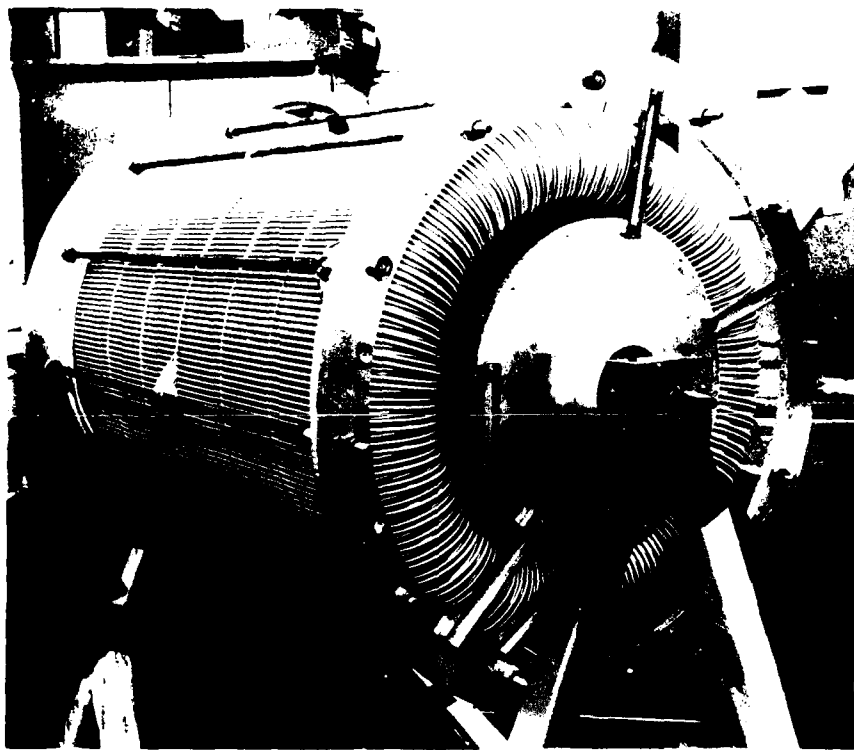
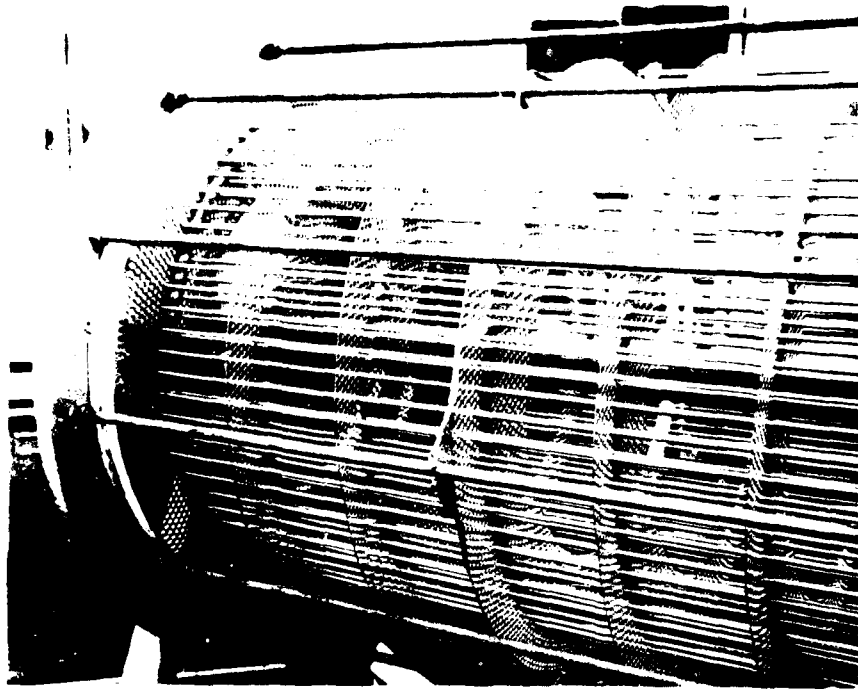


Figure 23. T-53 Gas Turbine Engine Recuperator.

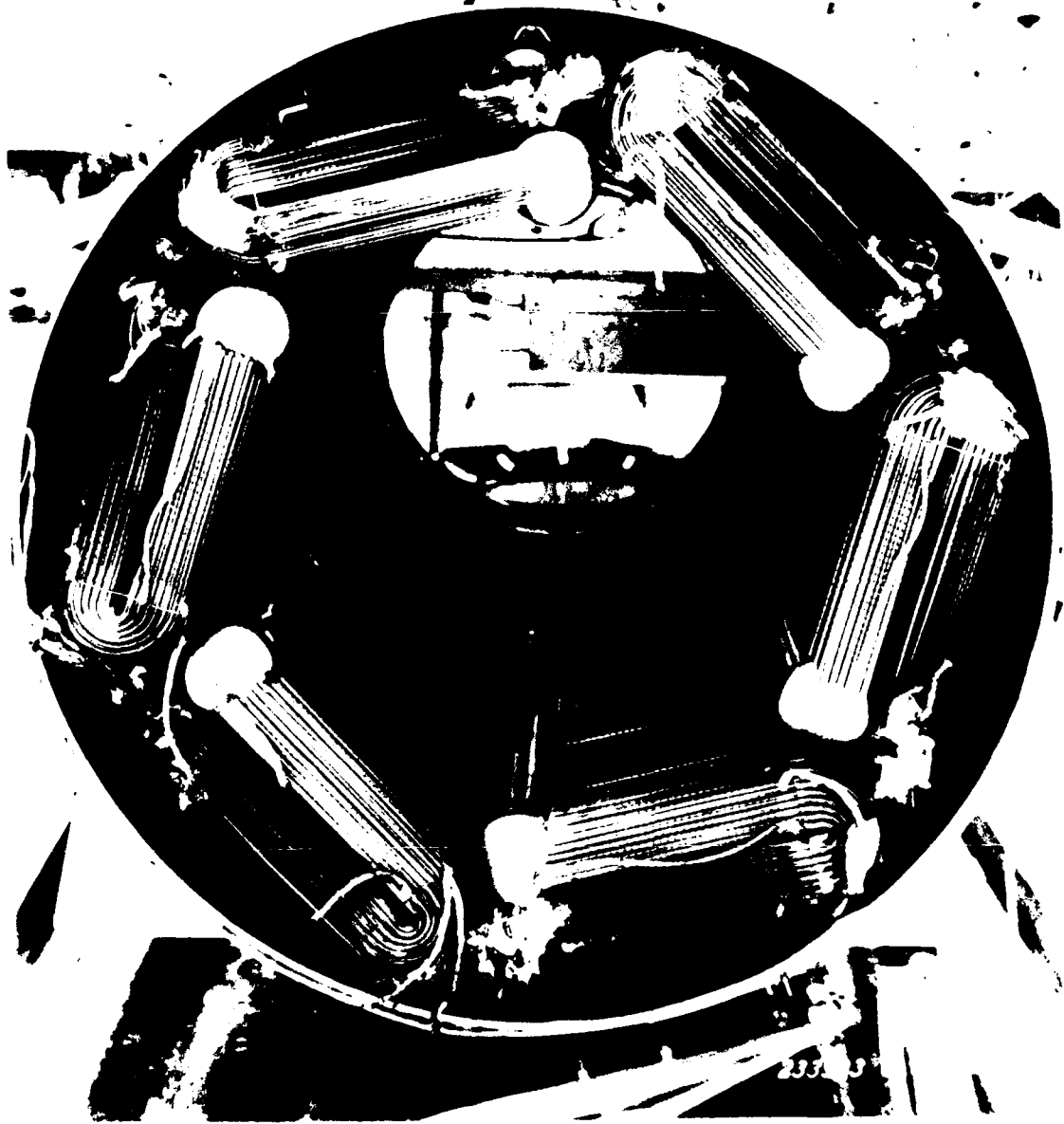


Figure 24. T-78 Recuperator.

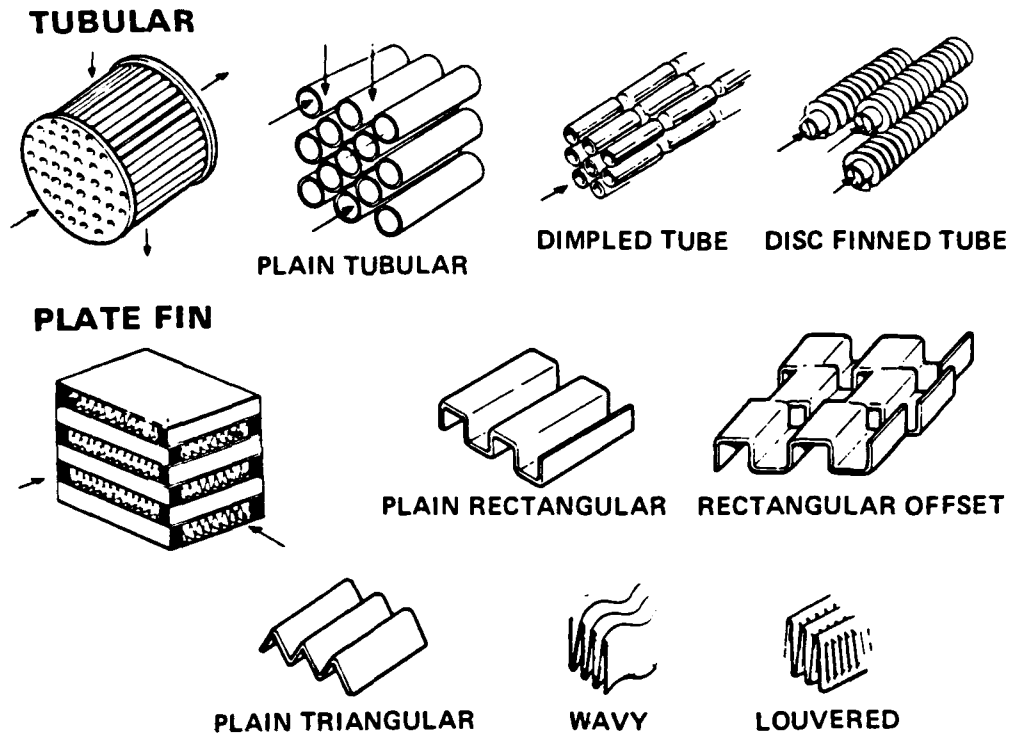
PLATE-FIN VERSUS TUBULAR

The two heat-exchanger concepts most likely to succeed for aircraft recuperator applications are the plate-fin and tubular construction. Figure 25 shows the heat-transfer surfaces typically used for each heat-exchanger type. Figures 26 and 27 are examples of tubular and plate-fin recuperator cores. The tubular unit shown in Figure 26 uses ring-dimpled tubes to increase the heat-transfer coefficient on the inside of the tubes. The plate-fin unit shown in Figure 27 uses very compact offset fins (37 fins per inch) on the air side for the same purpose. The units are typical of the type of design for the present applications.

For a fixed set of gas and air inlet conditions and allowable pressure drops, the effectiveness of the recuperator is the major performance parameter that influences the size and weight of the recuperator. The definition of effectiveness is given in Figure 28. For the present application, the optimum overall engine cycle can be expected to be in the effectiveness range of 0.7 to 0.8. In this range, tubular recuperators tend to be lighter than corresponding plate-fin units. Their lower weight is partly due to the simplicity of construction and partly to the excellent inherent pressure-containment characteristics associated with tubes. With high-pressure differentials present between hot and cold fluids in the recuperator, the high-pressure fluid can be made to flow inside a small diameter tube bundle while the low-pressure gas flows outside. In this way, full advantage is taken of the pressure-containment capability of the tubes while keeping the weight of the external shell low. Furthermore, because of their configuration, tubular heat exchangers can be readily packaged into an annular envelope with efficient use of space inside that envelope.

5
F

However, tubular heat-exchanger-design concepts, while simpler than their plate-fin counterparts, are less compact from a heat-transfer surface viewpoint. Although the tubes can be arranged in a staggered pattern for better heat transfer, and their spacing and diameter varied to suit design requirements, tubular units are not as flexible as plate-fin units in their geometry. The main disadvantage of tubular designs is the poor internal heat-transfer coefficient because of boundary-layer buildup. This can be alleviated in part by the use of ring-dimpled tubes. This causes a breakup of the boundary layer on the tube walls giving improved heat transfer. However, it also exacts a penalty in terms of pressure drop. Also, addition of external fins to the tubes seldom results in a smaller, lighter recuperator because the heat transfer coefficient inside the tubes controls the design. Thus, essentially the same surface area is available on the air and gas sides of the core.



5
B

Figure 25. Heat Transfer Surfaces.

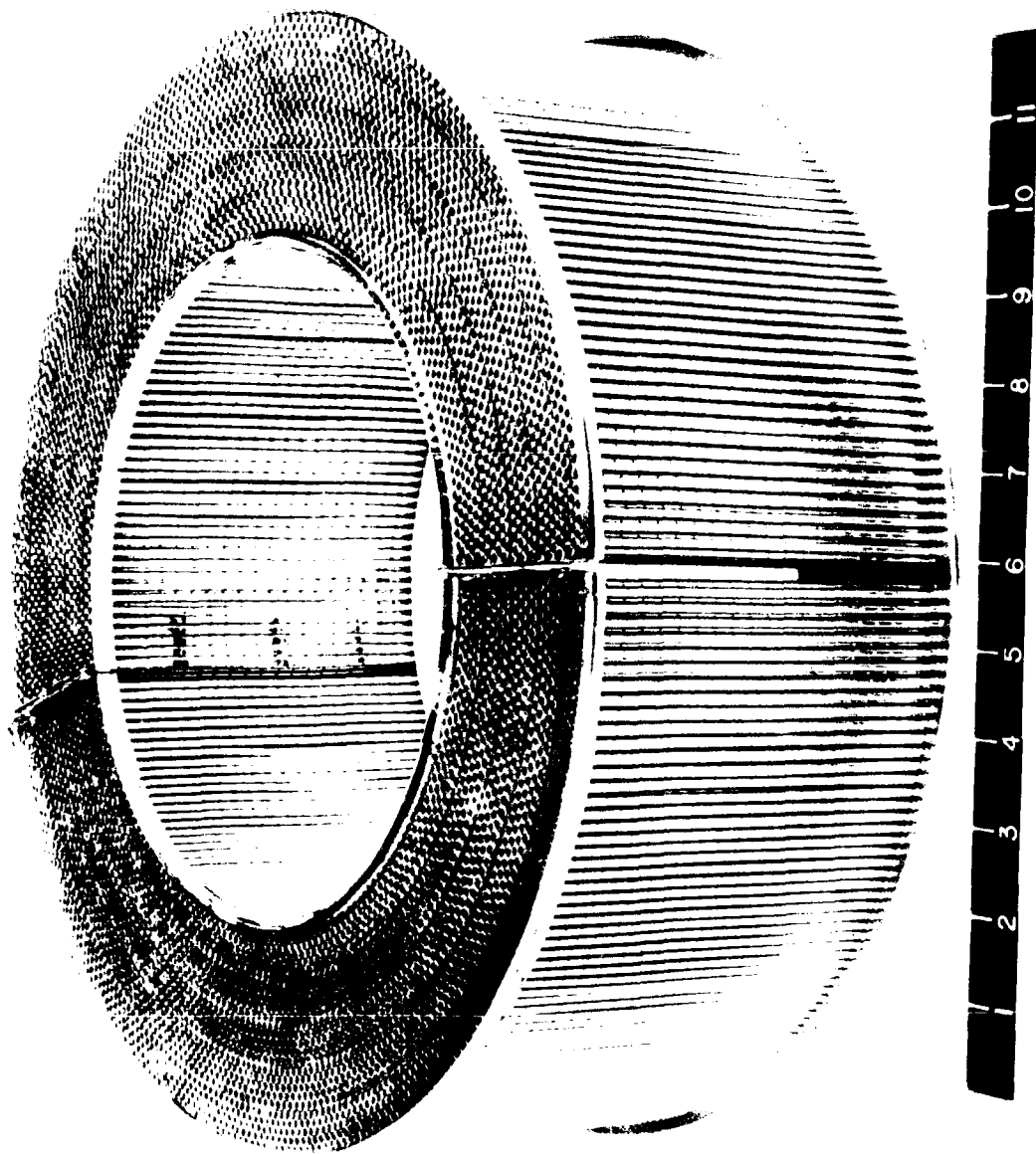


Figure 26. T-63 Regenerator Core Assembly.

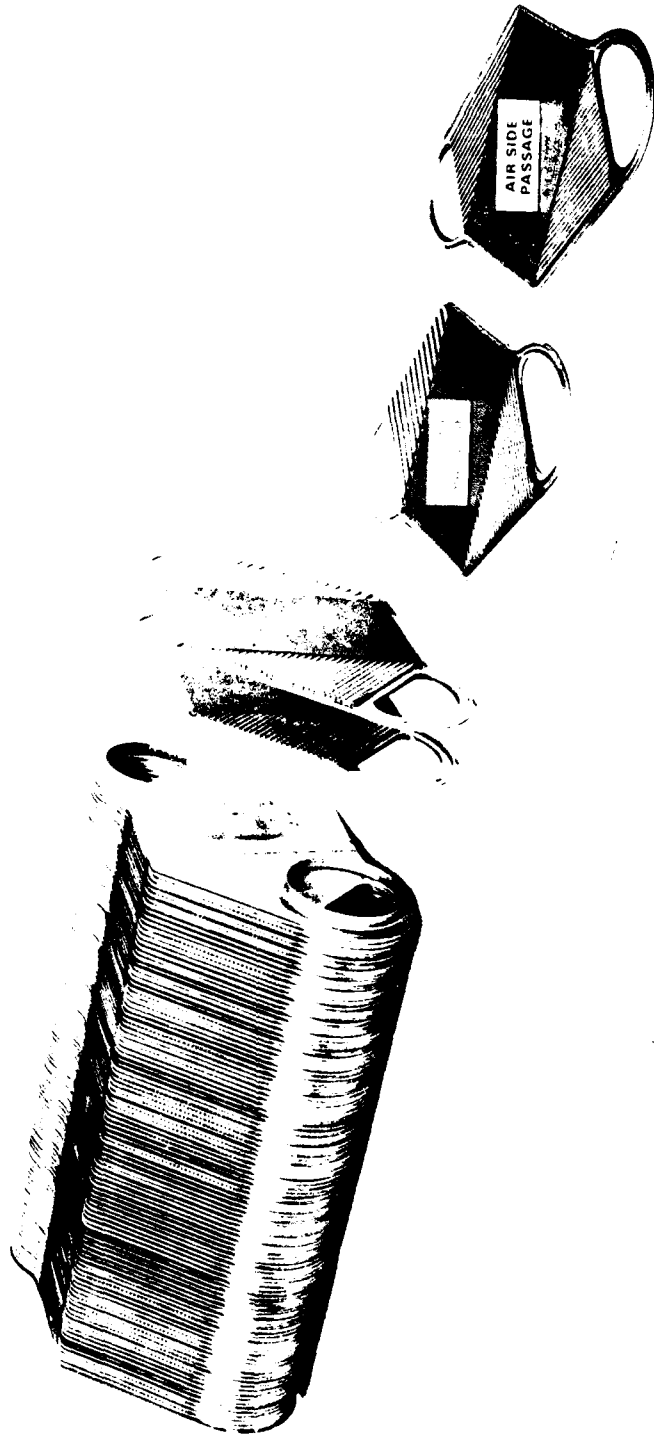


Figure 27. Fin-Tubeplate Subassemblies GT-601 Recuperator.

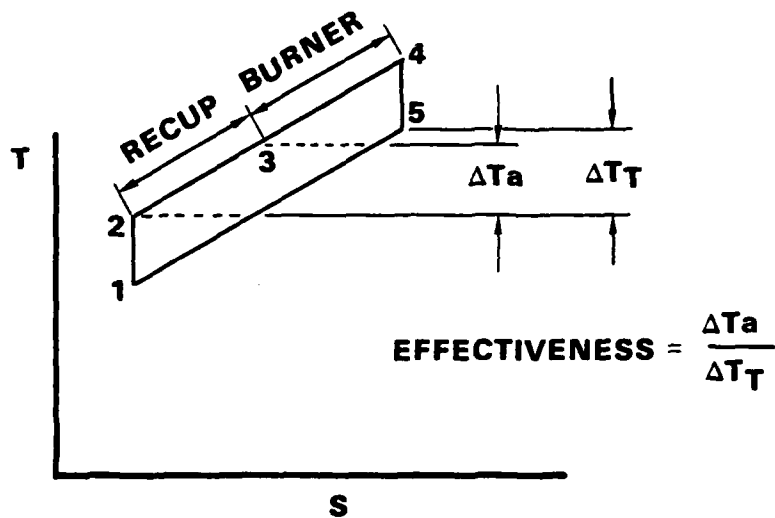
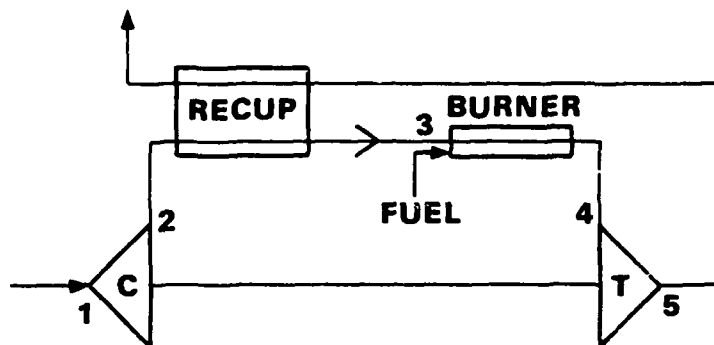


Figure 28. Recuperated Engine Cycle.

In the plate-fin recuperator construction, the hot and cold fluids are separated by parallel plates. Heat transfer in the fluid passages is enhanced by the presence of fins attached between the plates. Because passage height and fin geometry can be varied independently for the two fluids, there is considerable flexibility in the heat-exchanger design geometry. Near optimum designs with high compactness and balanced heat-transfer conductances can thus be achieved.

However, because of the flow arrangement inherent in the plate-fin concept, additional minimum requirements are placed on the heat-exchanger size. Thus, flow distribution and pressure-drop requirements dictate a minimum size for the ducting and manifolds leading the hot and cold fluids in and out of the core. Additionally, structural considerations impose minimum-flow length and core-aspect-ratio restrictions. These also affect the recuperator size adversely from a cylindrical packaging viewpoint.

Figure 29 is a comparison of plate-fin and tubular recuperator weight as a function of air-side effectiveness for engine condition numbers 34 and 36. The units of each type have been optimized to minimize their respective weights. At the lower end of the effectiveness range, the weight advantage of the tubular unit is nearly 2 to 1. Though this weight advantage decreases at higher effectiveness, on the basis of weight the tubular concept is clearly the best choice. For this reason, plate-fin units were not considered in the major part of the parametric studies conducted in this program. Spot checks were made, however, to ensure that the plate-fin design was not overlooked as a good candidate design.

TUBULAR DESIGN PARAMETERS

Based on experience with other aircraft recuperators^{1,3}, the range of tubular-design parameters to be investigated in this study can be reduced to those given in Table 14. Then by parametric evaluation of recuperator designs over the range of parameters indicated in Table 14, the best set of design parameters can be selected. The parametric evaluation was limited to plain tube and ring-dimpled tubes with the tube bundle arrangements shown in Figure 30. Though other tube configurations such as spiral tubes could be included in the program, these are not expected to survive the vibration environment.

³. McDonald, Colin F., "Study of a Lightweight Integral Regenerative Gas Turbine For High Performance", USAAVLABS Technical Report 70-39, Fort Eustis, Virginia: US Army Aviation Materiel Laboratories, 1970; AD877464.

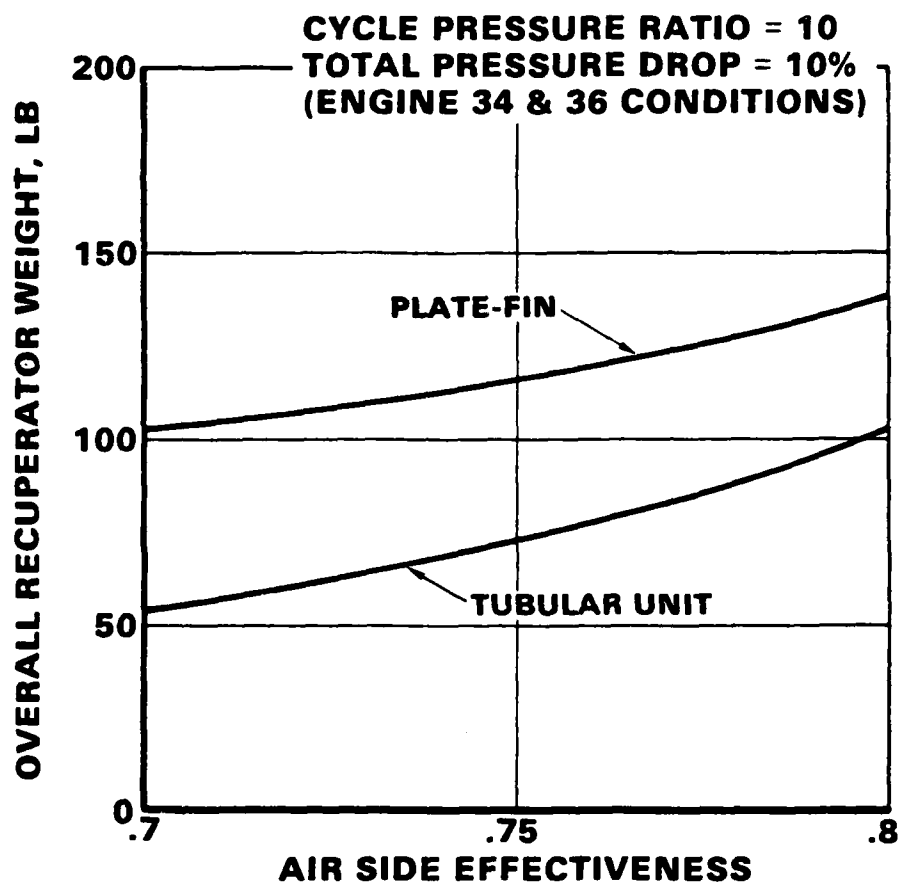


Figure 29. Weight Comparison of Typical Tubular and Plate-Fin Units (Stainless Steel Unit).

● PLAIN TUBE

● RING DIMPLED TUBE $\psi = .03, .05, .06, .08$

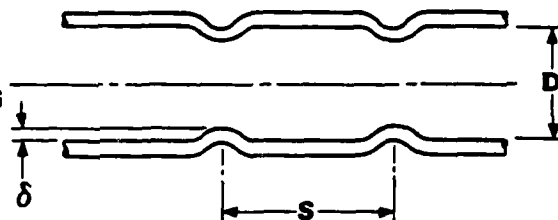
$$\psi = \left(\frac{\delta}{D} \right) / \sqrt{\frac{S}{D}}$$

WHERE

D = TUBE I.D.

δ = DIMPLE DEPTH

S = DIMPLE SPACING



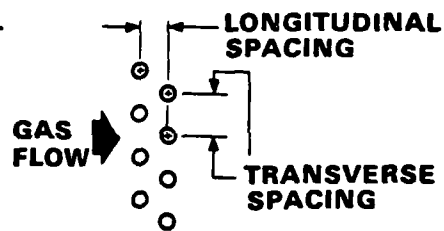
● TUBE BUNDLE ARRANGEMENT

SB 125100

SB 135100

SB 150100

SB 200100



EG. SB 125100 = STAGGERED TUBE PATTERN WITH 1.25 TUBE DIA.
PITCH TRANSVERSE TO FLOW & 1.0 TUBE DIA.
IN LONGITUDINAL FLOW DIRECTION

Figure 30. Tubular Heat Exchanger Surface Geometries.

TABLE 14. TUBULAR RECUPERATOR DESIGN PARAMETER RANGES

Tube Diameter	0.1 to 0.2 inch
Gas Stream Pressure Loss	20 to 80 percent of total $\Delta P/P$
Air Manifold Pressure Loss Allowance	5 to 20 percent of total $\Delta P/P$
Tube Ring Dimple Geometry (4)	0.03 to 0.08 and plain tube
Tube Module Arrangement Transverse Spacing	1.25 to 2.0 tube diameter
Longitudinal Spacing	Tube OD

Figure 31 gives the influence of the ring-dimple geometry as compared with plain tubes. This evaluation was conducted using an average engine design problem statement (Engine No. 75)--similar results can be expected for the other engines covered by this study. Several design characteristics become apparent upon review of Figure 31. The ring-dimple tubes give lighter weight recuperators with shorter overall length; the short tube length is beneficial to overall engine C.G. balance. The number of tubes and the core diameter both increase as the dimples get deeper. The number of tubes is an important cost consideration where the cost increases with the number of tubes. At a ψ (see Figure 30) of 0.05, a near minimum weight is obtained with a reasonable tube count and short overall length.

Figure 32 gives the influence of tube diameter and pressure drop on core diameter, tube length, number of tubes, and tube weight. Here it is shown that smaller tube sizes result in lighter recuperators; however, as the tube size decreases, the number of tubes increases. A realistic choice of tube size is 0.125-in. OD, where a lightweight design is achieved at a reasonable tube count. Figure 32 also shows that the optimum weightwise pressure-drop split between the gas and air sides of the recuperator is around 60 percent of the total $\Delta P/P$ for the gas side (i.e., 60 percent of the total allowable of 5 percent for 3 percent on the gas side).

Figure 33 gives the influence of the ratio of transverse tube spacing to tube OD on the major design characteristics of the recuperator. For ratios below 1.5, there is a drastic change in the core diameters due to the restricted gas-flow area over the tubes. At ratios over 1.5, there is a great deal of latitude in selecting the tube spacing.

EFFECTIVENESS = 0.7
 TOTAL $\Delta P/P = 5\%$
 TUBE O.D. = 0.125 IN.
 TUBE SPACING = SB 150100
 RING DIMPLE $\psi = \frac{\delta/D}{\sqrt{S/D}}$

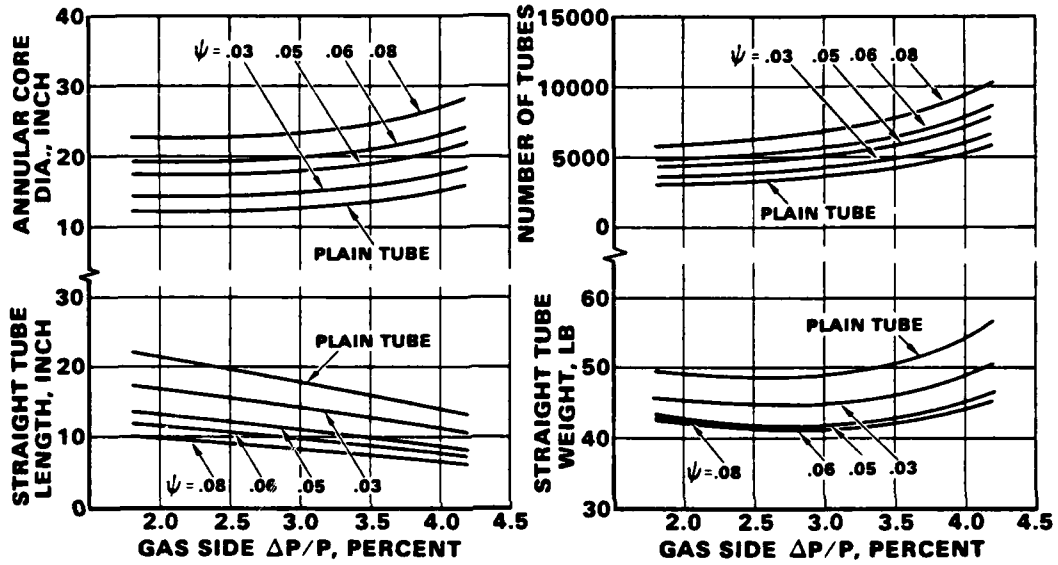


Figure 31. Tubular Recuperator, Study Effect of Tube Ring Dimple on Recuperator Characteristics.

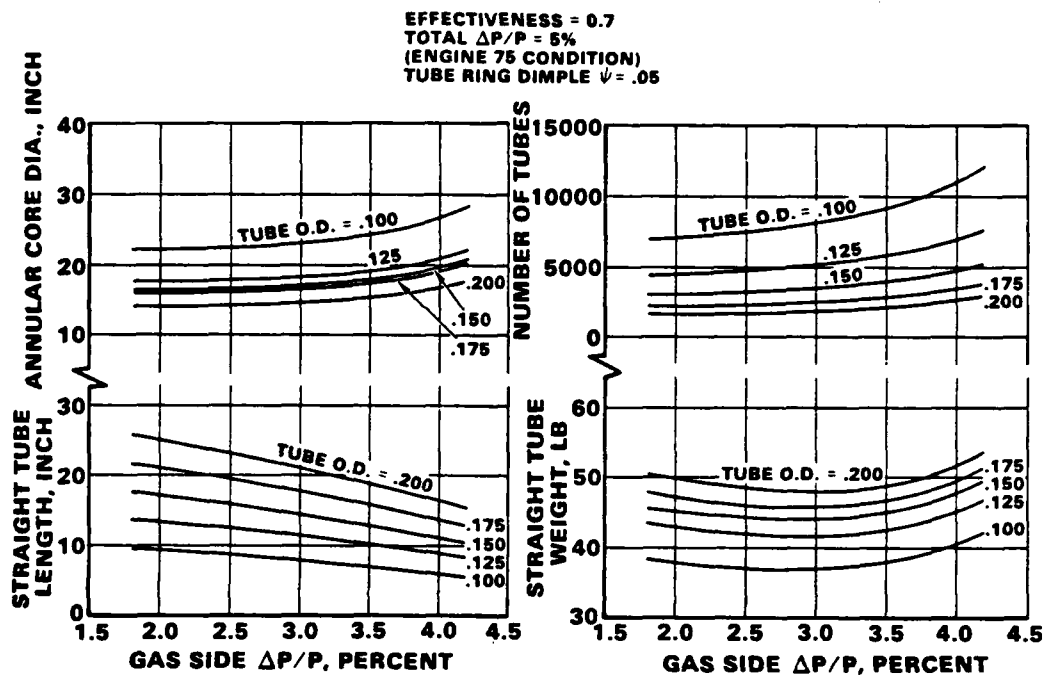


Figure 32. Tubular Recuperator, Study Effect of Pressure Drop and Tube Diameter on Recuperator Characteristics.

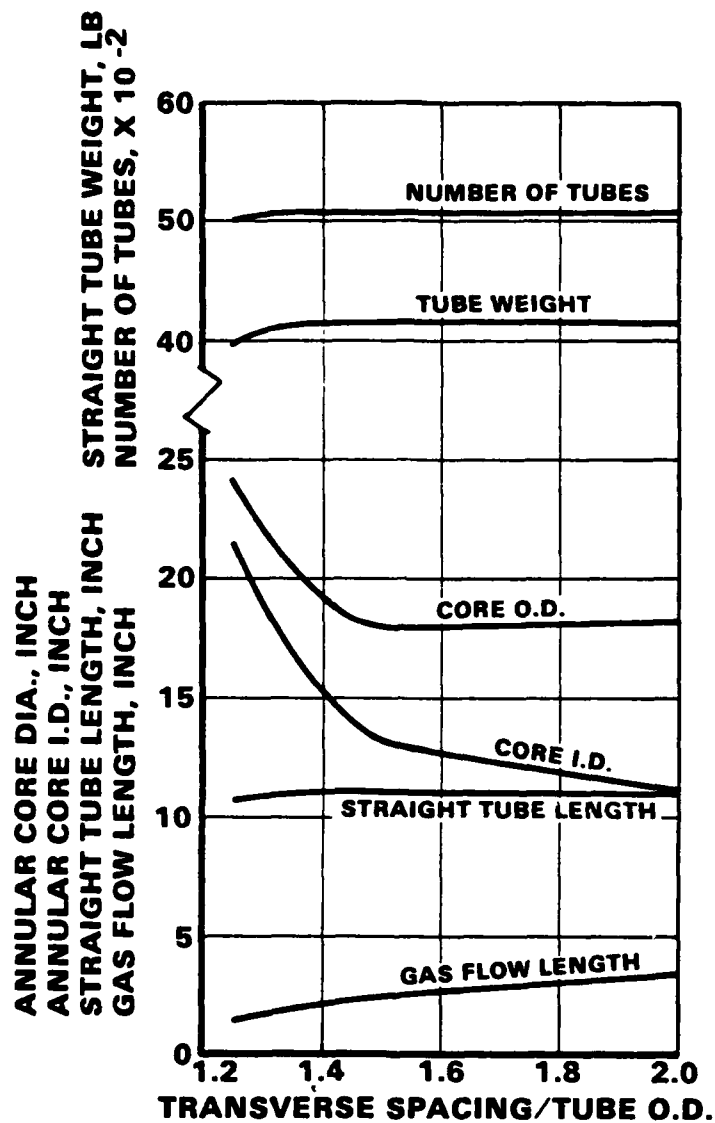


Figure 33. Tubular Recuperator, Study Effect of Tube Bundle Spacing on Recuperator Characteristics.

Based on the results of the parametric study represented in Figures 30 through 33, the parameters given in Table 15 were selected for use in developing recuperator designs for the 90 engines that were evaluated in this study. The choice of each parameter is based on obtaining a low-weight design that is cost effective with respect to its fabrication.

PARAMETRIC STUDY

- (a) Preliminary Screening - From the previous discussion, the basic heat-exchanger configuration of a tubular two-pass cross counterflow and the tubular heat-transfer geometry given in Table 15 were selected for the parametric study. The parametric study covered 90 engines in a preliminary screening process. To facilitate the work, the engines were divided into 18 groups based on recuperator effectiveness, recuperator $\Delta P/P$ and cycle pressure ratio. The values of these parameters are given in Table 16. Each group consisted of engines for three turbine-inlet temperatures and one or two compressor stages, with two-stage compressors only for the pressure ratio of 13.

Within each group of engines, a recuperator was designed for flow rates in the middle of the ranges. Recuperator weights could then be obtained for other engines in the same group by linearly scaling with flow rate. The other recuperator characteristics such as tube length, diameters, and number of tubes were based on the scaled weights. The results of this preliminary screening study yielded the recuperator characteristics given in Tables 17 and 18. This data was provided to the engine study for a selection of the most promising engine cycles.

- (b) Off-Design Performance - To aid in the screening process, off-design performance data was also generated. Pressure-drop performance of specific recuperators can be obtained by similarity to the pressure-drop characteristics of flow through and across tube banks. This allows the use of a simplified process to accurately estimate the off-design pressure drop of the tubular recuperators. The solid lines in Figure 34 represent the hot- and cold-side pressure drop of a specific recuperator (i.e., that designed for the fixed-geometry Engine No. 17). To estimate the pressure drop of other recuperators, it is only necessary to calculate the full-power corrected flow (W_{CORR}) defined in Figure 34 and draw a line parallel to the appropriate solid line. The dashed lines represent an example calculation giving the pressure drop of both the gas and air sides of a candidate design.

TABLE 15. SELECTED PARAMETER VALUES

Tube Diameter	0.125 inch
Pressure Drop Used on Gas Stream	60 percent of total $\Delta P/P$
Air Manifold Pressure Loss Allowance	5 percent of total $\Delta P/P$
Tube Ring Dimple Geometry, ψ	0.05
Tube Bundle Arrangement	Varied for each recuperator design

TABLE 16. 500-HP ENGINE TUBULAR RECUPERATOR DESIGN STUDY

Divide 90 engines into 18 groups based on combinations of:

3 Recuperator effectiveness	= 0.6, 0.7, 0.8
2 Recuperator $\Delta P/P$	= 5%, 10%
3 Cycle Pressure Ratio	= 7, 10, 13

TABLE 17. SCREENING STUDY RESULTS

For Each Engine, Supplied	Range
Tube Weight	15.5 - 96 lb
Overall Weight	28.7 - 178 lb
Tube Length	5.3 - 18.1 in.
Overall Length	7.1 - 20.4 in.
Outer Diameter	12.5 - 27.4 in.
Inner Diameter	7.3 - 23.9 in.
Cost	12 - 50K \$
Number of Tubes	2704 - 9632

TABLE 18. PRELIMINARY RECUPERATOR CHARACTERISTICS

Engine No.	Straight Tube Wt., lb	Overall Weight, lb	Core OD, in.	Core ID, in.	Straight Tube Length, in.	Overall Length, in.	No. of Tubes
1	25.0	46.2	7+	7	5.3	7.1	6408
2	20.8	38.5	8+	8	5.7	7.7	4950
3	44.1	81.6	9+	9	7.8	9.7	7608
4	37.0	68.4	10+	10	8.4	10.6	5926
5	89.8	166.2	47+	47	12.8	15.2	9488
6	73.8	136.5	48+	48	13.5	16.2	7356
7	23.3	43.1	27.4	23.9	5.3	7.1	5984
8	19.4	35.9	19.6	15.7	5.7	7.7	4612
9	41.2	76.2	26.4	22.5	7.8	9.7	7106
10	34.5	63.8	19.1	14.7	8.4	10.6	5526
11	84.0	155.4	47+	47	12.8	15.2	8870
12	68.8	127.3	48+	48	13.5	16.2	6860
13	21.9	40.5	7-	7	5.3	7.1	5626
14	18.2	33.7	8-	8	5.7	7.7	4332
15	38.7	71.7	9-	9	7.8	9.7	6680
16	32.4	59.9	10-	10	8.4	10.6	5186
17	79.0	146.1	47-	47	12.8	15.2	8340
18	64.6	119.6	48-	48	13.5	16.2	6446
19	22.1	40.9	25+	25	6.5	8.1	4698
20	18.4	34.0	26+	26	6.9	8.3	3606
21	38.7	71.5	27+	27	9.3	11.1	5610
22	32.2	59.5	28+	28	10.0	11.6	4324
23	77.2	142.9	65+	65	15.0	17.2	6962
24	63.5	117.5	66+	66	16.0	18.5	5362
25	20.5	37.9	21.5	18.3	6.5	8.1	4358
26	17.0	31.5	17.7	15.0	6.9	8.3	3340
27	35.9	66.4	21.1	17.5	9.3	11.1	5210
28	29.8	55.1	17.5	14.3	10.0	11.6	4006
29	71.7	132.7	65+	65	15.0	17.2	6464
30	58.9	109.0	66+	66	16.0	18.5	4970

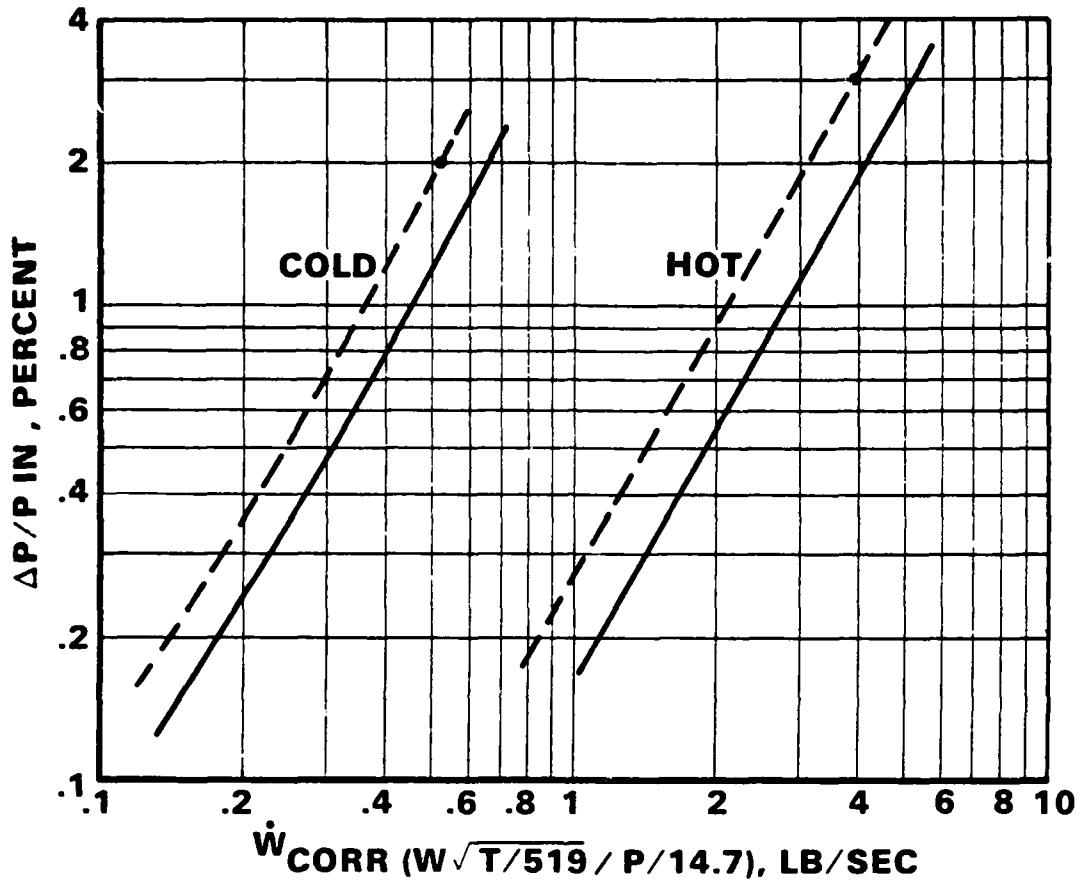
TABLE 18. Continued.

Engine No.	Straight Tube Wt., lb	Overall Weight, lb	Core OD, in.	Core ID, in.	Straight Tube Length, in.	Overall Length, in.	No. of Tubes
31	20.7	38.4	25-	25	6.5	8.1	4410
32	15.9	29.4	26-	26	6.9	8.3	3120
33	33.6	62.2	27-	27	9.3	11.1	4876
34	27.9	51.6	28-	28	10.0	11.6	3746
35	67.1	124.2	65-	65	15.0	17.2	6050
36	55.0	101.8	66-	66	16.0	18.5	4644
37	23.9	44.3	7+	7	5.3	7.1	6146
38	19.9	36.9	8+	8	5.7	7.7	4738
39	42.3	78.2	9+	9	7.8	9.7	7292
40	35.4	65.5	10+	10	8.4	10.6	5670
41	86.2	159.4	47+	47	12.8	15.2	9102
42	70.5	130.5	48+	48	13.5	16.2	7034
43	22.4	41.5	7-	7	5.3	7.1	5756
44	18.6	34.5	8-	8	5.7	7.7	4428
45	39.6	73.3	9-	9	7.8	9.7	6836
46	33.1	61.2	10-	10	8.4	10.6	5302
47	80.7	149.3	24.1	19.2	12.8	15.2	8524
48	66.0	122.1	17.7	12.3	13.5	16.2	6582
49	21.1	39.1	7-	7	5.3	7.1	5426
50	17.5	32.5	8-	8	5.7	7.7	4170
51	37.4	69.1	9-	9	7.8	9.7	6442
52	31.2	57.7	10-	10	8.4	10.6	4992
53	76.1	140.8	47-	47	12.8	15.2	8042
54	62.2	115.0	48-	48	13.5	16.2	6198
55	21.5	39.8	25+	25	6.5	8.1	4578
56	17.9	33.1	26+	26	6.9	8.3	3510
57	37.7	69.8	27+	27	9.3	11.1	5472
58	31.3	58.0	28+	28	10.0	11.6	4210
59	75.3	139.2	65+	65	15.0	17.2	6784
60	61.9	114.4	66+	66	16.0	18.5	5220

TABLE 18. Continued.

Engine No.	Straight Tube Wt., lb	Overall Weight, lb	Core OD, in.	Core ID, in.	Straight Tube Length, in.	Overall Length, in.	No. of Tubes
61	20.0	37.1	25-	25	6.5	8.1	4258
62	16.6	30.7	26-	26	6.9	8.3	3258
63	35.1	64.8	27-	27	9.3	11.1	5086
64	29.1	53.8	28-	28	10.0	11.6	3908
65	70.0	129.5	19.7	15.2	15.0	17.2	6310
66	57.6	106.6	14.5	9.5	16.0	18.5	4862
67	18.8	34.7	25-	25	6.5	8.1	3990
68	15.5	28.7	26-	26	6.9	8.3	3050
69	32.9	60.8	27-	27	9.3	11.1	4772
70	27.2	50.4	28-	28	10.0	11.6	3658
71	65.7	121.5	65-	65	15.0	17.2	5920
72	53.8	99.5	66-	66	16.0	18.5	4540
73	22.4	41.4	79+	79	7.3	8.8	4126
74	18.8	34.7	80+	80	8.0	9.3	3176
75	38.6	71.4	81+	81	10.6	12.3	4908
76	32.3	59.7	82+	82	11.5	13.0	3786
77	76.6	141.6	83+	83	16.9	19.0	6116
78	63.6	117.6	84+	84	18.1	20.4	4720
79	20.6	38.1	19.6	16.5	7.3	8.8	3794
80	17.2	31.8	16.1	13.5	8.0	9.3	2914
81	35.5	65.7	19.4	15.9	10.5	12.3	4518
82	29.6	54.8	16.0	13.0	11.5	13.0	3474
83	70.4	130.2	18.6	14.4	16.9	19.0	5624
84	58.3	107.9	13.7	9.0	18.1	20.4	4330
85	19.1	35.4	79-	79	7.3	8.8	3526
86	16.0	29.5	80-	80	8.0	9.3	2704
87	33.0	61.0	81-	81	10.6	12.3	4198
88	27.5	50.8	82-	82	11.5	13.0	3226
89	65.5	121.2	83-	83	16.9	19.0	5232
90	54.1	100.1	84-	84	18.1	20.4	4020

6
F



6
B

Figure 34. Estimated Off-Design Pressure Drop, 500 HP Engine Recuperator ($\Delta P/P_T = 5\%$).

Typical off-design thermal performance of tubular recuperators is given in Figure 35. Here, the effectiveness of recuperators for three engines is given as a function of the ratio of actual flow to the design flow. For these data, the ratio of hot-to-cold flow was held constant and equal to that at full power.

Figure 35 shows a characteristic inherent of two-pass cross-counterflow tubular units; the effectiveness does not greatly increase at reduced flow. This can influence the fuel savings at part power settings. For comparison, Figure 36 represents the effectiveness of a counterflow plate-fin unit designed for Engine 36. Here it is seen that the effectiveness is significantly higher at reduced flow. Thus, though plate-fin units are heavier than their tubular counterparts, they have better off-design performance at part-power-flow rates.

WEIGHT MODEL

Detail weight analysis of tubular heat exchangers is a tedious process, requiring considerable time. For parametric analyses, it is impractical to perform detail weight calculations. Fortunately, reasonably accurate weights of tubular units can be obtained by using a wrap-up factor obtained by taking the ratio of total unit weight to tube weight for heat exchangers of similar construction. The DC-10 precooler unit presently in production is similar to the present recuperators and was used as the basis for the wrap-up factor used in the parametric. The resulting wrap-up factor is 1.85 which includes the following:

- Tube weight based on computer calculations for 0.007-in. wall thickness tubing
- Total weight based on "Wrap-up" factor for DC-10 precooler

Wrap-up Includes

Egg-crate headers (2)
Manifolds (2)
Sound suppression baffles
Tube support plates
Anti-fretting ferrules
Side plates
Bracing
Mounts

Does Not Include

Hot gas ducting
tubing for U-bends

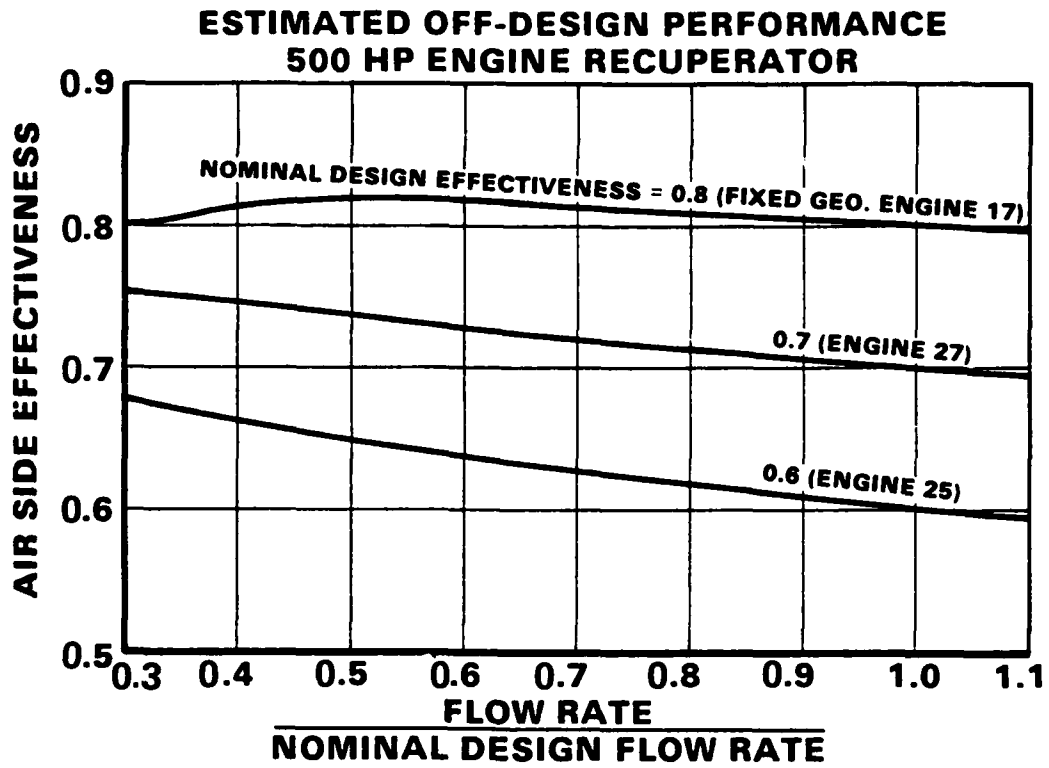


Figure 35. Tubular Unit Off-Design Performance.

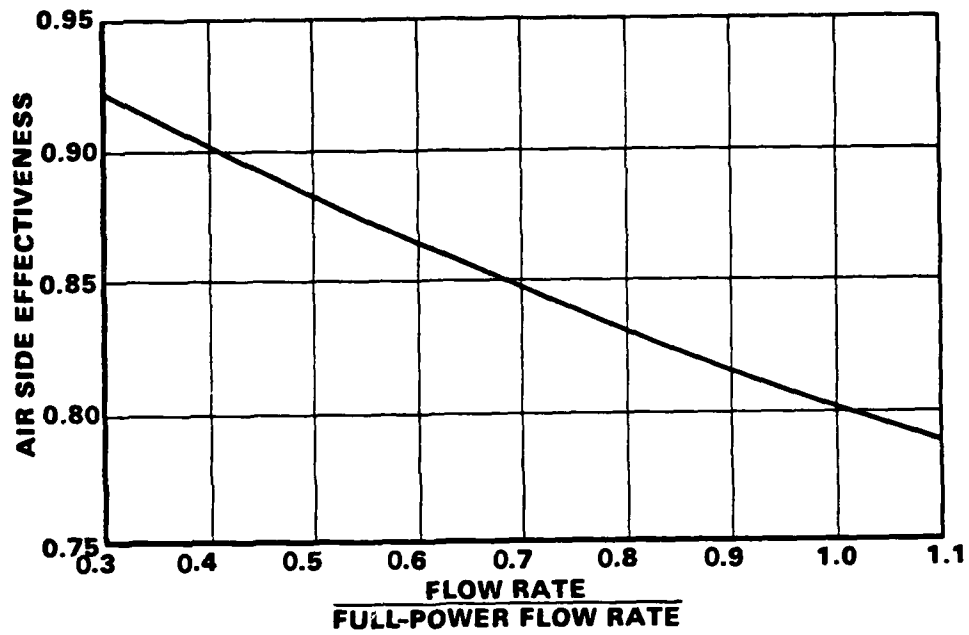


Figure 36. Estimated Off-Design Performance Plate-Fin Recuperator for 500 HP Engine No. 36.

- Total weight = 1.85 x tube weight

COST MODEL

For the parametric analysis, a cost model was developed to allow comparisons between the recuperators for the various engines. This model includes the cost elements listed in Table 19. The model is expressed in terms of material type, weight, number of tubes, tube length, and a fixed cost. U-tube construction is assumed in the interest of structural integrity. The relative-cost model is expressed as:

$$C = \{ WM + NT (K_1 + K_2 L + K_3 \text{INT} (\frac{L}{4})) + K_4 \} K_5$$

where:

C = Acquisition Cost

W = Straight tube weight, lb

M = Material factor, a function of hot side inlet temperatures

<u>Inlet Temp, °F</u>	<u>Material of Construction</u>	<u>M</u>
$t_i < 1340$	347 Stainless Steel	5.96
$t_i \geq 1340$	Inconel 625	10.43

NT = Number of tubes

K_1 through K_5 = Constants

L = Straight tube length

$\text{INT}(\frac{L}{4})$ = Rounded integer value of $\frac{L}{4}$

The unit cost from this model is based on a production rate of 300 units per year. The use of this model should be limited to comparisons rather than absolute cost evaluations.

REFINED RECUPERATOR DESIGNS

Following the parametric study, the recuperator designs were refined for the more promising engine cycles. The basic design data for the recuperators is given in Table 20. This data was provided to the engine study to aid in the final engine selection for the Phase 2 effort.

TABLE 19. TUBULAR HEAT EXCHANGER COST MODEL ELEMENTS

Component	Basis	
Tubing	Weight and material	
Dimpling	Length	
Balance of material	Weight and material	
Support plates		
Drill	Cost per plate is function of No. tubes	No. of plates is function of tube length
Ferrules		
Install ferrules		
Headers		
Drill	Per hole	
Install egg crate	Per hole	
Stacking	Per tube	
Final assembly		
Acceptance test	Fixed cost per heat exchanger	
Ship		
Profit G & A etc., based on sales to U.S. Army		

TABLE 20. REFINED RECUPERATOR DESIGN CHARACTERISTICS

Engine Number	Engine Geometry	Design Gas Flow, lb/sec	Overall Weight, lb	Core OD, in.	Core ID, in.	Overall Length, in.
34	Variable LPT	3.212	52.5	14.1	8.7	12.0
70	Variable LPT	3.137	51.3	13.9	8.5	12.0
88A	Variable LPT & IGV	3.264	49.6	12.5	7.3	13.2
*34A	Variable LPT	1.801	34.6	13.5	9.0	9.0
5	Fixed	3.508	178.2	22.3	15.5	16.9
17	Fixed	3.070	140.0	20.5	14.3	15.7
35	Fixed	2.969	115.6	16.6	10.9	17.4
41	Fixed	3.366	170.6	21.5	14.6	16.9
53	Fixed	2.961	134.7	19.8	13.6	15.7
71	Fixed	2.905	113.0	16.2	10.6	17.4

*Bypassed recuperator

PLATE-FIN CHARACTERISTICS FOR ENGINE NO. 36

To provide comparative data between plate-fin and tubular units, the detail characteristics of a plate-fin unit designed for the conditions of Engine 36 are presented here. This plate-fin unit consists of six modules; the individual module configuration is shown in Figure 37. The detail characteristics are given in Table 21, which also includes the characteristics of a plate-fin design for engine No. 34. The modules are counterflow with triangular end sections as shown. Six modules are required per engine; these are arranged around the diffuser in an annular package. The air side employs very compact offset fins (37 fins per inch); the gas side also uses offset fins with a fin count of 22 fins per inch. These are the same fins used in the GT601 recuperator and are near optimum weightwise for this application. The unit weight is 138 pounds compared with 102 pounds for its tubular counterpart.

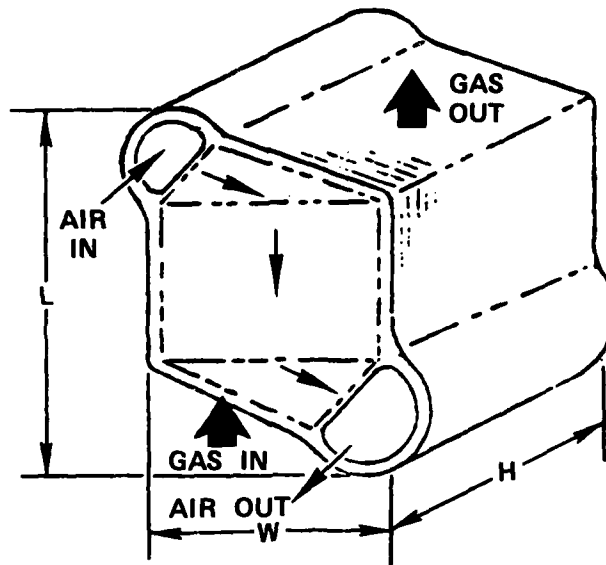


Figure 37. Plate-Fin Module Configuration for Engine 36.

TABLE 21. PLATE-FIN CHARACTERISTICS FOR ENGINE NOS. 34 AND 36.

Effectiveness	0.7	0.8
Total $\Delta P/P$, %	10	10
<hr/>		
Engine Number	34	36
<hr/>		
Module		
Width, W, in.	5.3	5.3
Length, L, in.	9.8	10.8
Stack Height, H, in.	8.3	9.7
Weight, lb	17	23
Total (6 modules)		
Weight, lb	102	138

Weight is based on stainless steel

The thermal performance of the unit is given in Figure 38. This figure shows the superior off-design performance of the plate-fin unit at reduced flows compared to its tubular counterpart. This performance characteristic can result in fuel savings for the plate-fin unit at part-power conditions. The off-design pressure-drop characteristics for the air- and gas-side fluid passages of the unit are given in Figure 39.

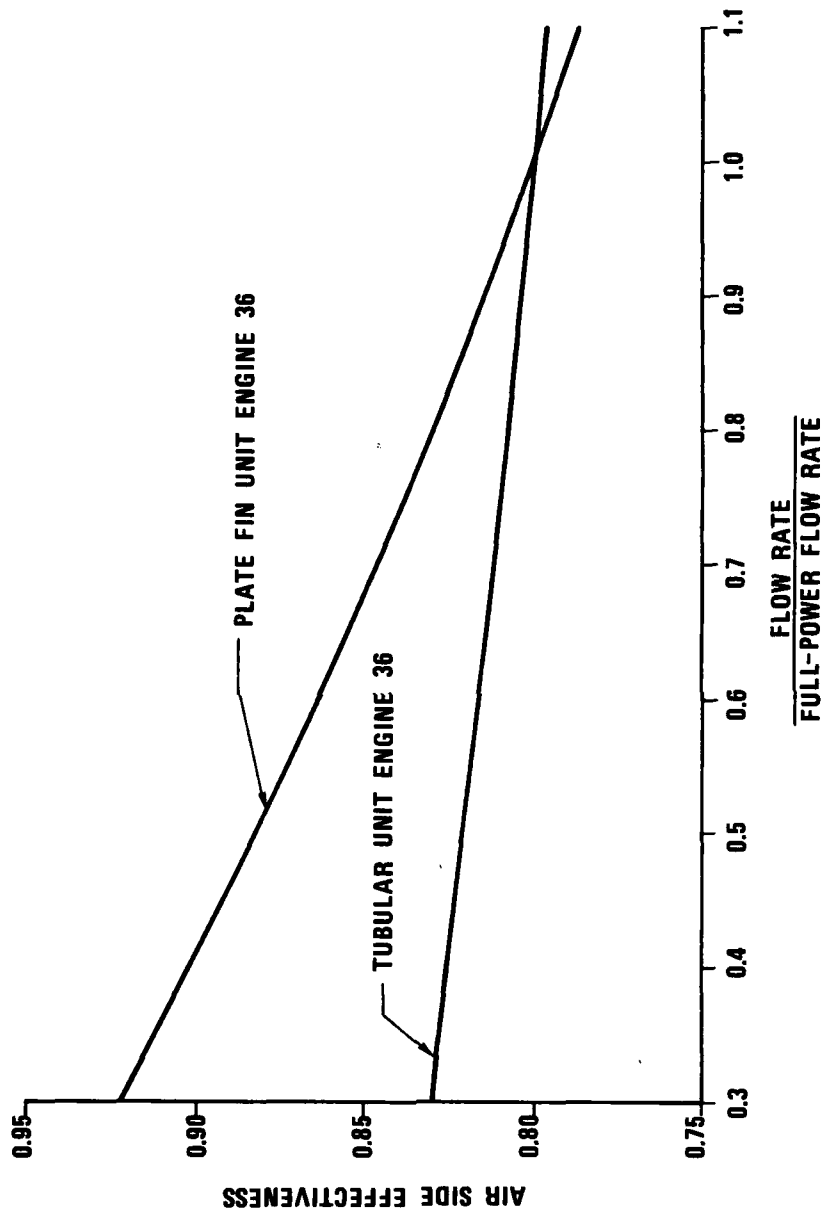


Figure 38. Estimated Off-Design Performance (Engine No. 36:
 $E = 0.8, \Delta P/P_T = 10\%$).

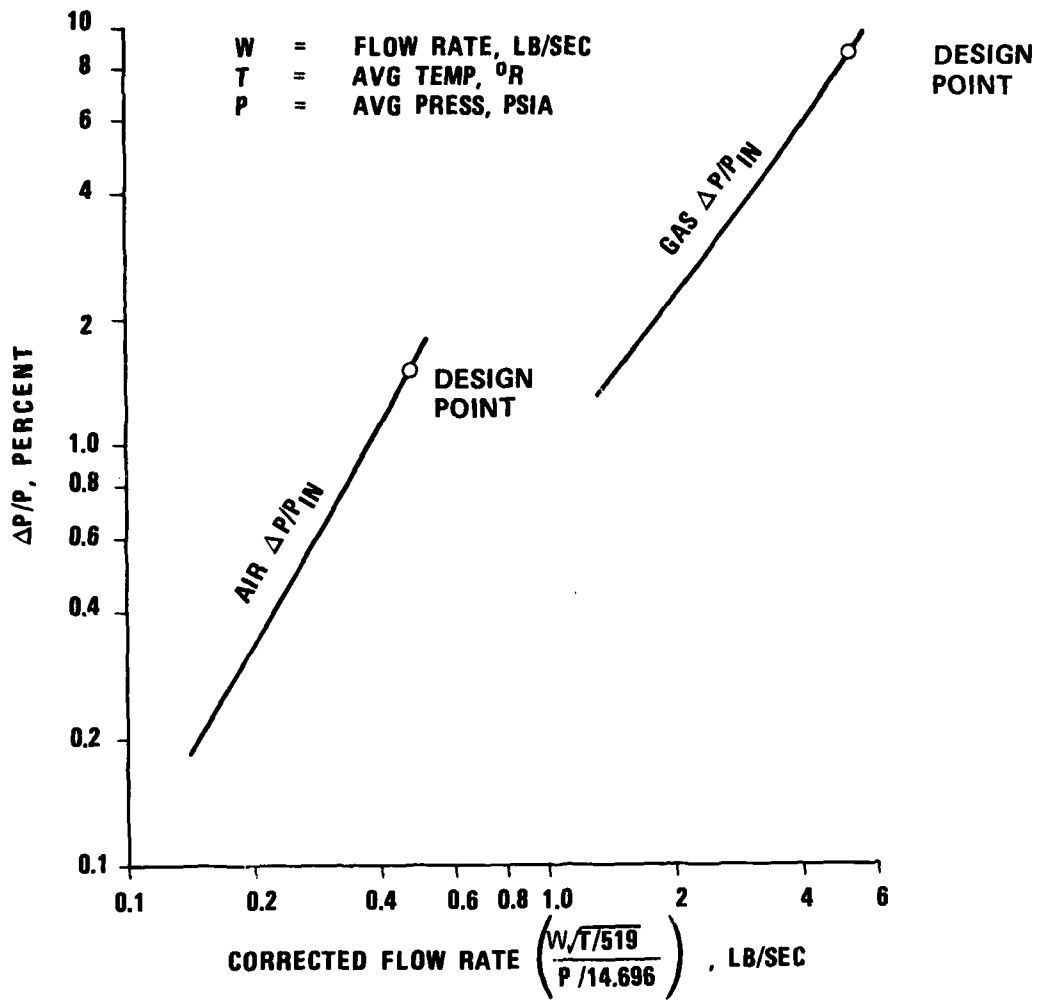


Figure 39. Estimated Off-Design Pressure Drop
 (Engine No. 36: $\Delta P/P_t = 10\%$, $E = 0.8$)

MOST PROMISING CYCLE PRELIMINARY DESIGN

A preliminary design of Engine 34 was performed to define engine and heat-exchanger configurations more representative of production designs, to specify component materials, to define weight and cost, and to prepare performance estimates for sea-level and cruise conditions.

ENGINE DEFINITION

The overall dimensions and center of gravity of the engine are shown in Figure 40, and the cycle parameters are given on Table 22. This design is essentially unchanged from that shown for Engine 34 in Figure 17. The aeromechanical design incorporates an inlet particle separator that includes an engine-driven scavenge blower for the bypass air, a spur gear set to reduce the 30,000-rpm power-turbine speed to an output-shaft speed of 20,000 rpm, a top-mounted accessory gearbox on which a starter-generator and the fuel-control package are mounted, a 10:1 pressure ratio centrifugal compressor based on a design currently under development at AiResearch for the Applied Technology Laboratory (ATL), a reverse-flow annular combustor developed by AiResearch under ATL sponsorship, a laminated, cooled, radial, high-pressure turbine also under development at AiResearch for ATL, a two-stage axial power turbine that incorporates a variable-geometry first-stage stator, and a tubular two-pass cross-counterflow heat exchanger that provides for recuperation of thermal energy from the engine exhaust to the combustor inlet air. The principal difference between the design shown in Figure 40 and that of Figure 17 is in the configuration of the heat exchanger and its attachment to the engine. The heat exchanger U-tube radii were increased for improved manufacturability, and bellows were incorporated in the ducts that connect the heat exchanger and the engine to allow for thermal growth between the engine and the heat exchanger. A more detailed description of the heat exchanger is given in the following section.

The materials selected for the principal engine components are listed in Table 23. Their selections were based on considerable experience with other engines and are representative of currently available technologies.

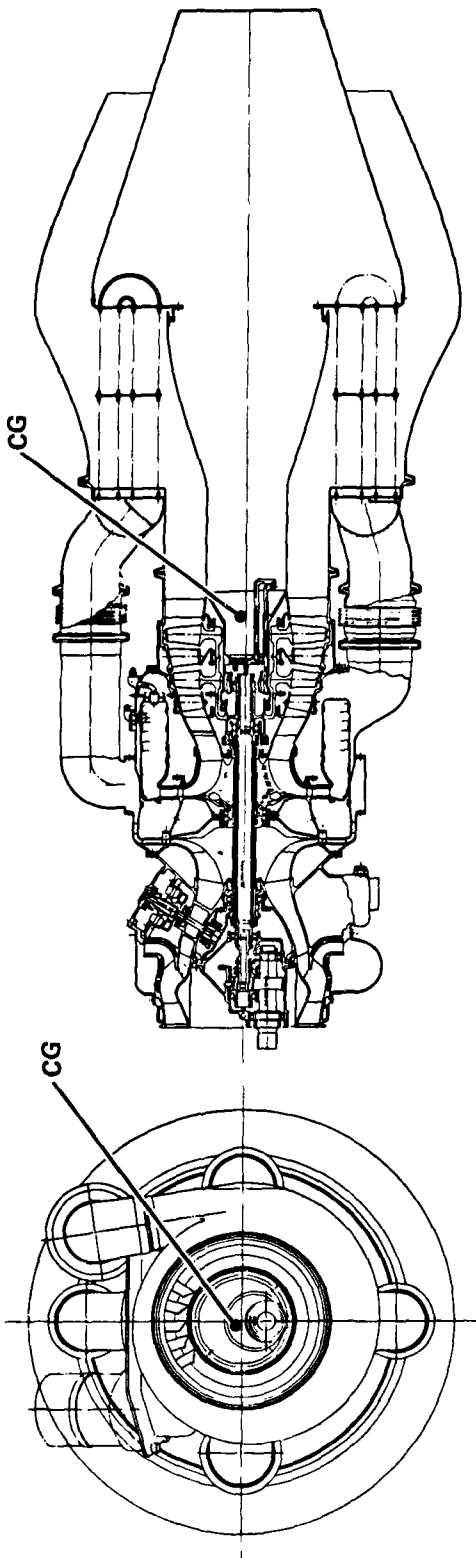


Figure 40. Turboshaft Engine TSE Model 1071.

TABLE 22. TSE MODEL 1071 CYCLE PARAMETERS
SEA LEVEL STATIC, 59°F

Output Shaft Horsepower	500	250
Compressor Pressure Ratio	10.0	5.48
Compressor Efficiency	0.768	0.773
Combustor Pressure Loss, $\Delta P/P$	0.035	0.035
Combustion Efficiency	0.998	0.998
Gas Generator Turbine Rotor Inlet Temperature, °F	2300	2300
Gas Generator Turbine Pressure Ratio	2.961	2.06
Gas Generator Turbine Efficiency	0.895	0.872
Power Turbine Pressure Ratio	2.678	2.324
Power Turbine Efficiency	0.885	0.861
Heat Exchanger Cold Side Pressure Loss, $\Delta P/P$	0.040	0.032
Heat Exchanger Hot Side Pressure Loss, $\Delta P/P$	0.060	0.025
Heat Exchanger Effectiveness	0.700	0.728
Specific Fuel Consumption, lb/hr-hp	0.425	0.437
Compressor Airflow, lb/sec	3.175	1.754

TABLE 23. TSE MODEL 1071 MATERIALS

IPS Scroll	Fiberglass
IPS Housing	Cast A356
Output Shaft	Bar H-11
Gearbox and Sump	Cast A356
Compressor Housing	Forged 15-5
Compressor Diffuser	Cast H556
Compressor Impeller	Forged Ti 6246
Combustor Case	Forged IN718
Combustor Liner	Sheet IN617
Combustor Inner Case	Forged IN718
Gas Generator Turbine Nozzle	Cast Mar-M 509
Gas Generator Turbine Rotor	Rolled Sheet Astroloy
Inter-Turbine Duct	Cast IN738
First Power Turbine Case	Forged IN718
First Power Turbine Stator	Cast IN738
First Power Turbine Rotor	Cast IN738
Second Power Turbine Case	Forged IN718
Second Power Turbine Stator	Cast IN713
Second Power Turbine Rotor	Cast IN738
Rear Frame	Cast IN713
Power Turbine Shaft	Forged IN718
Heat Exchanger Ducts	Cast H556
Heat Exchanger	Sheet IN625
Gears, Accessory Drive	Forged 6260
Gears, Output Shaft	Forged SAE 9310

Performance for the TSE Model 1071 is shown in Figures 41, 42, and 43 for static and flight conditions at three altitudes. (The performance at the sea-level static, 59°F condition is identical to that given earlier for Engine 34 on Table 6 and in Figure 13.) Also shown in these figures are the limits of operation at constant turbine rotor inlet temperature. The variable low-pressure-turbine nozzle is used to maintain a constant rotor inlet temperature as power is reduced. However, at low-power operations engine/recuperator limits are encountered, and rotor inlet temperature must be reduced. The constraining limit at

AD-A096 113

AIRESEARCH MFG CO OF ARIZONA PHOENIX
REGENERATIVE ENGINE ANALYSIS PROGRAM (REAP).(U)
JAN 81 R W HELDENBRAND, W S MILLER

F/G 21/5

DAAK51-79-C-0057

UNCLASSIFIED

21-3668

USAAVRADCOM-TR-81-D-2

NL

2 of
206 (11)

END
DATE
FORMED
4-11-81
DTIC

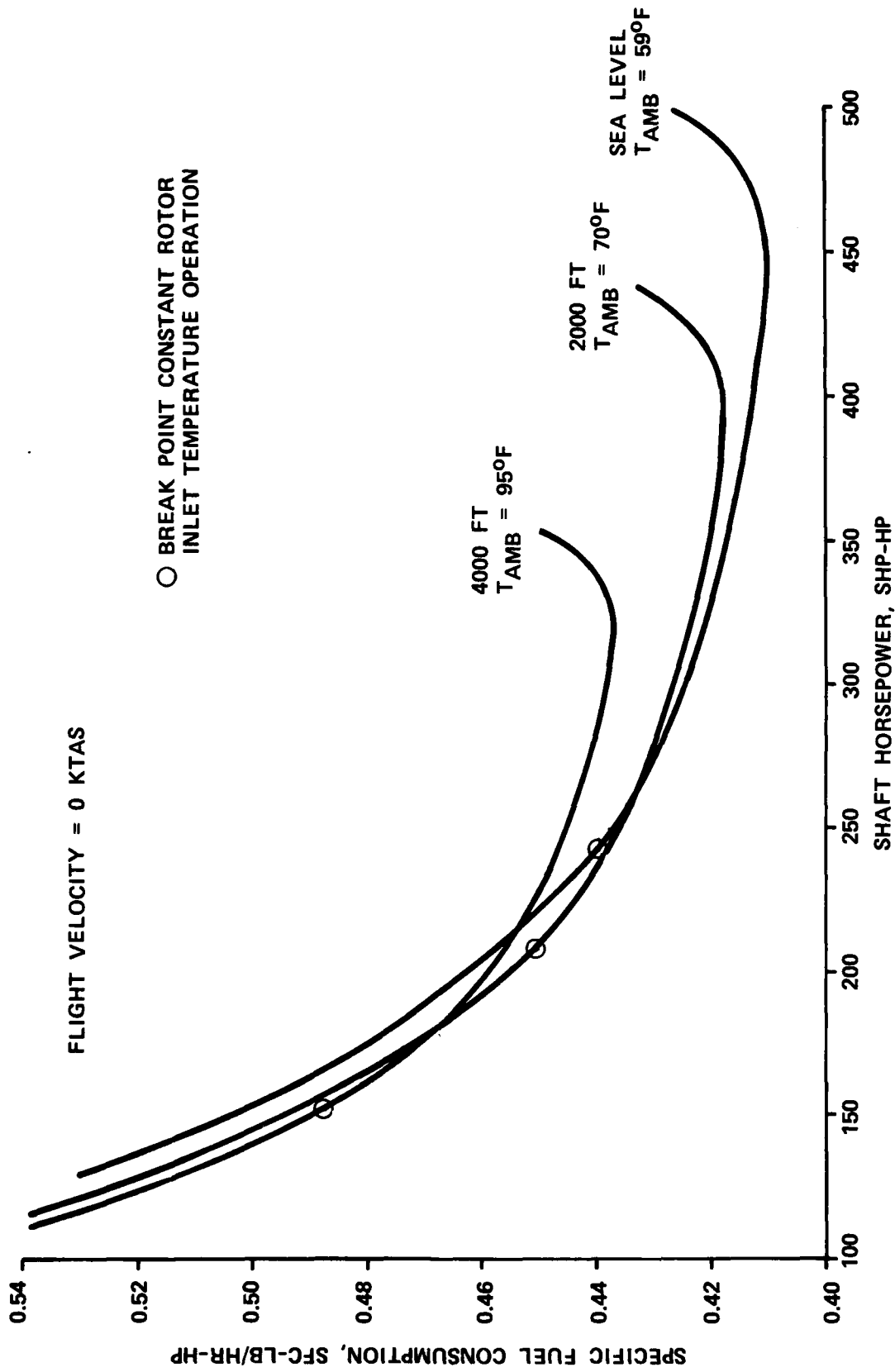


Figure 41. TSE Model 1071 Performance.

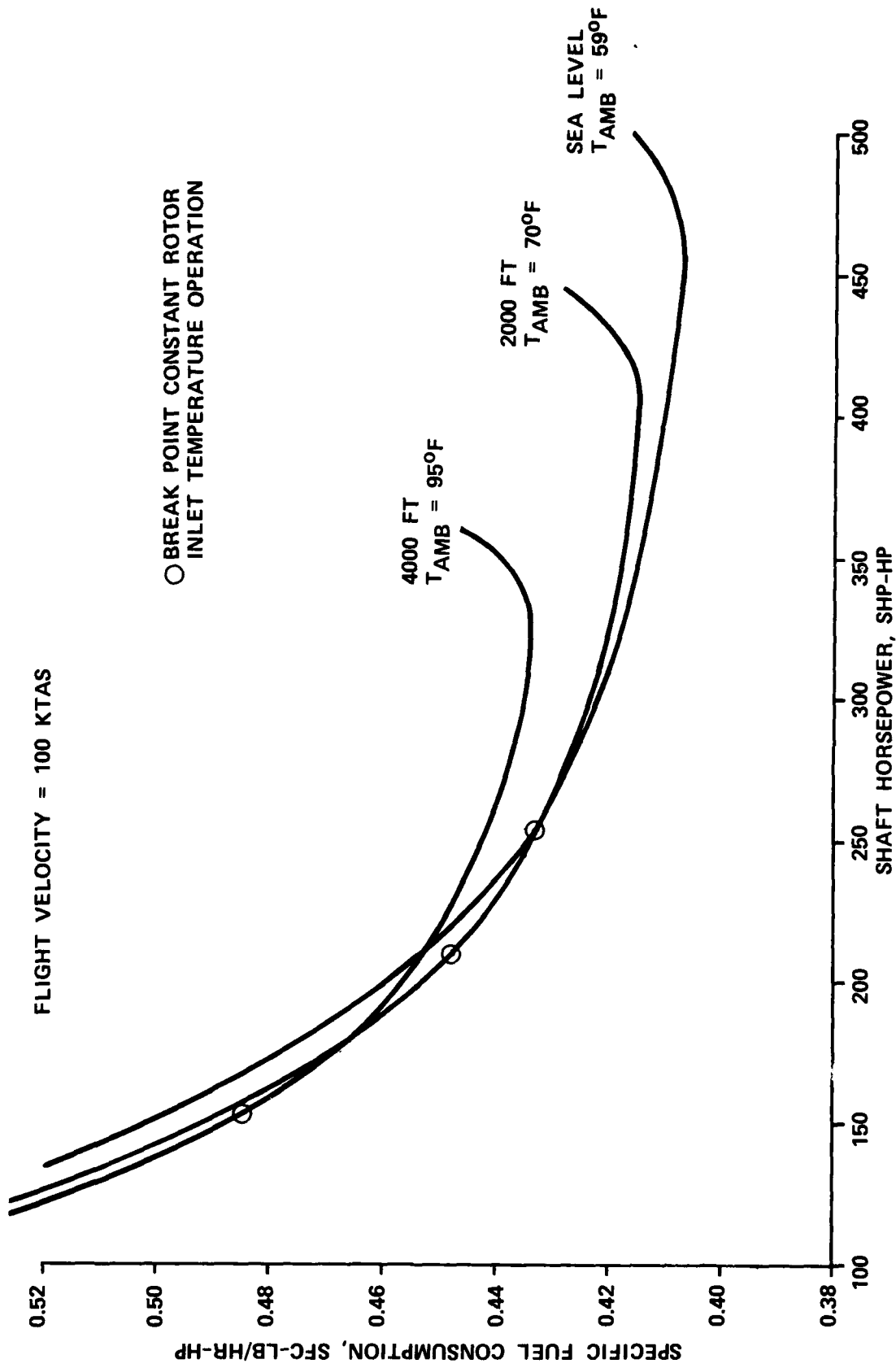


Figure 42. TSE Model 1071 Performance.

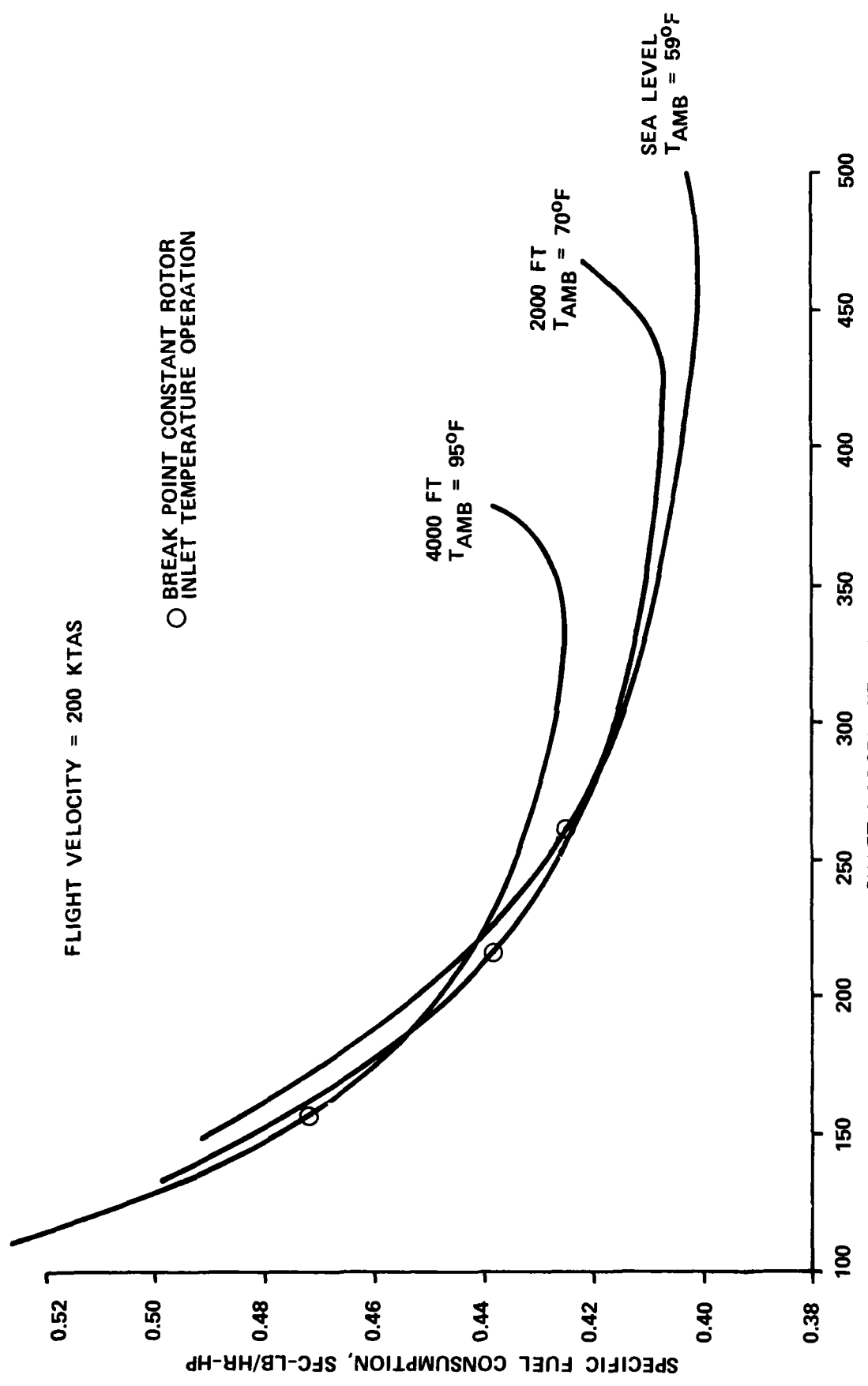


Figure 43. TSE Model 1071 Performance.

59°F sea level and 2000 feet 70°F is surge margin. The constraining limit at 4000 feet 95°F is recuperator inlet temperature. Operation at power levels lower than the breakpoint is accomplished at reduced turbine rotor inlet temperatures. Table 24 presents data from these curves in tabular form.

TABLE 24. TSE MODEL 1071 TRENDS AND LIMITS.

Flight Velocity, KTAS	Zero	100	200
At sea level, 59°F			
Maximum shp	500	500	500
SFC	0.425	0.416	0.402
SFC at 250 shp	0.437	0.435	0.429
Break Point - Constant TRIT* Operation	250	254	261
SFC	0.437	0.433	0.424
At 2000 ft, 70°F			
Maximum shp	439	445	468
SFC	0.432	0.429	0.421
SFC at 250 shp	0.435	0.434	0.426
Break Point - Constant TRIT* Operation	207	209	215
SFC	0.451	0.448	0.438
At 4000 ft, 95°F			
Maximum shp	353	360	378
SFC	0.450	0.447	0.438
SFC at 250 shp	0.445	0.443	0.434
Break Point - Constant TRIT* Operation	152	153	157
SFC	0.487	0.484	0.472

*TRIT - Turbine Rotor Inlet Temperature

The weight of the TSE Model 1071 was estimated by using component volume and material density relationships combined with known weights of externally mounted components. A breakdown of the engine weight is given in Table 25 and includes weights for a starter-generator and a hydraulic pump. The weights for these accessories are arbitrary and can vary over a wide range depending on the aircraft requirements and the capacities of the units. The engine weight shown in Table 25 is greater than the weight estimated for the parametric analysis (Table 6) or the weight estimated for the engine cross-section drawing shown in Figure 17 because, as the study progressed, additional refinements (e.g.; details of the control system; heat exchanged ducts, flanges, bellows, etc, and accessories) were included to better define the propulsion system. These details were not included in the parametric analysis since their weight would not change from engine to engine and their influence in the weight fraction of the FOM equation would be insignificant.

TABLE 25. TSE MODEL 1071 ESTIMATED WEIGHT

<u>Engine (Major Modules)</u>	
Gearbox and Inlet	29.9
Compressor	28.0
HP Turbine and Burner	48.7
LP Turbine and Exhaust	71.5
Fuel Control and Pump	19.0
Starter Generator	26.5
Hydraulic Pump	<u>4.5</u>
Subtotal	228.1 LB
 <u>Recuperator</u>	
Heat Exchanger	56.0
Ducts	10.9
Bellows and Flanges	<u>4.0</u>
Subtotal	<u>70.9 LB</u>
Total	299.0 LB

The acquisition of the TSE Model 1071, given in Table 26, was estimated on the basis of manufacturing experience with similar engines and components for a production rate of 300 units per year and a total of 2500 engines. The cost of the heat exchanger was estimated on the same production basis with the cost model described previously. Accessory costs are not included since they were not included in the 90-engine parametric study. These figures represent relative acquisition costs and are valid for comparisons within the engine families defined in this study.

TABLE 26. TSE MODEL 1071 ESTIMATED ACQUISITION COST*

<u>Engine (Major Modules)</u>	
Gearbox and Inlet	\$22,700
Compressor	13,100
HP Turbine and Burner	28,400
LP Turbine and Exhaust	31,900
Controls	15,700
Assembly and Test	<u>13,200</u>
Subtotal	125,000
<u>Recuperator</u>	
Heat Exchanger	20,000
Ducts	<u>6,300</u>
Subtotal	26,300
TOTAL	<u>\$151,300</u>

*ROM 1980\$

HEAT EXCHANGER DEFINITION

This section describes preliminary design data of a recuperator for the 500-hp helicopter engine selected from the engine parametric study. The problem statement for the recuperator summarized in Table 27 is identical to that of Engine 34 in the parametric study.

TABLE 27. RECUPERATOR DESIGN REQUIREMENT FOR PHASE III
500-HP HELICOPTER ENGINE.

Parameter	Hot	Cold
Fluid	Exhaust gas	Air
Flow Rate, lb/sec	3.212	2.792
Inlet Temperature, °F	1282.2	674.3
Inlet Pressure, psia	15.63	141.35
Effectiveness	--	0.7
Total Pressure Loss, %		10.0

DESIGN PHYSICAL CHARACTERISTICS

The designed recuperator, shown in Figure 44, is a tubular heat exchanger with tubes oriented in an axial direction and arranged in an annular bundle around the diffuser outlet. The engine exhaust gas flows radially outward, making a single pass through the heat exchanger core, while the air makes two transverse passes inside the tubes in an overall counterflow direction to the gas flow. Interpass turns on the air side are accomplished with U-tubes. While the D-shaped return pan usually results in more compact packaging, the U-tube configuration provides structural advantages in that the tubes are free to accommodate large differential thermal expansions as will be realized in this application. Due to engine exhaust-gas temperature being higher than 1340°F at part-power conditions, Inconel 625 is used as material for the heat exchanger.

The physical characteristics for the recuperator are summarized in Table 28. Ring dimpling of the tube walls is employed to promote air-stream turbulence and thus increase the inside heat-transfer coefficient.

When tubes are arranged in an annular bundle with U-tubes for interpass return, a large variation in tube spacing between the first and last tube rows results. However, a relatively uniform tube spacing can be achieved when more tubes are used in a row as the tube bundle diameter increases. This has been accomplished by connecting two rows of inner-pass tubes to a single row of outer pass where the two diameters for each pass differ greatly. For the present design, the first six rows of the inner pass are connected to three rows of the outer pass; the first two rows to the outermost row, the next two rows to the second outermost row, and so on through the sixth inner row. The succeeding six inner rows each connect to a separate outer row. Thus, 12 rows of tubes are used for the inner pass and 9 rows for the outer pass. This results in a total of 21 rows of tubes per bundle for a heat-exchanger core. Based on this arrangement, the average center-to-center transverse pitch is 0.188 inch, and the spacing between the tube rows is 0.125 inch.

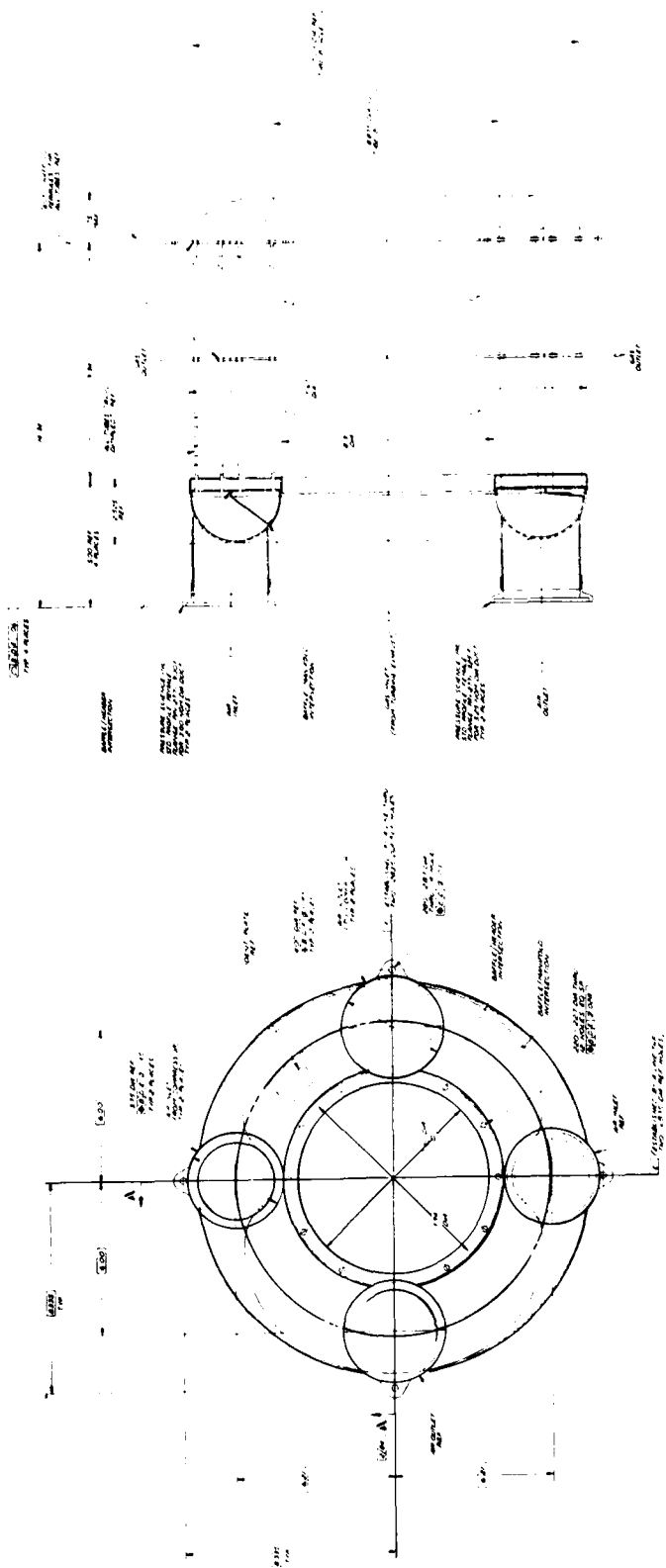


Figure 44. Recuperator Outline, Turbine Exhaust.

TABLE 28. RECUPERATOR DESIGN SUMMARY

Tube OD	0.125 in.
Tube wall thickness	0.007 in.
Tube type	Ring-dimpled
Dimple depth	0.0122 in.
Dimple spacing	0.375 in.
Number of tube rows on outer pass	9
Number of tube rows on inner pass	12
Number of passes	2
Average tube spacing	0.188 in.
Tube row spacing	0.125 in.
Total number of U-tubes	2070
Straight tube length (core only)	9.3 in.
Overall gas flow length	3.3 in.
Core ID	8.75 in.
Core OD	15.23 in.
Air-side manifold sizes	
Manifold diameter	3.5 in.
Maximum inlet flow area	3.3 in. ²
Minimum inlet flow area	0.2 in. ²
Maximum outlet flow area	4.5 in. ²
Minimum outlet flow area	1.4 in. ²
Number of inlet ports	2
Number of outlet ports	2
Inlet port OD	3.0 in.
Outlet port OD	3.25 in.
Maximum package dimensions	
Inside diameter	7.3 in.
Outside diameter	17.4 in.
Axial length	16.1 in.
Core tube weight	30.3 lb
Estimated heat exchanger weight	56.0 lb
Material of construction	Inconel 625

The recuperator manifolds are designed to achieve uniform airflow distribution to the tubes. Sizing is accomplished through use of an AiResearch computer program, the Incompressible Manifold Pressure Profile and Core Flow Distribution Analysis Program. For given input manifold sizes, the program calculates the static pressure profile along the two manifolds (inlet and outlet) and the resultant flow distribution in the core, as well as the overall pressure loss. Balanced flow conditions are obtained by running the computer program iteratively for several input values of the manifold areas.

The initial analysis indicated that separate air inlet and outlet manifolds extending over the face of the two tube passes did not provide sufficient flow area unless an excessive number of inlet and exit ports were used. More than four inlet and outlet ports are required for such a manifold arrangement to provide a reasonable pressure drop and flow distribution. A manifold using the full radius over the overall gas flow length, with a divider between the inlet and outlet passes, provides over twice the flow area and has the added advantage of providing for the use of larger inlet and exit ports. With this configuration, and using two inlet and outlet ports, uniform-flow distribution in the tubular core is achieved by employing variable-area inlet- and outlet-manifold flow passages. Z-flow (inlet and outlet ports at opposite ends of the heat-exchanger core) as used here requires the inlet-manifold flow to be accelerated to have parallel static-pressure profiles along the inlet and outlet manifolds. The inlet-manifold flow area is thus maximum at each inlet port (about 70 percent of the total manifold area) and reduces rapidly as shown in Figure 44, while outlet-manifold area increases rapidly to a maximum at the outlet port to match the inlet-manifold static-pressure profile. In addition to this manifold configuration, two inlet and two outlet ports (180-degrees apart as shown) were employed to satisfy the overall heat-exchanger pressure-loss requirement. The weight breakdown of the unit is given in Table 29.

A summary of performance at design-point conditions is presented in Table 30. The design requirements were satisfied, yielding an air-side effectiveness of 0.7 and an overall pressure loss of 10 percent; 5.8 percent for gas side and 4.2 percent for air-side pressure loss. Air-side overall pressure drop in Table 28 represents total-to-total pressure losses from inlet ports to outlet ports, including losses in manifolds and ports. Pressure losses associated with air-flow-distribution ducting to and from the ports are not included here. Gas-side pressure loss is core-pressure drop only and does not include losses associated with exhaust ducting to the atmosphere.

TABLE 29. RECUPERATOR WEIGHT SUMMARY

Description	Gauge	No. Req.	Weight (Lb)
Tubes 0.125 in. OD	0.007	630	10.65
Tubes 0.125 in. OD	0.007	600	10.75
Tubes 0.125 in. OD	0.007	840	16.11
Header Plate - In and Out	0.050	1	1.98
Header Plate - In and Out	0.050	1	1.52
Header Plate - Turning	0.090	1	2.14
Plate - Tube Separation	0.063	1	1.43
Tubes - Chaffing 0.143 in. OD	0.006	8280	1.43
Braze	--	AR	0.52
Core Assembly			(46.53)
Pan - Air, In and Out	0.050	1	2.60
Baffle	0.050	1	1.20
Duct - Air Inlet, 3 in. OD	0.050	2	0.72
Flange - Air Inlet	3 in. dia	2	0.72
Duct - Air Outlet, 3.25 in. OD	0.050	2	0.78
Flange - Air Outlet	3.25 in. dia	2	0.78
Weld and Miscellaneous	--	--	2.67
Total			56.0

TABLE 30. PRELIMINARY DESIGN RECUPERATOR PERFORMANCE SUMMARY AT DESIGN POINT

	Gas Side	Air Side
Flow rate, lb/sec	3.212	2.792
Inlet temperature, °F	1282.2	674.3
Outlet temperature, °F	933.4	1099.8
Effectiveness	0.574	0.7
Inlet pressure, psia	15.63	141.35
Core pressure drop, psi	0.90	4.71
Overall pressure drop, psi	0.90	5.92
Overall pressure drop, percent	5.8	4.2

Estimated off-design performance and pressure loss of the recuperator for a wide range of flow rates are given in Figures 45 and 46. The thermal performance is given as a function of the ratio of actual flow to the design flow. The pressure loss in terms of percentage to inlet pressure is given as a function of corrected flow for the hot- and the cold-side fluid passages of the unit. The performance predicted in Figure 45 is based on the assumption that the design-point, hot- and cold-flow-rate ratio is maintained for part-power conditions. The air-side pressure loss in Figure 46 is total-pressure differential between inlet and outlet ports, while the gas-side pressure loss is from exhaust-gas diffuser exit to the outlet of the core.

Recuperator performance at engine off-design operating conditions is estimated as follows. Air-side effectiveness is obtained from Figure 45 by simply comparing flow rate to design flow rate. Corrected-flow rates at heat-exchanger average condition are then calculated to find pressure loss from Figure 46. Fluid average temperature in the heat exchanger can be found by using the air-side effectiveness obtained above. For rule of thumb estimation, air-side pressure loss is considered to be proportional to flow to the 1.9 power, while the 1.8 power should be used for gas-side pressure loss.

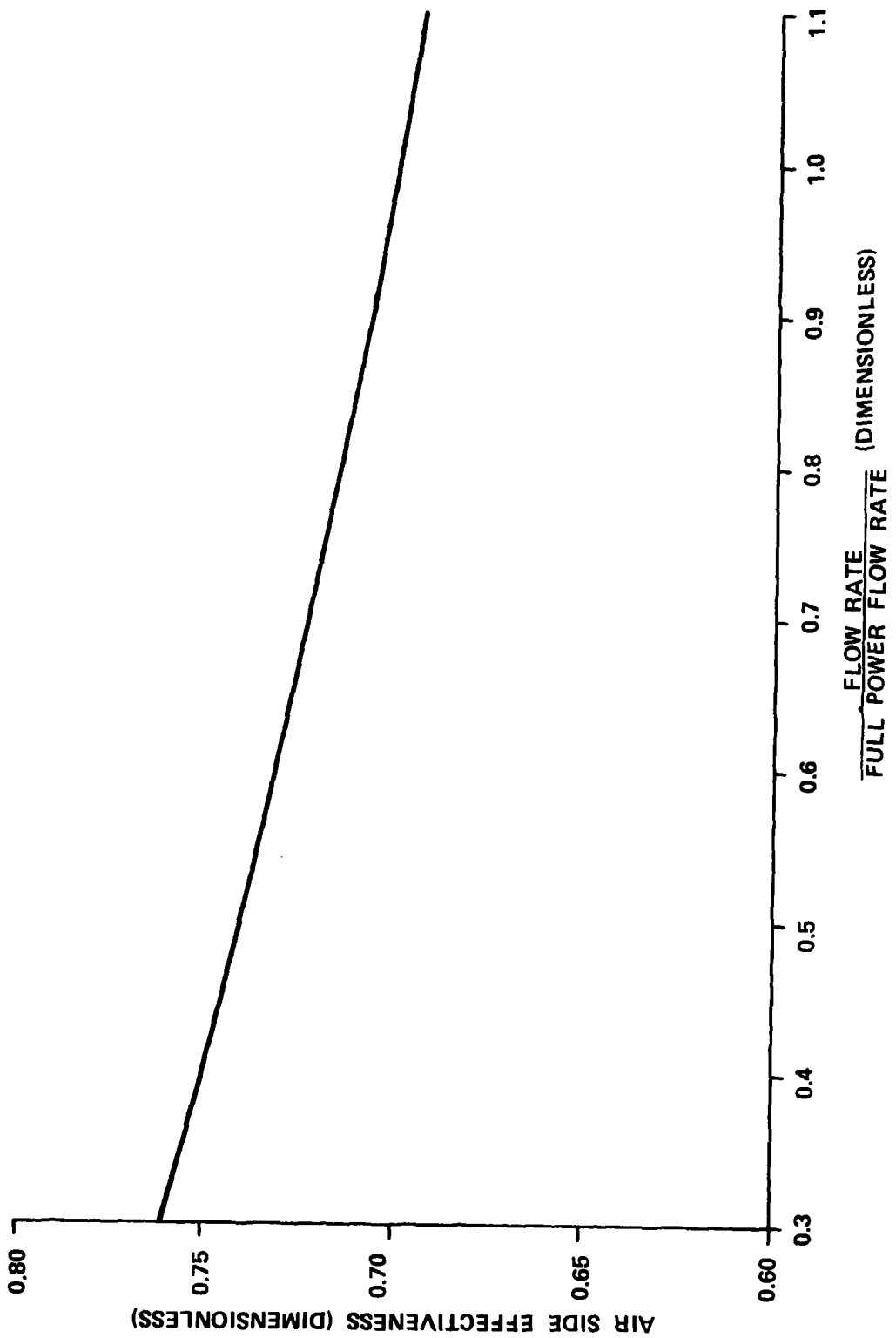


Figure 45. Estimated Recuperator Off-Design Performance.

W = FLOW RATE, LB/SEC
 T = AVG. TEMP., °R
 P = AVG. PRESS., PSIA

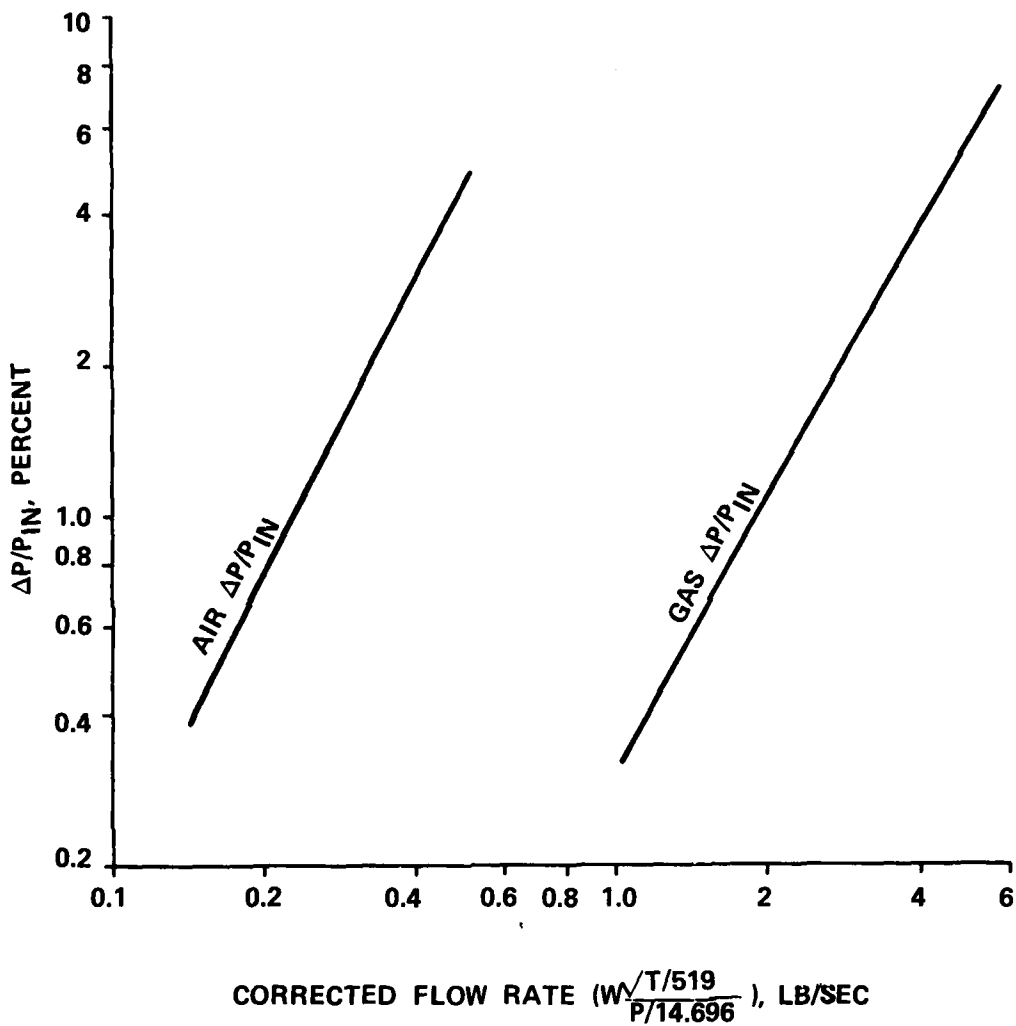


Figure 46. Estimated Recuperator Off-Design Pressure Loss.

TEN YEAR TECHNOLOGY ADVANCEMENTS

The engines evaluated throughout this study were based on technology levels consistent with those of a demonstrator engine available in 1980. As part of the study, the effects of engine and heat-exchanger component-technology improvements that could be achieved within the next 10 years were also identified.

ENGINE TECHNOLOGY

Engine-cycle analyses were performed with component improvements projected for the 1990 time period using the cycle of Engine 34 at the 50-percent power condition. Achievement of these improvements is expected through the use of advanced analysis techniques to better define the internal losses, three-dimensional flow characteristics, and component boundary layer effects. The results show that with the anticipated improvements in aerodynamic component efficiencies, a 10-percent reduction of specific fuel consumption can be anticipated, and that comparable improvements in engine weight and cost could be achieved. The overall results are given in Table 31. This table also shows the expected reduction in vehicle weight that would result from the improved SFC based on vehicle sensitivities. Vehicle sensitivities for weight and cost as functions of engine weight and cost were not available and could not be derived for this study.

TABLE 31. ESTIMATED 10-YEAR TECHNOLOGY IMPROVEMENTS.
BASED ON ENGINE 34 AT 50-PERCENT POWER

	Current	10-Year	Δ , %
Compressor Efficiency	0.773	0.814	4.1
Gas Generator Turbine Efficiency	0.872	0.896	2.4
Power Turbine Efficiency	0.861	0.882	2.1
Recuperator Effectiveness	0.728	0.728	-
Cold Side $\Delta P/P$, Percent	3.22	3.20	-
Hot Side $\Delta P/P$, Percent	2.47	2.56	-
Output Power, HP	250	250	-
Specific Fuel Consumption, (Lb/Hr)/Hp	0.437	0.392	-10.3
Estimated Total Engine Weight, Lb	299.0	242.3	-19.0
Estimated Relative Cost	1.000	0.868	-13.2
Estimated Relative Vehicle Weight	1.000	0.958	-4.2

Coincident with the aerodynamic improvements are projected improvements in materials and manufacturing techniques that will permit operation at higher temperatures, improve reliability and life, and reduce the costs of fabrication and assembly. Engine and component improvements in the areas of performance, materials, and fabrication are being pursued under numerous other government and privately sponsored programs. However, a delineation of those programs was not considered within the scope of this study, and primary emphasis has been given to the heat-exchanger technology advancements.

HEAT-EXCHANGER TECHNOLOGY

The heat exchangers designed for this study are primarily of the tubular type, with the construction material dependent on the level of hot-gas inlet temperature. These units have several advantages which include:

- Minimum weight construction
- Flexibility in packaging
- Ease of manifolding
- Reasonable volume
- Minimum thermal stress
- Pressure contained in circular passages

With so many characteristics that tend to favor the use of a heat exchanger of this type, the obvious question then becomes, what are the major drawbacks, and which of them are expected to improve a significant amount during the next 10 years. The desirable areas for improvement are:

- Lower weight
- Smaller volume
- Lower cost

WEIGHT REDUCTION

There are two potential changes in the recuperators that could lead to lower weight. One is a reduction in the amount of heat-transfer surface required, and the other would involve the use of reduced-thickness materials. In order to reduce the amount of heat-transfer surface required to achieve a given performance, an increase in heat-transfer coefficient (with no increase in pressure loss) is required. This type of improvement in heat transfer is considered very unlikely to occur during the next 10 years.

Weight reduction by use of thinner-gauge materials is also a possibility. The tube wall thickness (0.007 inch) and the wrap-up factor for this study have been chosen consistent with proven practice in aircraft today and are based on experience with several fully developed heat exchangers. However, the assumptions are, of necessity, somewhat generalized. When the full

operational spectrum is defined for the helicopter engine, including such items as vibrational and crash-loading requirements, a weight-reduction program should be identified as part of the detail design phase, and also carried throughout development.

The weight-reduction program referred to above is, however, a normal portion of flight-weight hardware development, and not a technology advancement. Significant weight savings due to the use of thinner material are thus expected only if the heat exchanger environment is more benign than that generally experienced today. The major exception to this premise would be if the advanced materials development discussed later allows significant reduction in materials thickness.

VOLUME REDUCTION

In general, the volume occupied by a plate-fin exchanger may be smaller than that of a corresponding tubular unit. However, the present study has shown that plate-fin involves a weight penalty, and thus, this alternate configuration will not be considered. In addition, no major breakthroughs in tubular heat-exchanger technology that would allow large volume reduction are envisioned. Thus, drastic change in this area does not appear to be forthcoming.

COST REDUCTION

This area is envisioned as offering the greatest potential for improvement. The tubular configuration has been chosen for all of the reasons discussed earlier, including lightweight and low thermal stresses. There are, however, drawbacks in the cost area. The manufacture of thin-gauge, small-diameter tubing inherently involves a significant amount of processing. Thus, the required heat-transfer surface tends to be relatively expensive on a per-square-foot basis. In addition, the labor content due to installing the large number of tubes tends to be high. A third area that tends to fall under cost reduction is the materials of construction. A number of the Phase I engine recuperators are constructed of Inconel due to material temperatures. This material, with the high nickel content, is not only expensive, but utilizes strategic materials. A definite need exists for low-cost, high-temperature/high-strength materials. Development of these may well show significant progress in the next 10-year period.

The major areas that are projected as subject to significant improvement by technology advancement may thus be summarized as (1) materials, and (2) low-cost fabrication methods. Each is discussed separately below.

ADVANCED MATERIALS

In general, the material operating limitations of a high-temperature heat exchanger are dictated by material damage due to creep, corrosion, or both. Thus, the ideal material will have increased resistance to these and also be available at reduced cost. The materials for a metal heat exchanger must also be readily reducible to thin gauges, and must be formable by techniques which bend, stretch, and shear. These requirements essentially dictate the use of wrought alloys, which have not improved in physical properties as rapidly as the cast alloys. It will also be noted that improved physical properties of metals at elevated temperatures are for the most part dependent upon the use of alloying constituents, which are very expensive and require increasingly unacceptable times for procurement.

At temperatures up to about 1300°F, stainless steels can be used as recuperator materials. For higher operating temperatures, superalloys are required, such as Inconel alloys 625 and 617, or Hastelloy X and Haynes 188. For recuperator operation at peak temperatures of 1500°-1600°F, Inconel 625 has sufficient strength. Of the conventional superalloys, Haynes 188 and Inconel alloy 617 have the highest creep-rupture strengths for materials that can readily be reduced to the required form and thickness of lightweight heat exchangers. Alternatives to these materials must be developed in order to reduce cost or increase operating temperatures.

8
F

Dispersion-strengthened alloys appear to be an acceptable answer for higher temperature requirements, since post fabrication heat treatment is not a necessity. However, the oxide-dispersion-strengthened alloys such as DS Nickel, MA754 (Ni-CR), and MA956 have very high mill costs, and depending on material, high fabrication costs. The high cost, of the order of \$50-60/lb for light gauges, is definitely a drawback, as is the generally low rupture ductility.

As a substitute for these costly oxide-dispersion-strengthened materials, AiResearch-California has been studying the nitride-dispersion-strengthened (NDS) stainless steels as candidates for application as high-temperature recuperator alloys. Because the NDS materials have an outstanding strength-to-cost ratio, they can potentially be substituted at a cost saving wherever a superalloy is now required. Typically, the dispersion-strengthened alloys exhibit excellent creep and rupture characteristics in high-temperature service and offer promise for extending the operating temperature of a metal recuperator to 1800°F and above.

The high strength and stability of dispersion-strengthened alloys are conferred by the incorporation of a uniformly-spaced array of a very fine and relatively insoluble (inert) dispersoid, such as an oxide, nitride, or carbide. Although the dispersoid

will tend to grow and become less finely spaced during prolonged elevated-temperature service, growth is generally quite slow. This is in contrast to conventional precipitation-hardened superalloys that lose strength at elevated temperatures because of dissolution of the precipitate.

Historically, dispersion-strengthened alloys have been expensive to produce because of complex procedures needed to ensure uniform particle distribution. However, a technique has been identified as having potential for significantly lowering the cost of production. By use of a gaseous ammonia treatment at high temperature, a stable TiN dispersoid is created, leading to the pronounced strengthening inherent to dispersion-strengthened metals. The nitriding process is analogous in almost all respects to the internal oxidation process, but is several orders of magnitude faster. The treatment time is only a few minutes for foil thicknesses (approximately 0.010 in. and less) and is relatively inexpensive.

Figure 47 presents the results of applying the high-temperature nitriding treatment to a steel based on 18Cr-12Ni-2Ti (a low-carbon, high-titanium modification of Type 321). Creep properties are shown in Figure 48, where the Larson-Miller master curve technique is used to compare current heat-exchanger alloys with the NDS alloy. This figure also indicates the temperatures at which the various materials may be operated for 10,000-hours life. The advantage of the NDS material is readily apparent. Because the NDS approach requires a minimum of costly strategic elements, application of this technology will be very cost-effective, both in recuperator manufacture and energy savings. Further, as evidenced by data in Figures 47 and 48, the NDS alloy will provide a strength advantage when substituted for superalloys such as Inconel Alloy 625. This advantage becomes more pronounced as the temperature is increased.

8
B

In work to date, the simple austenitic stainless steel based on Type 321 has exhibited the best overall combination of ease of nitriding and high-temperature strength. This material is well characterized relative to the required nitriding temperatures and times as a function of titanium level and gauge. Since this composition represents a relatively minor modification of an existing grade of stainless, minimum risk would be incurred in scaling up to steel mill production levels. This is a critical point, as it will be only through use of conventional mill practices that the cost of finished tubing or strip at recuperator gauge can be held to a reasonable premium over the base for the existing grade. Although some adjustments in chemistry may be necessary, e.g., to compensate for coatings, use of a fairly standard alloy system makes it possible to address the implementation of an NDS alloy to a high-temperature heat-exchanger system on a near-term basis.

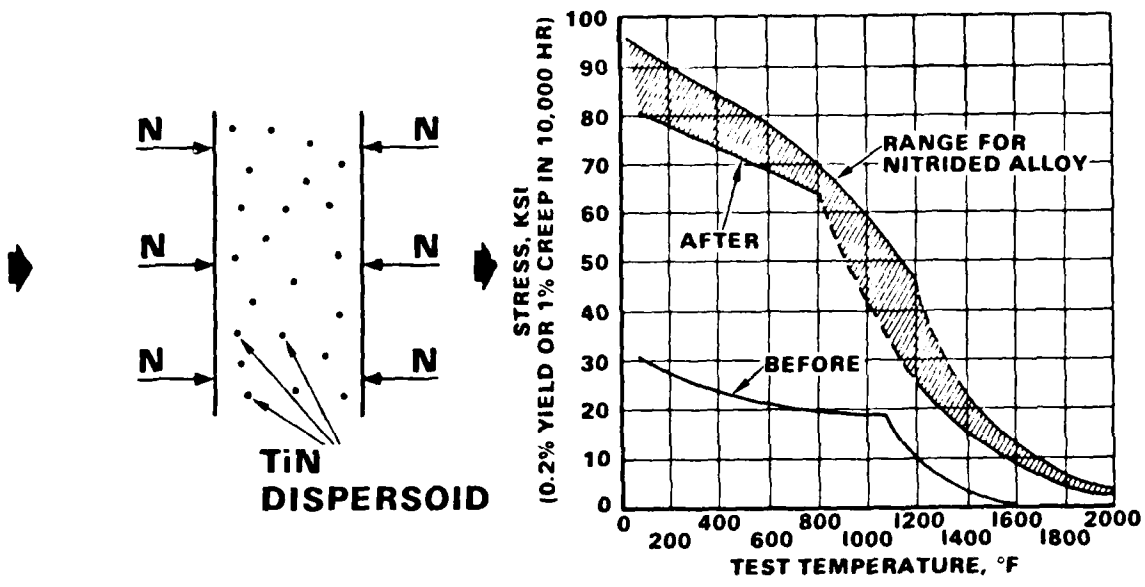
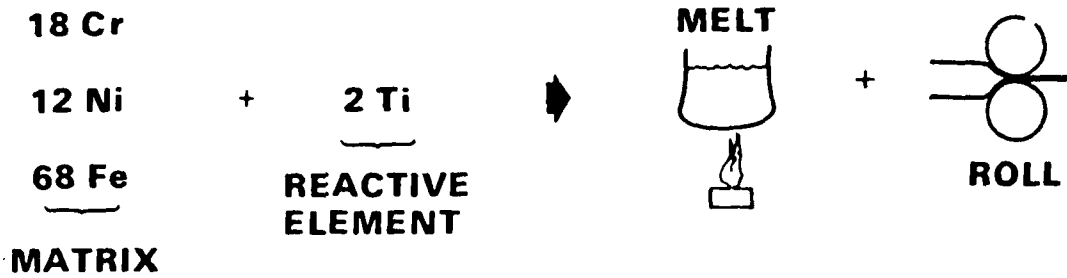


Figure 47. Application of High-Temperature Nitriding Process to Modified Type 321 Stainless Steel Sheet.

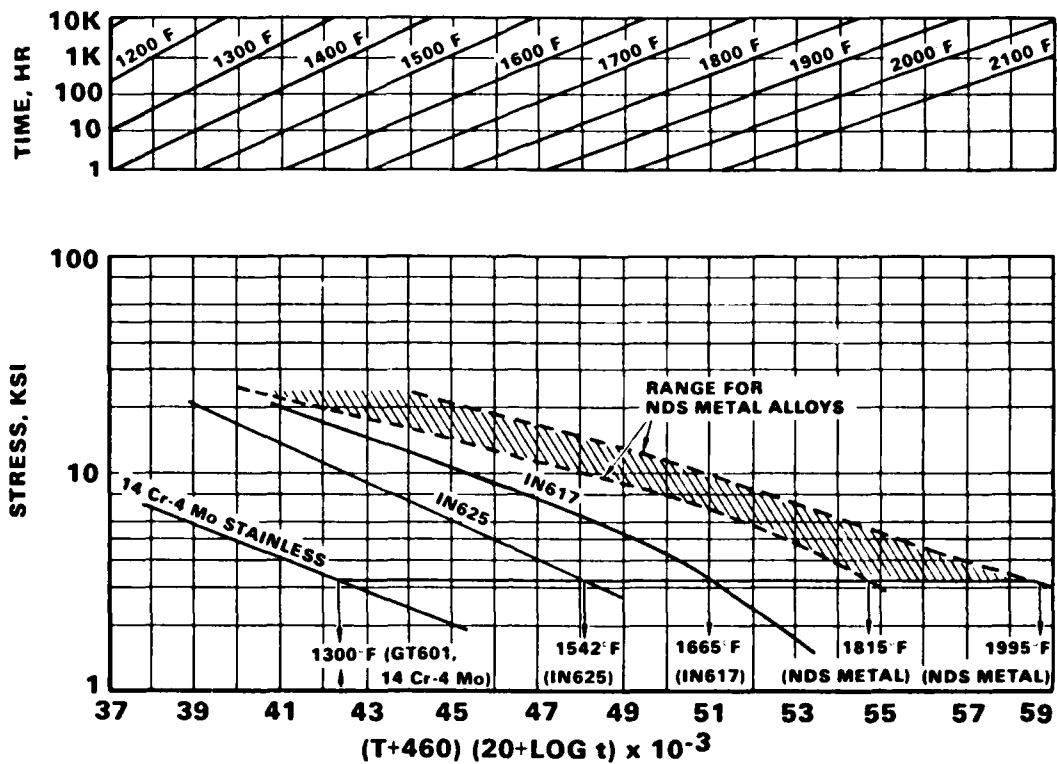


Figure 48. Master Rupture Plot Showing Temperatures for 1-Percent Creep in 10,000 Hours.

In addition to development of material and recuperator fabrication processes, a coating process is required in order to provide oxidation and corrosion resistance at the operating temperatures. One promising method is to coat the entire heat exchanger, after fabrication, by a gaseous diffusion treatment process such as chromizing or aluminizing. It would not be satisfactory to pretreat the material prior to shearing because of the untreated raw edges that would be present in the final assembly.

Although chromium is known to confer resistance to hot-corrosion damage (especially in iron- and cobalt-based alloys), high chromium surface treatments generally have not found application in gas turbine engines because of the volatility of the protective oxide in high-velocity gas. In a heat exchanger, however, gas velocities are low, typically less than Mach 0.2 at full power, and even lower at part power, where the higher temperatures are encountered. This potentially allows the use of a simple chromizing treatment for service in the 1800°F range, which can be applied to a fully assembled heat exchanger without leaving untreated areas. With normal diffusion times for chromizing and with a typical thin-gauge heat-exchanger material, the chromium will become a part of the metal (unlike a coating). This would typically raise the material composition at the surface to over 35-percent chromium. Such a technique will use the minimum amount of chromium to provide the maximum resistance to the environment. A diffusion coating of chromium should be compatible with the TiN particles; the normal treatment time of 5 to 6 hours at a temperature of 1900°F will not alter the strength of the base NDS alloy.

LOW-COST FABRICATION METHODS

The tubular heat exchanger possesses many advantages. It is "all prime surface", it contains pressure in the "ideal" round passage, and thermal stresses are minimized by the U-tube configuration. However, this type of heat exchanger is inherently expensive. Small diameter, thin-wall tubing costs several dollars per square foot of heat-transfer surface. A considerable amount of labor is also involved in installing the tubes. The most unfortunate characteristic is that costs do not tend to be reduced greatly as production is increased. Thus, alternate designs should be evaluated from a cost versus engine penalty standpoint.

The plate-fin type of construction should be evaluated in depth from this standpoint. Another type of construction that should also be compared is a plate-type "all prime surface" unit. In this type of construction, the heat-transfer surface is formed by stamping individual plates and then stacking them together, which is an extension of the AiResearch technology employed in formed-tube-plate heat exchangers. This approach tends to provide the required heat-transfer surface with several hundred

pieces as opposed to several thousand tubes, and thus may conceptually reduce assembly labor. Both analytical and fabrication studies are presently being pursued at AiResearch on other engine applications.

FUEL SENSITIVITY

As discussed previously, the figure-of-merit (FOM) equation used in the 90-engine cycle parametric study described previously was based on a military attack mission of approximately 2.5-hours duration with fuel cost fixed at \$0.60 per gallon. As the study progressed, and as domestic fuel costs increased, it was decided to investigate the effects of other mission types and of higher fuel costs. Accordingly, two additional FOM equations were developed by AiResearch, and two other equations were acquired from Bell Helicopter Textron. These five equations are presented in Table 32. Also shown are the mission and fuel-cost assumptions. The equations were normalized so that the three coefficients on the SFC, weight and cost ratios would equal unity when summed. In each case, the coefficient on the SFC ratio was predominant and was higher for higher fuel costs or longer missions. This trend resulted in considerably lower emphasis on weight and cost.

Each of the five equations in Table 32 was used to calculate the FOM for all 90 of the engines in the parametric study to determine the sensitivity to fuel. It was assumed that the increasing value of the SFC coefficient (K_1) in the equation was a valid measure of either a longer-mission duration or an increase in fuel cost. From these calculated FOMs, the engines with the 10 lowest FOMs were tabulated, and their FOM position was plotted versus the value of the SFC coefficient in each equation. This plot, shown in Figure 49, presents the engines with the lowest FOM in Position 1 and successively higher FOMs in higher numbered positions. Each point on the plot is identified with its engine number, and each point is coded to identify heat-exchanger effectiveness -- open points, $\epsilon = 0.6$; points with plus signs $\epsilon = 0.7$; solid points, $\epsilon = 0.8$.

Two major items emerged from the plot of Figure 49. First, the choice of Engine 34 as the most promising cycle was confirmed. The plot shows that the figures of merit for both Engines 33 and 34 were among the lowest 10 FOMs for each equation, and although Engine 33 ultimately had the lower FOM of the two engines, this fact was not revealed until the study had progressed to the evaluation of the three promising cycles, and Engine 34 had already been selected for additional study.

The second item was the trend toward higher heat-exchanger effectiveness, as the SFC coefficient increased in value, in spite of the higher heat-exchanger weights and costs. This trend is more clearly shown in Figure 50, in which the average values of effectiveness, SFC, relative weight, and relative cost are shown versus the SFC coefficient, K_1 , for each group of 10

TABLE 32. FIGURE OF MERIT (FOM) EQUATIONS

<u>AIRESEARCH</u>	$FOM = K_1 \frac{SFC}{SFC_{BL}} + K_2 \frac{WT}{WT_{BL}} + K_3 \frac{\$}{\$_{BL}}$				
ATTACK MISSION: (2.5 HOURS) (1977 FUEL: \$0.60/GAL)	FOM = 0.55	+	0.14	+	0.31
	$\frac{SFC}{SFC_{BL}}$		$\frac{WT}{WT_{BL}}$		$\frac{\$}{\$_{BL}}$
CRUISE MISSION: (3.4 HOURS) (1977 FUEL: \$0.60/GAL)	FOM = 0.56	+	0.19	+	0.25
	$\frac{SFC}{SFC_{BL}}$		$\frac{WT}{WT_{BL}}$		$\frac{\$}{\$_{BL}}$
ATTACK MISSION (2.5 HOURS) (1980 FUEL: \$2.00/GAL)	FOM = 0.729	+	0.153	+	0.118
	$\frac{SFC}{SFC_{BL}}$		$\frac{WT}{WT_{BL}}$		$\frac{\$}{\$_{BL}}$
<u>BELL</u>					
100-MILE RADIUS MISSION (1975 FUEL: \$0.50/GAL)	FOM = 0.63	+	0.30	+	0.07
	$\frac{SFC}{SFC_{BL}}$		$\frac{WT}{WT_{BL}}$		$\frac{\$}{\$_{BL}}$
200-MILE RADIUS MISSION (1975 FUEL: \$0.50/GAL)	FOM = 0.83	+	0.16	+	0.01
	$\frac{SFC}{SFC_{BL}}$		$\frac{WT}{WT_{BL}}$		$\frac{\$}{\$_{BL}}$

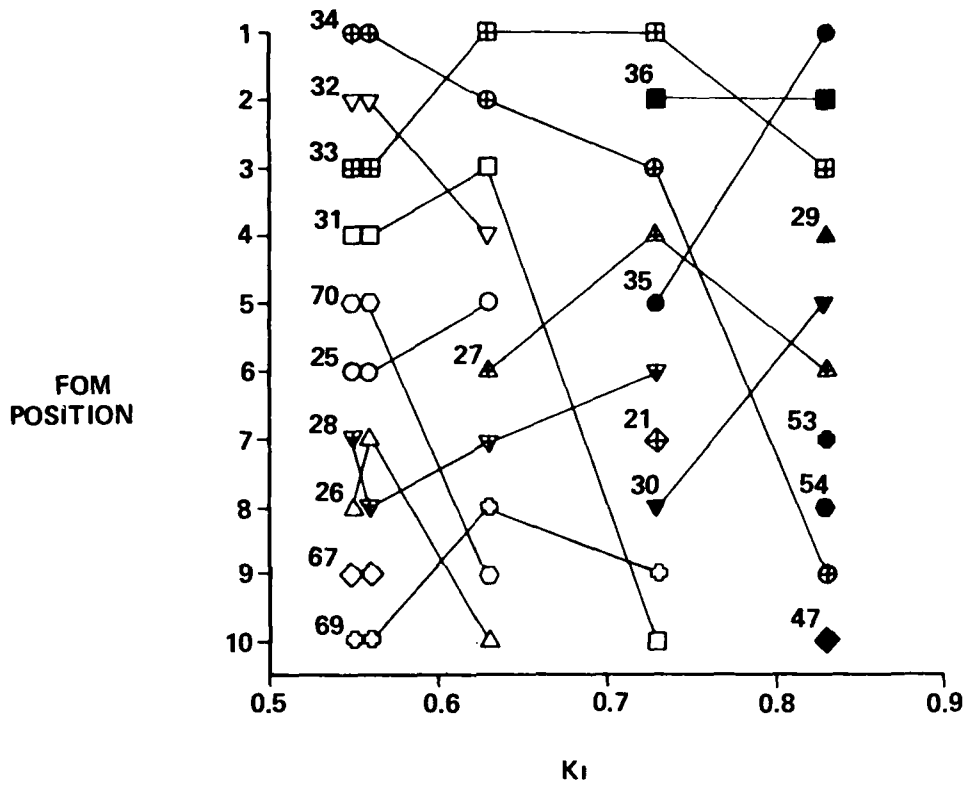


Figure 49. Fuel Sensitivity.

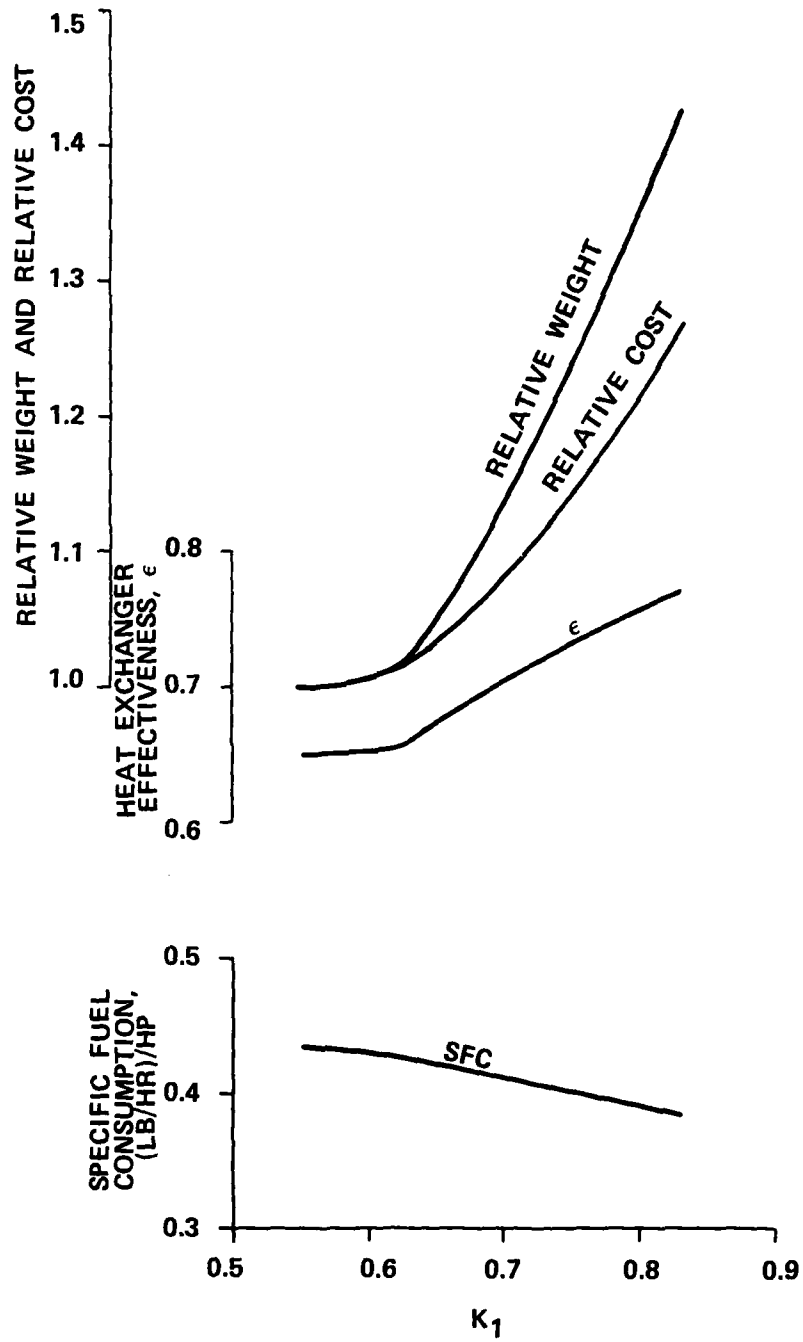


Figure 50. Fuel Sensitivity Trends.

engines shown in Figure 49. A review of these trends led to the following conclusions:

- As fuel (either cost or necessity for a long mission) becomes more critical, a higher heat-exchanger effectiveness, with the resulting lower SFC is desirable if not mandatory.
- As heat-exchanger effectiveness is increased, propulsion-system weight and cost are not penalizing factors since their influences on the FOM (life-cycle cost) diminish rapidly.

Accordingly, since the influence of weight was far less significant, it was considered worthwhile to again investigate the merits of the plate-fin heat exchanger. The cycle of Engine 36 was used for this investigation. Engine 36 is identical to Engine 34 except that the heat-exchanger effectiveness is 0.8 rather than 0.7. A plate-fin heat exchanger was configured for the engine, and the five FOM equations were calculated using weight and cost estimates for the plate-fin configuration. The results are plotted versus the FOM SFC coefficient, K_1 , in Figure 51. At the lower values of K_1 , the plate-fin unit has a slightly lower FOM; however, as K_1 increases, the advantage changes to the tubular unit. An examination of the FOM equations shows that as K_1 increases, K_2 (the weight coefficient) remains relatively constant (changing only from 0.14 to 0.16, ignoring the spike to 0.30), while for K_3 the cost coefficient drops drastically from 0.31 to 0.01. Therefore, even though the tubular heat exchanger is 60 percent more costly than the plate-fin unit, it is the plate-fin unit's weight in the weight fraction of the FOM equation that results in the higher FOMs for the plate-fin configuration.

It is acknowledged that the differences between the FOMs for the tubular and plate-fin units in Figure 51 are small -- differing by a maximum of 3 percent at the highest K_1 . Therefore, at this point, it appears that the selection of one or the other becomes a matter of judgement by the airframe manufacturer based ultimately on installation characteristics for a particular vehicle. The configuration of the tubular unit, as shown in Figure 40, was acknowledged to be acceptable, and in fact, attractive. The configuration of the plate-fin unit configured for Engine 36 is somewhat less attractive in that it consists of six modules, as shown earlier in Figure 37, and arranged around the engine exhaust in an annular array, as described previously. The maximum diameter for this annular package would exceed that of the tubular installation by a minimum of 3 inches, and would result in a somewhat higher wrap-up weight due to the larger-diameter ducts required for the exhaust gas and to the larger number of interconnecting ducts required for the compressor-discharge air.

ENGINE COMPRESSOR 36
 1-STG 10:1 P/P
 2300°F

	TUBULAR	PLATE-FIN
T ₄	0.8	0.8
H-X	0.1	0.1
ε	16.0*	10.8**
ΔP/P	102	138
LENGTH, IN.	1.000	0.634
WEIGHT, LB.		
REL COST		

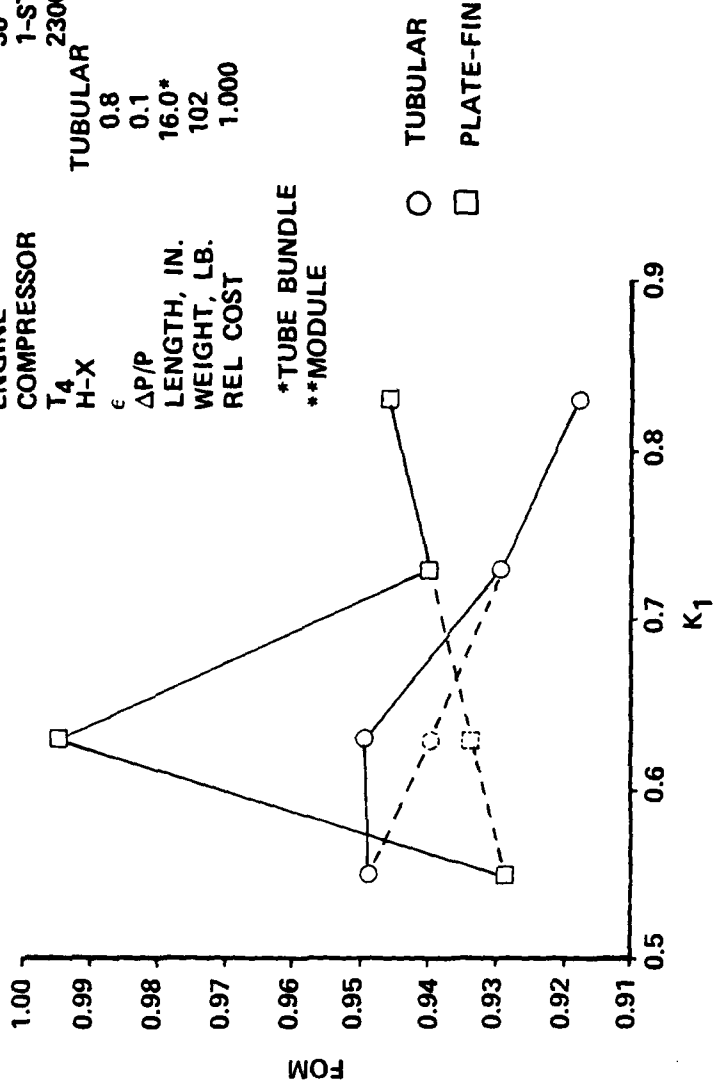


Figure 51. Heat-Exchanger Trades.

INSTALLATION CHARACTERISTICS

The integration of a unique propulsion system such as that evaluated in this study involves the consideration of a larger than usual number of installation characteristics or features, including:

- (a) Mounting loads
- (b) Accessibility
- (c) Maintenance
- (d) Accessory pads
- (e) Survivability
- (f) Starting methods
- (g) Inlet Particle Separator
- (h) Inlet/Exhaust losses
- (i) Bleed air capability
- (j) IRS/RCS/Noise

Discussions with airframe manufacturers have indicated that, while some of these considerations are generic in nature and therefore applicable to most helicopter engine installations, some, because of the introduction of the heat exchanger, require extra consideration. It was not the purpose nor within the scope of this study to provide definitive solutions for each of the potential problems posed by these features. However, the following paragraphs offer brief discussions of alternative considerations for each.

A single-engine vehicle will normally have the engine mounted aft of the mast. The heat exchanger will obviously impose an extra aft center-of-gravity load and must be accounted for in the overall vehicle design. However, in a twin-engine vehicle, it has been suggested by Bell, that engine mounts on either side of the main transmission with right-angle drives into the transmission may bring the center-of-gravity of the dual propulsion system forward sufficiently to place it in line with the mast. Of course, the vehicle vibratory and landing forces must be considered in the design of the heat exchanger and its attachments to the engine and the vehicle.

Items (b) through (d), above, are closely interrelated. The survivability (or vulnerability) of the engine is not only a function of its location on the vehicle but also a function of the location of its controls, accessories, and other vital components, including, in this case, the heat exchanger. The airframe manufacturer must decide, in conjunction with the engine manufacturer and the ultimate customer, whether top-mounted accessories

are desirable, whether heat-exchanger armor protection is necessary, whether shielding from ground arms is more important than maintenance accessibility, and on a host of other trade-offs, before the final airframe/engine configuration can be established.

The 500-hp class engines are normally started with a battery energy source and an electric starter-generator. However, batteries are heavy items, and, depending on the electrical requirements of the vehicle, it may be advantageous to employ either an air-bottle/air-turbine-motor system or an accumulator/hydraulic-motor system. Again, depending on the vehicle mission, military or civilian, and accessibility to alternative ground power units, a trade-off may be warranted.

For this program, the inlet-particle separator was considered an integral part of the engine. This may also be true of some civilian operations. However, other civilian operations, e.g., business flights or inter- or intra-city shuttles, would not encounter such foreign-object contamination and would benefit by eliminating the inlet-particle separator and its attendant losses.

Inlet and exhaust losses are other items that require close coordination between the airframe and engine manufacturers. Inlet designs can be either the plenum or pitot type and are largely a function of the engine location. However, with the heat exchanger and its inherent back pressure on the engine, extreme care must be employed to minimize exhaust losses. It is obviously advantageous to utilize any remaining energy in the engine exhaust in a jet nozzle to aid forward propulsion as indicated with the concept shown in Figure 40. This, of course, requires that the exhaust gas turn 90 degrees to enter the heat-transfer matrix and an additional 90 degrees after leaving the matrix to enter the nozzle. It would be possible to reconfigure the matrix to reduce or eliminate these turns; however, any such configurations would involve trade-offs of additional weight, cost, and installation complexity. Alternative exhaust schemes include upward, sideward, or downward exit configurations. Upward exits introduce the possibility of interference from main rotor down wash pulses. Side exits could compromise the rear rotor field. Side and down exits may cause interference with personnel during ground operations.

Bleed-air capability was not considered for the engine cycles evaluated in this study; nevertheless, any analysis of future helicopter requirements must include provision for the vehicle air conditioning, deicing, or other pneumatic system needs.

The addition of a heat exchanger to the engine exhaust offers distinct advantages with respect to the vehicle infrared (IR)

signature, the aft radar cross section, and the exhaust noise. Reducing the exhaust-gas temperature and blocking the direct view of the hot turbine and exhaust duct metal with the heat exchanger effects a major reduction in the IR signature. Further reductions might be achieved with the introduction of bleed or ambient air to the exhaust gas. While the radar cross section (RCS) is a combined function of the configuration and the materials, a significant reduction in RCS will be effected by eliminating the line-of-sight view of the final turbine stage. The heat exchanger might also be designed to act as an exhaust muffler to reduce the engine core (or combustion) noise. Helicopter noise has recently been the subject of FAA rule making and will require additional study for future applications.

In summary, a review of the Engine 34 configuration by airframe manufacturers did not reveal any major compromises associated with recuperated engines with respect to weight, volume, or location. While several installation options are available, none of the options appears to be objectionable to these airframe manufacturers with respect to the overall vehicle characteristics, including configurations, handling, drag, accessibility, or maintainability.

SPECIAL DEVELOPMENT ASPECTS

The study revealed several areas in addition to the usual performance and durability problems that are pertinent to the engine and the heat exchanger that would require special emphasis during development. These include:

- (a) Scaling
- (b) Transient operation
- (c) Infrared reduction
- (d) Noise
- (e) Survivability/Vulnerability
- (f) Heat exchanger materials
- (g) Heat exchanger cleaning

Scaling of small, high-operating-temperature turbine engines can pose some unique problems. Particular consideration must be given to the compressor and turbine running clearances (which do not scale) and, in the case of scaling to a smaller size, to the design of the turbine cooling scheme, which can be difficult at best for small turbines. Adequate cooling is required for good component life; however, the cooling air imposes a penalty on the overall cycle, and a careful trade-off is necessary. Other scaling problems include leakage control, Reynolds number, and boundary-layer effects in the aerodynamic components. These latter items are, of course, unique to individual designs. However, the components used as the baselines for this program are within 20 percent of the size required for the selected REAP engine. For example, the design corrected air-flow rate of the tested single-stage 10:1 pressure ratio compressor used as a baseline for Engine 34 is 2.8 pounds per second. Scaling this compressor to the 3.26 pounds per second flow rate required for the REAP engine without performance loss is entirely feasible. This is equally true of the laminated turbine and the combustor since their original design flow rate is also 2.8 pounds per second. In general, scaling of overall engine parameters within a moderate shaft power tolerance band (e.g., +20 percent of a baseline (BL) value) can be performed for preliminary-design purposes with the following relationships for common configurations and technology levels:

Performance: SFC = Constant

$$\text{Weight: } WT/WT_{BL} = \left[\text{SHP/SHP}_{BL} \right]^{1.00}$$

$$\text{Length: } L/L_{BL} = \left[\text{SHP/SHP}_{BL} \right]^{0.40}$$

$$\text{Diameter: } D/D_{BL} = \left[\text{SHP/SHP}_{BL} \right]^{0.50}$$

The use of a variable-area nozzle on the power turbine permits operation of the gas generator spool at high turbine temperatures over a broad output-power range. This feature results in optimum heat-exchanger performance and low specific fuel consumption. However, it also results in operation of the gas generator spool over a broad speed range from full load to part load as shown in Figure 16. In large engines, transient operation from a low spool speed at part load to the higher speed at full load could impose a potentially unsafe condition because of the time required to overcome the spool inertia. In small engines with their much smaller spool inertias, time constants are considerably reduced, and transient operations should be significantly quicker and safer. This is illustrated in Figure 52, which shows the operating line for Engine 34 plotted on the compressor map. At 50-percent load (Point A), the operating point is near the surge line with a surge margin of 5.0 percent, while at 100-percent load (Point B), the operating point is well away from the surge line with a surge margin in excess of 14 percent. During acceleration from part load to full load, fuel flow must be scheduled to increase speed within the surge margin available. The 5-percent surge margin at 50-percent load would result in a slow acceleration. However, with the variable-geometry power turbine, opening the power turbine nozzle prior to modulating fuel flow can provide additional surge margin as shown in the shaded region of Figure 52 and would provide very good transient performance. As the power turbine nozzle is opened to 100 percent of the design area, the gas generator spool will begin to accelerate because of the unbalanced torque between the HP turbine and the compressor. At this point, fuel flow must be reduced to lower the HP turbine inlet temperature, and then gradually increased to continue the acceleration and restore the turbine inlet temperature to the rated value. This acceleration mode is subject to limitations imposed by thermal gradients in the engine and heat exchanger, and it is expected that a controls system development program would be required to properly integrate and define the nozzle area, fuel flow, temperature, and speed functions.

9
F

As mentioned earlier, the use of the heat exchanger will reduce the infrared signature of the engine. The lower exhaust gas temperature will result in a much lower plume intensity, and the blockage of the direct view of the last turbine stage and the hot engine exhaust duct will eliminate the high-temperature metal signature. The degree to which the plume-signature intensity can be reduced can be predicted with analytical techniques presently available; however, development tests would be required to verify the predictions. The prediction of the engine exhaust plume infrared signature is a complex analysis, which is beyond the scope of this program. However, a first approximation, based on exhaust gas temperatures only, would indicate that the intensity of the recuperated engine exhaust could be as low as one-fourth that of a comparable unrecuperated engine.

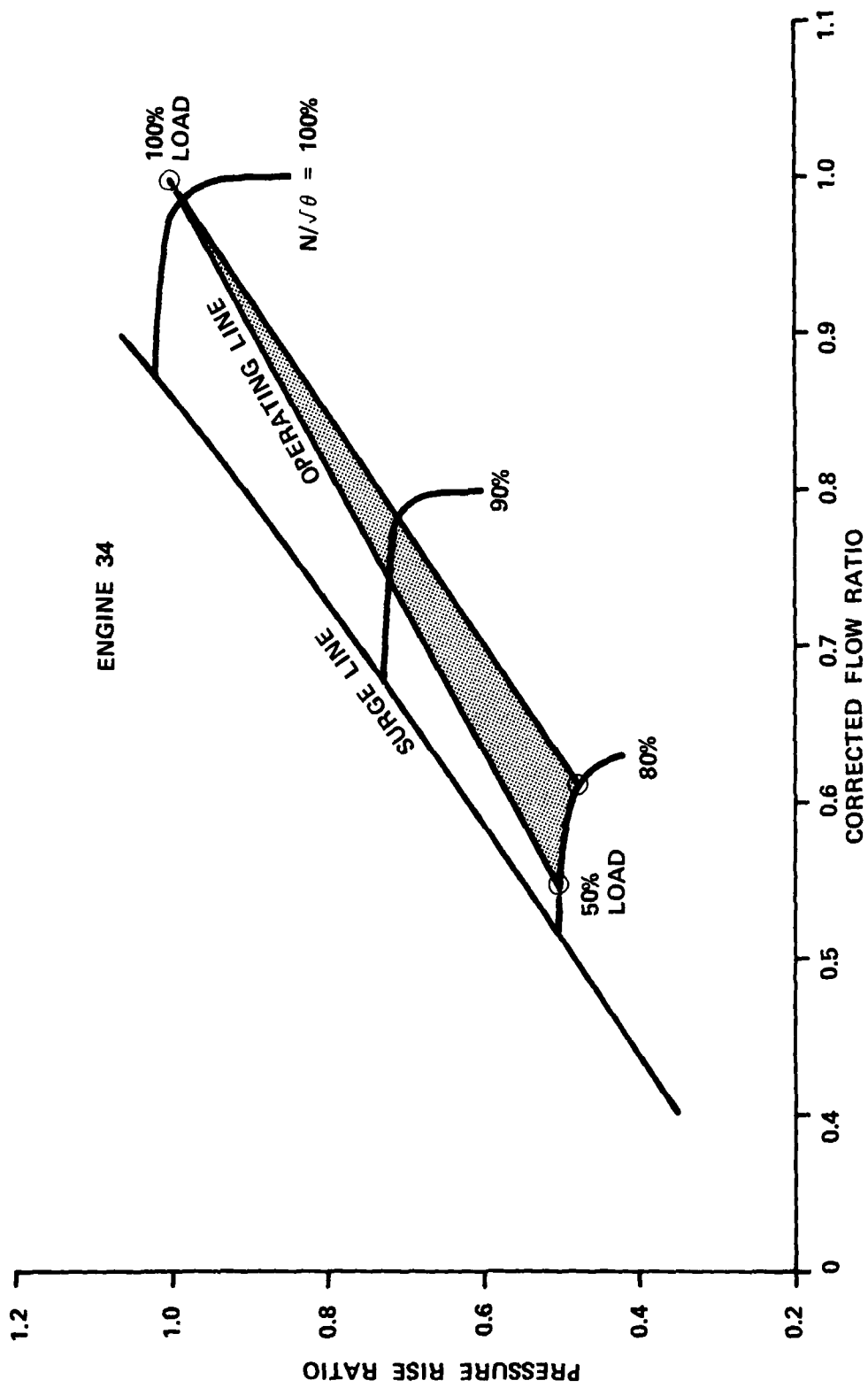


Figure 52. Engine 34 Compressor Map.

The recent (November 1979) FAA notice of proposed rule making (NPRM) regarding helicopter noise has caused airframe manufacturers to seek means for reducing main- and tail-rotor noise signatures. As these sources are controlled, engine noise will become dominant. While effective means are available for controlling compressor inlet noise, and jet noise for turboshaft engines is essentially nonexistent, core (combustor) noise is extremely difficult to reduce. One method that has been demonstrated is the use of a large exhaust muffler. Such a device is impractical for most engine installations because of weight and bulk considerations. However, the aft-mounted heat exchanger offers the opportunity to incorporate muffler-type treatment with a minimum weight and size penalty.

The survivability and vulnerability (S/V) problems associated with military helicopter engines are the subjects of numerous analyses, and S/V has become a highly-specialized area of the military/aerospace community. Consideration of that aspect of the engine itself was not within the scope of this study and would logically be a part of the engine final design. However, the survivability of the heat-exchanger will require careful consideration for military applications. The heat exchanger is, necessarily, a large, highly exposed and vulnerable target. Puncture by small arms rounds or shrapnel could result in severe leakages that would impose large penalties on engine performance. As an example, penetration of the Engine 34 recuperator by a single 7.65 millimeter NATO type round could rupture 36 of the 4140 tubes, plus the outer case. (This assumes straight line trajectory with no tumbling.) This would result in leakage of nearly one percent of the compressor discharge airflow to mix with the exhaust gas in the recuperator plenum, with a consequent slight reduction of heat-exchanger effectiveness and a shaft power loss of approximately 14 horsepower from the full-load condition. Repairing such damage typically consists of simply plugging the damaged tubes, with the consequent effectiveness and pressure-drop effects shown in Figures 53 and 54. As indicated, these effects are relatively minor until a significant percentage (greater than 10 percent) of tubes is plugged. Means for reducing this vulnerability will require unusual and creative design and development.

As discussed previously, the application of new materials and processes for heat exchangers warrants investigation. The potential weight and cost advantages require further exploration and evaluation, and if these advantages are verified, their implementation will require special development emphasis.

As discussed previously, nitride dispersion-strengthened (NDS) stainless steels appear to be the best candidate for future use in lieu of the baseline Inco 625 material. Development of NDS stainless steels in sheet metal form has received considerable attention, and this effort is expected to continue. Development for tubular units can be expected to be much more costly

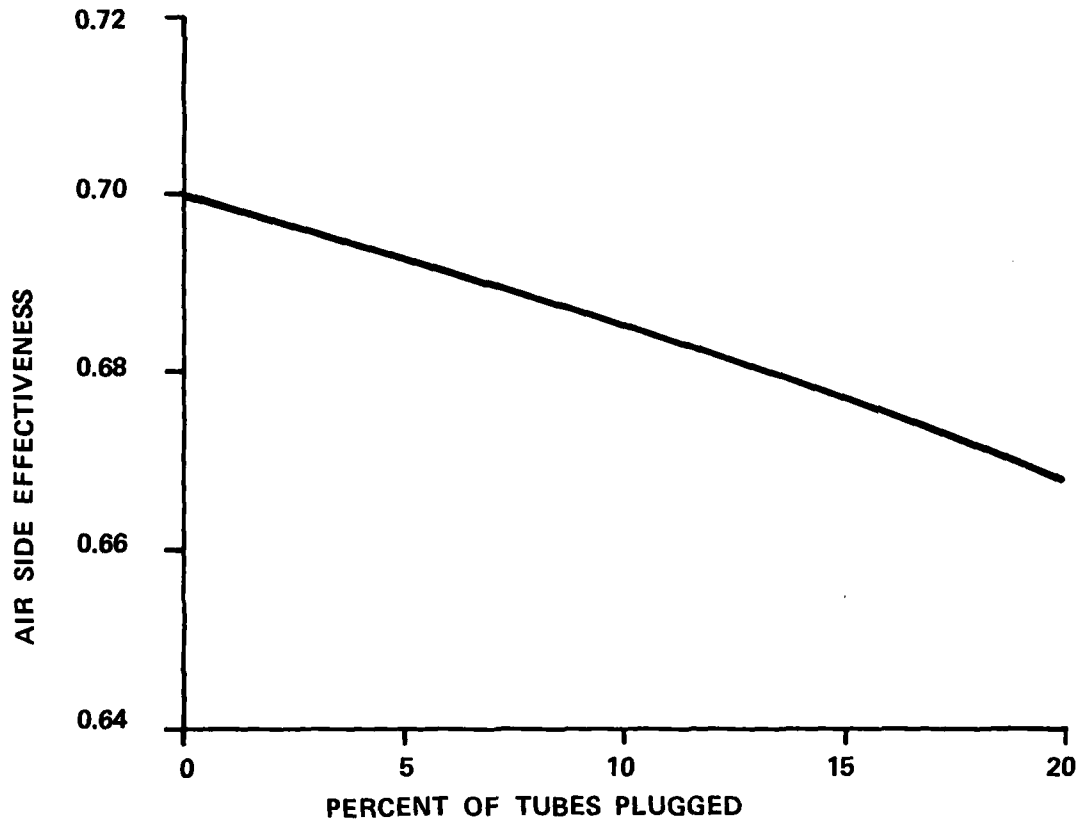


Figure 53. Sensitivity of Tubing Blockage to Recuperator Performance.

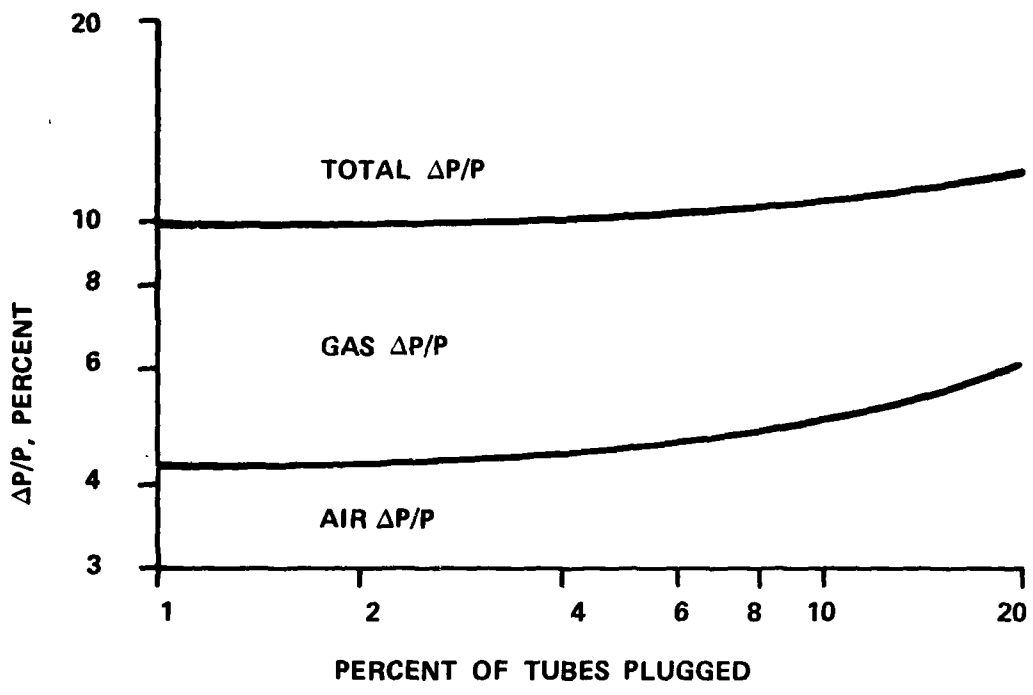


Figure 54. Sensitivity of Tubing Blockage to Recuperator Pressure Drop.

requiring special mill runs of large quantities of tubes. For this reason, it is recommended that development of tubular units using the NDS process be deferred until the process is fully developed for sheet metal (plate-fin) units.

The baseline tubular recuperator cost is not overly sensitive to the material of construction. If the material were free, the cost would be decreased by only 25 to 30 percent compared to the baseline design. If the operating temperatures allowed the use of 347 stainless steel, the cost could be decreased by 12 to 15 percent.

Reduction of heat-exchanger weight can only be achieved at this time by eliminating material. If improved designs permit reduction of tube wall thickness, for example, weight reductions as shown in Figure 55 are possible.

Maintenance and cleaning of heat exchangers exposed to aircraft gas turbine exhaust conditions are functions for which relatively little experience or data exists. The modest amount of information available for automotive and truck applications indicates that rotary regenerators are essentially self-cleaning and that stationary recuperators can be cleaned simply by blowing shop air through the heat-transfer matrices. An intrinsic part of the overall engine-development program will entail monitoring the condition of the heat exchanger for integrity, contamination, and performance (heat-transfer effectiveness and pressure losses) as a function of operating time.

The sensitivity of the effectiveness of the baseline tubular design to fouling factor is given in Figure 56. Unfortunately, these data cannot be related to operating hours on the basis of existing data. If uniform fouling on the outside of the tubes is assumed, a fouling factor of $0.002 \text{ ft}^2\text{-hr}^\circ\text{F}/\text{Btu}$ is equivalent to a deposit of lamp black 0.001-inch thick⁴. This can be misleading because lamp black, which is a loosely packed form of carbon, has a thermal conductivity of $0.042 \text{ Btu/hr-ft-}^\circ\text{F}$. This thermal conductivity is about the same as a good insulation material. In reality, it would be expected that any fouling deposit would be more densely packed with thermal conductivities an order of magnitude greater than lamp black. For example, on the other end of the scale, packed coke has a thermal conductivity of $2.9 \text{ Btu/hr-ft-}^\circ\text{F}$. With coke as the fouling scale -- neglecting blockage of the flow area by the scale -- it would take a deposit layer thickness of 0.069 inch, or roughly 10 times the tube wall thickness, to bring about the two points drop in effectiveness.

⁴Standards of Tubular Exchanger Manufacturers Association, 6th ed., 1978.

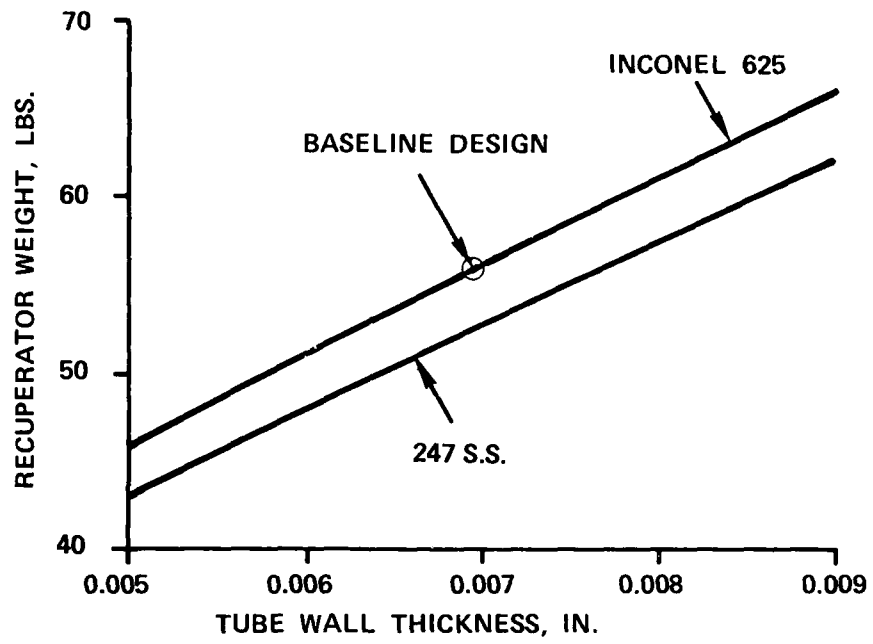


Figure 55. Recuperator Weight as a Function of Tube Wall Thickness.

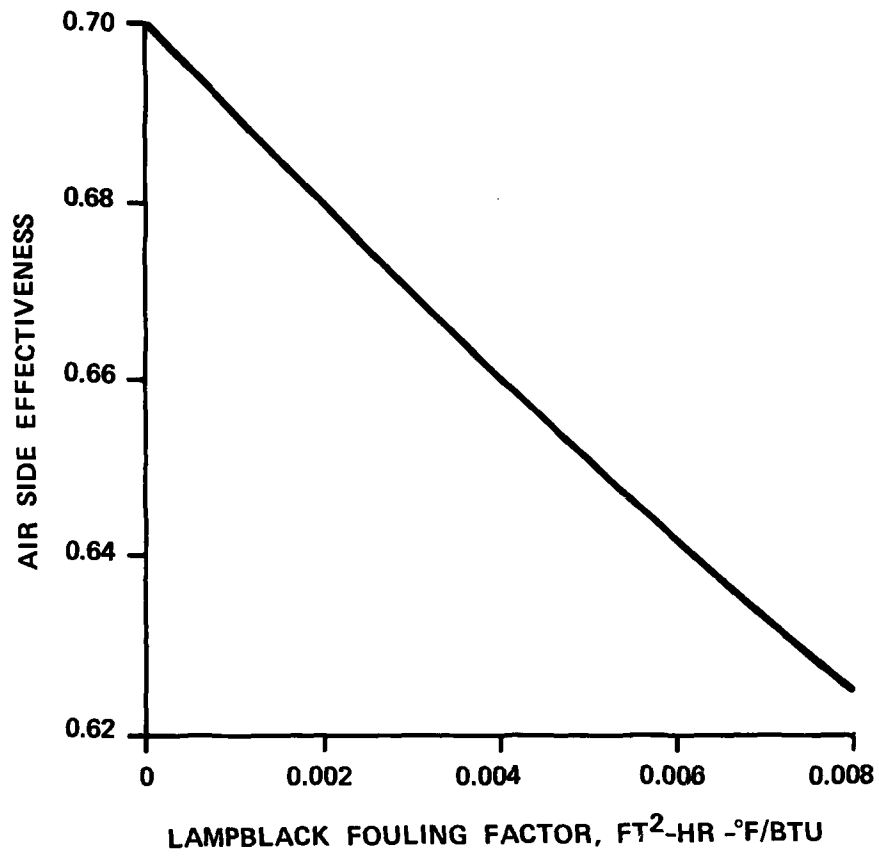


Figure 56. Sensitivity of Fouling on Tube Outside Surface to Recuperator Performance.

Any real fouling deposit would be expected to have a thermal conductivity between those of lamp black and packed coke, with deposit thicknesses approaching the 0.007-inch tube wall thickness required to bring about a two-point drop in effectiveness. This is a significant amount of deposit, which probably represents an upper limit.

Fouling does not affect tubular and plate-fin units in an identical manner. Tubular units are all prime surface units, and the fouling is a direct thermal resistance on this surface. Plate-fin units are part prime surface and part extended surface (the fins). As deposits form on the fins, the overall resistances to heat transfer is increased, but this is partly offset by an increase in fin effectiveness. The thermal performance of plate-fin units, therefore, degrade less than tubular units for the same fouling factor; this behavior is shown in Figure 57. This is not to say, however, that for a like operating time, a plate-fin unit will degrade less in performance than tubular units. There are insufficient data to be sure; it is expected, however, that plate-fin units are, in general, more susceptible to fouling than their tubular counterparts.

The influence of fouling on pressure drop is very difficult to assess. Pressure drop calculations can be made if all surfaces are assumed to receive a uniform deposit of material. In the actual case, however, the leading edge of the fins and tubes are expected to accumulate the major part of any fouling deposits. In this case, the assumption of uniform deposits could lead to a very optimistic pressure drop prediction. In view of these considerations, it is expected that development emphasis would be placed on discovering causes for contamination, finding means for minimizing or eliminating those causes, and determining effective cleaning methods.

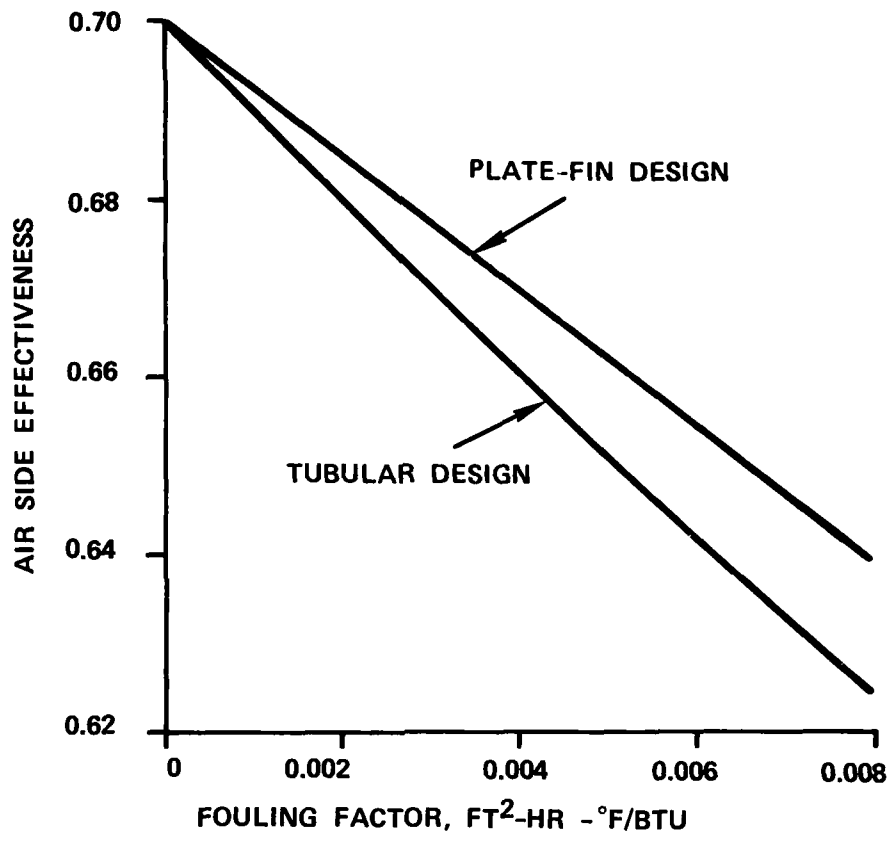
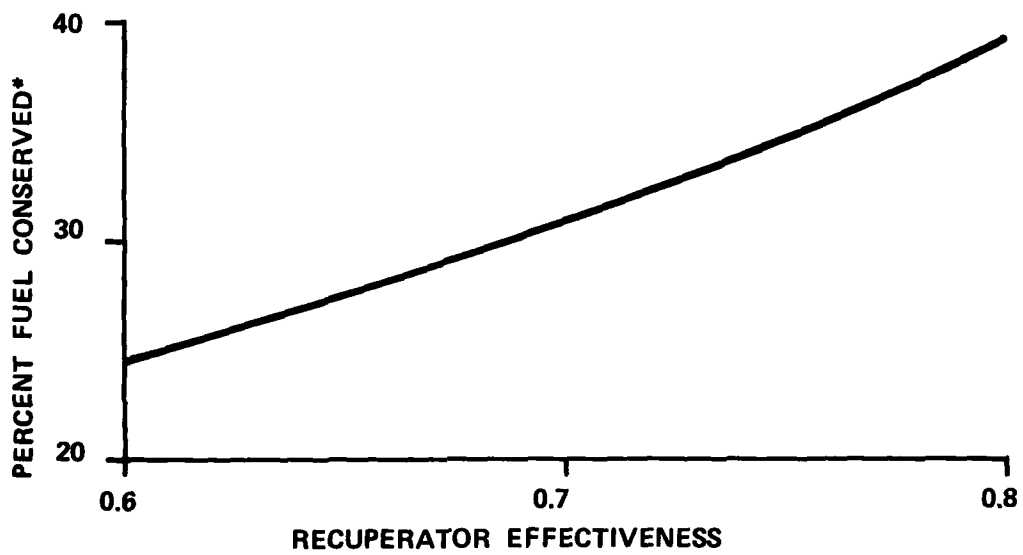


Figure 57. Comparison Between Tubular and Plate-Fin Heat Exchanger.

CONCLUSIONS

Current conditions associated with the cost and availability of fuel have warranted the reexamination of the regenerated or recuperated turboshaft engine cycle for helicopters with particular emphasis on promising heat-exchanger concepts. After examination of the engine-cycle advantages, various heat-exchanger configurations, weight and cost effects, and potential installation problems, the following conclusions were reached:

- (a) Based on up-to-date, life-cycle-cost analyses that consider performance, weight, and acquisition cost, the propulsion system SFC is the overriding factor in determining the relative merits of various systems.
- (b) Whereas earlier studies rarely considered mission times longer than one hour, the current studies have examined missions of 2.5 to 3.5 hours for which the weight of the fuel saved on a single mission more than offsets the added weight of the heat exchanger. This is illustrated in Figure 58, which shows the fuel conserved by a recuperated engine at 50-percent IRP as a percentage of the fuel that would be burned by an unrecovered engine. For a 2.5-hour mission, the weight of the fuel saved could exceed the heat-exchanger weight by as much as 40 percent.
- (c) Heat exchangers can be packaged in a manner that will not interfere with the accessibility or maintainability of the engine nor do they impose unacceptable drag characteristics on the vehicle.
- (d) The civilian helicopter community finds the regenerated turboshaft engine acceptable and attractive in the present fuel situation and would support immediate development of these engines for the 2,000- to 8,000-lb gross-weight vehicles.
- (e) The cycles of the recuperated engines examined in this program are quite similar to the cycles of nonrecuperated engines in this size class since, due to the relatively small size of the turbomachinery, it is impractical to consider very high pressure ratios and temperatures for the conventional engines. Accordingly, any component technology programs undertaken for either type would also benefit the other.
- (f) The variable geometry low pressure turbine, in conjunction with the recuperator, offers a significant payoff in the form of reduced fuel consumption at part power.



***SHOWN AS A PERCENT OF FUEL BURNED
BY AN UNRECUPERATED ENGINE**

**Figure 58. Fuel Conserved By A Recuperated Engine
At 50 Percent IRP.**

- (g) The recuperated engines offer significant life-cycle cost advantages and warrant technology development. In particular, recuperator technology development is required to validate the design estimates made in this program.
- (h) Both single- and two-stage compressors are viable configurations for recuperated engines. For the application considered in this program, compressor efficiency at part power is the important consideration. A detailed study of fixed- and variable-geometry options is required to optimize configurations.

RECOMMENDATIONS

As indicated earlier in this report, the engine concept that was designated Engine 34 and later the TSE Model 1071 was favorably appraised by both Bell and Hughes. Also the general concept of a recuperated engine was received enthusiastically, and AiResearch was encouraged to pursue the concept into hardware development. These companies are primarily concerned with the civilian applications, which may differ from the objectives of a military program; nevertheless, the results of this study support the conclusion that a recuperated turboshaft helicopter engine is not only fuel efficient, but no longer imposes disadvantages of weight and cost. Accordingly, the following programs are recommended:

- (a) An exploratory recuperator-development program to address packaging and installation and the important aspects of recuperator reliability and durability. Specifically, the program should include testing to demonstrate the effects of vibration, thermal cycles, corrosion/sulfidation/oxidation, and erosion. The objective of the program is to determine failure modes, tube support methods, materials, wall thicknesses, and brazing alloys. Following completion of the recuperator program, and depending on its results, initiate the following recuperated engine program.
- (b) Development of an advanced-technology recuperated engine that incorporates, as a minimum, a cooled-gas-generator turbine and a variable-geometry power turbine. (Variable-compressor geometry might be incorporated for optimum efficiency at part power or if required to maintain adequate surge margin. It is also recommended that military and civilian requirements be integrated to meet the shorter-life, higher-performance objectives of military aircraft, as well as the higher utilization and longer TBO periods of the civilian environment.

